The Effects of Wheat Flour, Water, Salt and Mixing on the Rheological Properties and the Gas Phase of Bread Dough

by

Xinyang Sun

A thesis submitted to the Faculty of Graduate Studies of

The University of Manitoba

In partial fulfillment of the requirements of the degree of

DOCTOR OF PHILOSOPHY

Department of Food and Human Nutritional Sciences

University of Manitoba

Winnipeg, Manitoba

Abstract

Health Canada recommends an approximately 30% reduction of sodium levels in bread products, which brings a great challenge for bakery industry due to dough handling difficulties and product quality issues induced by sodium reduction. In order to address this challenge, the effects of wheat cultivar, water content and mixing time on the response of dough's rheological properties and gas phase to salt (NaCl) reduction were investigated to develop processing strategies for improving the breadmaking performance of reduced salt content doughs.

The rheological properties of doughs with a wide range of formulations were examined using the mixograph, dynamic oscillatory rheometry and creep-recovery tests. Outcomes from these rheological studies indicated that doughs with a better tolerance to salt reduction were prepared at higher water contents, and/or optimal mixing time. The gas phase parameters, *i.e.*, the gas volume fraction and the volumetric bubble size distribution, of doughs were examined using synchrotron X-ray microtomography. In terms of the time evolution of the bubble size distribution in unyeasted doughs, increased water content, reduced salt content, and/or increased mixing time were seen to promote disproportionation in the dough. Dough gas phase studies also confirmed a cultivar-dependent response of dough to salt reduction and suggested that the optimal-mixing condition developed the doughs to be more tolerant to salt reduction compared to under- and over-mixing conditions.

In conclusion, formulation and mixing conditions play an important role in determining dough's response to salt reduction. The type of wheat flour (associated with the cultivar's tolerance to salt reduction), water content and optimal mixing time need to be considered when improving the breadmaking performance of reduced-salt doughs.

Acknowledgements

I would like to express my great appreciation to my advisor, Dr. Martin G. Scanlon, for his intellectual guidance, incredible support and intensive knowledge, directing me through the entire Ph.D. study. I am so grateful for having benefited from his scientific insights and teaching philosophy. I would like to give my sincere thanks to my co-advisor, Dr. Filiz Koksel, for her intellectual input and continuous motivation throughout my research and writing of this thesis. My sincere gratitude also goes to my internal examiners Dr. Michael T. Nickerson, Dr. Nancy P. Ames and Dr. Harry D. Sapirstein, and my external examiner Dr. Vassilis Kontogiorgos, for their insightful comments and encouragements. I want to thank Ms. Kim Kuzminski, Mr. Dave Niziol, Dr. Francis Zvomuya, Dr. Aleksandar Yovchev, Dr. Reine-Marie Guillermic, Dr. George Belev, Dr. Adam Webb, and Dr. Serdar Aritan for their technical support.

I am also grateful to my friends Pamela, Nasibeh, Ali, Nazanin, Victoria, Kabo, Lovemore, and Carly for their help and support during my Ph.D. program. I appreciate the financial support provided by Canada Bread Corp. (Toronto, Canada), the Saskatchewan Agricultural Development Fund, the Western Grains Research Foundation, the joint NSERC (Natural Sciences and Engineering Research Council of Canada)-CIHR (Canadian Institute of Health Research) Institute of Nutrition, Metabolism and Diabetes Funding Initiative for Sodium Reduction in the Canadian Food Supply, CSC (China Scholarship Council), UMGSA (University of Manitoba Graduate Student Association) and AACCI (American Association of Cereal Chemists International) Student Travel Awards.

Last but not the least, I greatly appreciate my family: my father Zhongmin Sun, my mother Yuzhen Lan, and my brother Wei Sun, for their unconditional love and support, spiritually motivating me to complete this thesis.

Table of Contents

List of Tables

List of Figures

List of Appendices

List of Abbreviations

Abbreviation	Description
σ	Stress
γ	Strain
$\dot{\gamma}$	Strain rate
η	Viscosity
ω	Angular frequency
$G'(\omega)$	Frequency-dependent storage moduli
$G''(\omega)$	Frequency-dependent loss moduli
G^*	Complex modulus
$G(t)$	Time-dependent stress relaxation
S	Gel strength
n	Gel exponent
$J(t)$	Time-dependent shear compliance
$J_c(t)$	Time-dependent creep compliance
$J_r(t)$	Time-dependent recovery compliance
$J_{c,max}$	Maximum creep compliance
$J_{r,\ max}$	Maximum recovery compliance
J_0,	Instantaneous compliance
J_1, J_2	Retarded compliance
λ, λ_1, λ_2	Retardation time
η_0	Zero shear viscosity
R_1, R_2	Elastic constant

η_1, η_2	Viscous constant
ΔP	Pressure difference
γ_s	Surface tension
D'	Bubble diameter
μ	Mean of the normal distribution
σ_n	Standard deviation of the normal distribution
R	Bubble radius
BSD	Bubble size distribution
R_0	Median of the lognormal distributed BSD
ε	Width of the lognormal distributed BSD
φ	Gas volume fraction
ρ_{atm}	Dough density at atmospheric pressure
ρ_{gf}	Gas-free dough density at zero pressure
$BVF(R)$	Radius dependence of bubble volume fraction

1. General Introduction

Excessive sodium consumption via common table salt (NaCl) brings a considerable number of health concerns, *i.e.*, cardiovascular diseases, high blood pressure, propensity for strokes, and obesity (Du Cailar, Ribstein, & Mimran, 2002; Elliott et al., 1996; World Health Organization, 2007). Canadians consume ~3500 mg of sodium per day, double the recommended Adequate Daily Intake (ADI) level of 1200-1500 mg/day (Fischer, Vigneault, Huang, Arvaniti, & Roach, 2009). Bread and cereal products have been reported to contribute approximately 30% to the daily intake of sodium in western diets (Noort, Bult, Stieger, & Hamer, 2010). To reduce or eliminate excessive sodium intake in the human diet, reducing the sodium content in bread products is a potential strategy. Canadian bread products have been reported to contain an average sodium level of 447 to 471 mg/100 g of bread (Arcand, Au, Schermel, & L'Abbe, 2014; Scourboutakos & L'Abbé, 2013). Health Canada's Sodium Working Group has targeted the sodium level in pan bread to reach ~330 mg sodium/100 g of bread (Yovchev et al., 2017b; Yovchev, Scanlon, & Nickerson, 2015). To meet this target, the baking industry needs to work on an approximate 30% reduction in sodium levels in bread products.

The reduction of salt (NaCl) in bread dough has been reported to affect its rheological properties, *i.e.*, decrease of dough strength (Casutt, Preston, & Kilborn, 1984) and increase of dough stickiness (Hutton, 2002; Jekle & Becker, 2011; Yovchev et al., 2017b). Salt reduction has also been reported to affect the gas phase of the dough during breadmaking, *i.e.*, increase the gas volume entrained into the dough at the end of mixing (Chin, Campbell, & Thompson, 2005; Koksel, Strybulevych, Page, & Scanlon, 2014) and increase the rate of bubble expansion in the dough during proving (Lynch, Dal Bello, Sheehan, Cashman, & Arendt, 2009; Miller & Hoseney, 2008). Salt reduction has also been reported to result in unexpected changes in the quality of bread (Belz, Ryan, & Arendt, 2012), for example, increase the number of larger-sized gas cells within bread

crumb (Lynch et al., 2009), promote a lighter colored crust (Czuchajowska, Pomeranz, & Jeffers, 1989), and produce a loaf lacking in flavor (Miller & Hoseney, 2008). As such, it is challenging to reduce the salt content in the dough, and concurrently control the rheological properties, the gas phase in the dough, and the quality of the bread baked from it.

As the dough is a mixture of wheat flour, water and salt, its rheological properties are affected by the interactions of gluten proteins, water and salt (Beck, Jekle, & Becker, 2012b; Belton, 2012). Therefore, the effect of salt reduction on dough rheological properties may be mitigated by manipulating the wheat cultivar and/or water content. Empirical rheological measurements have been conducted to investigate the effect of salt reduction on dough rheological parameters (Danno & Hoseney, 1982a; Galal, Varriano-Marston, & Johnson, 1978; Preston, 1989). The response of a dough's mixograph and extensigraph parameters to salt reduction has been reported to differ according to wheat cultivar (Butow, Gras, Haraszi, & Bekes, 2002). However, the relationship between wheat cultivar strength and its sensitivity to salt reduction has not yet been clarified. In terms of dough consistency measured by a farinograph, higher water content has been reported to lower the sensitivity of dough to salt reduction (Hlynka, 1962). But it may not be wise to confirm this hindering effect of higher water content on dough's sensitivity to salt reduction from the measurement of only one parameter.

Fundamental rheological studies, *e.g.*, dynamic oscillatory rheometry and creep-recovery tests, have been conducted to examine how salt reduction affects dough viscoelasticity in terms of the frequency-dependent storage $G'(\omega)$ and loss $G''(\omega)$ moduli (Larsson, 2002; Lynch et al., 2009; McCann & Day, 2013; Salvador, Sanz, & Fiszman, 2006), as well as the time-dependent creep and recovery compliance $J(t)$ (Beck, Jekle, & Becker, 2012a). A negative relationship between dough elasticity and salt reduction has been indicated by the instantaneous and retarded elastic

compliance from Burgers modeling of *J(t)* (Beck et al., 2012a). However, other studies of dough viscoelasticity have shown contradictory results, *i.e.*, with salt reduction, dough's *G′(ω)* decreased (Lynch et al., 2009; McCann & Day, 2013; Salovaara, 1982) or increased (Larsson, 2002). This difference in the response of dough's *G′(ω)* to salt reduction has also been observed for noodle doughs, with salt reduction from 3% to 0% leading to a decrease in the *G′(ω)* of doughs made from a wheat cultivar with a lower protein content, and an increase in the *G′(ω)* of doughs made from a wheat cultivar with a higher protein content (Wu, Beta, & Corke, 2006). Further investigation is needed for bread doughs to confirm if there is a cultivar-dependent response of dough viscoelasticity to salt reduction. Although the softening effect of water on dough has been widely demonstrated by decrease in *G′(ω)* and *G″(ω)* (Berland & Launay, 1995b; Dreese, Faubion, & Hoseney, 1988; Létang, Piau, & Verdier, 1999; Mani & Trligardh, 1992; Masi, Cavella, & Sepe, 1998; Navickis, Anderson, Bagley, & Jasberg, 1982; Upadhyay, Ghosal, & Mehra, 2012), and an increase in the maximum creep compliance (Jekle & Becker, 2012; Yovchev et al., 2017a), how water content affects the response of dough viscoelasticity to salt reduction has not been reported yet.

Constitutive models have been used to investigate the viscoelasticity of doughs for a range of formulations. *G′(ω)* and *G″(ω)* have been characterized using power-law models with only two parameters (Bohlin & Carlson, 1980; Georgopoulos, Larsson, & Eliasson, 2004; Peressini, Sensidoni, Pollini, & Cindio, 2000; Upadhyay et al., 2012). *J(t)* has been characterized using the Burgers model with four parameters (Beck et al., 2012a; Lazaridou, Duta, Papageorgiou, Belc, & Biliaderis, 2007; Skendi, Papageorgiou, & Biliaderis, 2010) or six parameters (Campos, Steffe, & Ng, 1997; Meerts, Cardinaels, Oosterlinck, Courtin, & Moldenaers, 2017; Van Bockstaele, De Leyn, Eeckhout, & Dewettinck, 2011). Although a modified expression of the power-law model,

i.e., power-law gel model, has been used for modeling the $G'(\omega)$, $G''(\omega)$ and $J(t)$ of dough (Ng, 2008), the Burgers model has not been used to characterize the $G'(\omega)$ and $G''(\omega)$ of dough yet.

Mixing is a critical process that develops the gluten network with an impact on dough rheological properties (Lee, Ng, Whallon, & Steffe, 2001). As dough is mixed towards its optimal development time, the G' of dough increases with increasing mixing time (Bohlin & Carlson, 1980; Gómez, Ferrero, Calvelo, Añón, & Puppo, 2011; Larsson, Eliasson, Johansson, & Svensson, 2000). Before the dough reaches its optimal development, interactions between gluten proteins are strengthened with longer mixing time, resulting in an increase in dough elasticity (Létang et al., 1999). After reaching the dough's optimal development, further increases in mixing time leads to a decrease in G' (Dreese et al., 1988; Mani, Eliasson, Lindahl, & Tragardh, 1992; Mani & Trligardh, 1992) due to the depolymerization of gluten proteins by overmixing the dough (Skerritt, Luch, & Bekes, 1999). As the composition of gluten proteins varies across wheat cultivars, it needs to be determined if there is a cultivar-dependent response of dough rheological properties to mixing time. With increasing mixing time, a higher volume of gas bubbles has been reported as being entrained into the dough from dough density measurements (Koksel & Scanlon, 2012), ultrasonic studies (Mehta, Scanlon, Sapirstein, & Page, 2009) and X-ray tomography analyses (Trinh, Lowe, Campbell, Withers, & Martin, 2013). However, there is a lack of investigation on how mixing time affects the size distribution of entrained bubbles and its evolution, likely because of the challenges of measuring the sizes of fragile bubbles in an optically opaque dough (Bellido, Scanlon, Page, & Hallgrimsson, 2006; Shimiya & Nakamura, 1997).

Investigation of the entrainment and evolution of gas bubbles in bread dough, *i.e.*, the gas volume (Chin & Campbell, 2005a, 2005b; Chin, Martin, & Campbell, 2005) and the size of entrained bubbles at the end of mixing (van Vliet, 1999) as well as their time evolution, is of great

importance if strategies are to be developed for predicting the structure of gas cells within the crumb of the bread loaf baked from the dough (Elmehdi, Page, & Scanlon, 2003). Synchrotron X-ray microtomography is a powerful imaging technique that produces high resolution images in a short scanning time. Therefore, it has been used for investigating the bubble size distribution (BSD) and its evolution in non-yeasted doughs (Guillermic et al., 2018; Koksel, Aritan, Strybulevych, Page, & Scanlon, 2016), the growth in sizes of the bubbles in yeasted doughs (Babin et al., 2006; Turbin-Orger et al., 2012, 2015), as well as the structure of gas cells in bread crumb (Babin, Della Valle, Dendievel, Lassoued, & Salvo, 2005; Falcone et al., 2004, 2005; Lassoued, Babin, Della Valle, Devaux, & Réguerre, 2007). However, there is still a lack of investigations on how the BSD and its evolution are affected by dough formulation.

The hypotheses of this thesis are:

1. Wheat cultivar and water content will affect the mechanical properties of reduced-sodium dough as measured by a mixograph.
2. The modeling studies of dough viscoelasticity will demonstrate the general applicability of power-law gel and Burgers models to a wide range of cultivar strength and formulations.
3. Dough formulation and mixing time will affect dough's gas phase at the end of mixing and how it evolves with time.

For aiming to produce reduced sodium breads with desirable product quality, the importance of strategies that can be used to improve the breadmaking performance of reduced salt content doughs is emphasized. Therefore, the overall objective of this thesis was to improve the formulation and processing conditions for reduced salt content bread doughs by studying the effects of wheat flour, water, salt and mixing on the rheological properties and the gas phase of bread dough. The specific objectives were:

1. To investigate using a mixograph how wheat cultivar and water content affect the response of dough rheological properties to salt reduction.
2. To screen for wheat cultivars with a better tolerance to salt reduction in terms of the mixograph results.
3. To evaluate the effects of wheat cultivar, water content, salt reduction and mixing time on dough viscoelasticity by dynamic oscillatory rheometry and creep-recovery tests.
4. To characterize the viscoelaticity of doughs over a wide range of formulations varying in wheat cultivar, water and salt content with the use of power-law gel and Burgers models.
5. To investigate how wheat cultivar, water content, salt reduction and mixing time affect the volume of gas bubbles entrained into the dough at the end of mixing by dough density measurements and synchrontron X-ray microtomography.
6. To examine the size distribution of bubbles entrained at the end of mixing and its time evolution for a range of dough formulations (*i.e.*, wheat cultivar, water and salt content) and various mixing conditions (*i.e.*, under-, optimal- and over-mixing) by synchrontron X-ray microtomography.

2. Literature Review

2.1. Rheological Studies on Bread Dough Properties

Under well-controlled laboratory conditions, bread dough properties can be studied by rheological methods that simulate dough processing behavior under practical conditions (Tanner, Qi, & Dai, 2008). Rheological studies of dough can be used for optimizing the breadmaking process. For example, empirical rheological methods, *i.e.*, farinograph and mixograph, were used to examine how certain additives and mixing time affected the properties of dough (Gómez et al., 2011; Singh, Inderpreet, Singh, & Hardeep, 2003), which in turn demonstrated the importance of dough rheological studies for understanding how to modify bread formulas and processing conditions.

2.1.1. The Importance of Studying Dough Rheology for Breadmaking

There are two primary reasons for studying dough rheology. Studying dough rheology benefits the bakery industry through screening wheat flours from different wheat cultivars for their suitability for breadmaking according to differences in their dough rheological properties (Janssen, Vliet, & Vereijken, 1996; Van Bockstaele, De Leyn, Eeckhout, & Dewettinck, 2008a, 2008b). Secondly, studying dough rheology contributes to a knowledge of dough handling properties that is an important factor throughout breadmaking processes (Bloksma & Bushuk, 1988). From empirical rheological studies, wheat flours with better baking performance were found to produce doughs that exhibited a greater resistance to extension and a higher extensibility (Kokelaar, van Vliet, & Prins, 1996). To achieve bread with desirable loaf volume and crumb structure, the extensibility of wheat flour dough should exceed a minimum level (Janssen et al., 1996). Fundamental rheological studies, *i.e.*, dynamic oscillatory rheometry and creep-recovery tests, have also been conducted to verify the rheological parameters that have a good ability to indicate

dough baking performance and the volume of bread baked from it (Autio, Flander, Kinnunen, & Heinonen, 2001; Van Bockstaele et al., 2008b, 2011).

2.1.1.1. Definition of Rheology

Rheology is defined as the science that studies the deformation and flow behavior of all materials (Steffe, 1996). Over a given time range, when a controlled stress or strain is applied to a material, the material has a response to the stress or strain. This response is measured and indicated as the material's rheological properties (Dobraszczyk & Morgenstern, 2003). In order to better characterize the rheological properties of a material, some rheological terms, *i.e.*, stress and strain, should be clarified.

Stress is defined as a force per unit area (Barnes, 2000; MenJivar, 1990; Steffe, 1996). It is, therefore, represented with units of Pascal (Pa or N/m^2). In terms of the direction, stresses are classified into two types: 1) shear stress acts in a parallel direction to the surface of the deformed material (Barnes, 2000); 2) normal stress acts in a perpendicular direction to the surface of the deformed material (MenJivar, 1990). Stresses are independent of the size and shape of the deformed material (Steffe, 1996).

Strain is defined as the measure of a material's deformation when it is subjected to external forces. In terms of rheological perspectives, strain is a quantification of the relative displacement between the particles of a material (MenJivar, 1990). Therefore, strain is calculated by one quantity relative to another quantity (Steffe, 1996). Both quantities use the units of length, indicating that strain is dimensionless (Steffe, 1996). When external forces are applied that lead to the flow of a material, the rate at which this flow occurs is defined as strain rate, which has units of reciprocal time (Barnes, 2000; MenJivar, 1990).

Defining the stress, strain and strain rate of a material allows us to determine the material's properties of rheological interest, *i.e.*, viscosity and elasticity. Shear viscosity is the most common type of viscosity reported in the literature (MenJivar, 1990). Under shear conditions, shear viscosity is the resistance of a material to flow (Barnes, 2000). A purely viscous fluid follows Newton's law which states the fluid's strain rate $\dot{\gamma}$ is directly proportional to the applied stress σ (MenJivar, 1990). As a result, a *Newtonian fluid* has a viscosity $\eta = \sigma/\dot{\gamma}$ with units of pascal over reciprocal second (Pa·s) (Barnes, 2000). A *Newtonian fluid* exhibits a positive linear relationship between the σ and $\dot{\gamma}$, and the intercept of the line fitted to the σ *vs.* $\dot{\gamma}$ is zero (Steffe, 1996). The elasticity of a material is defined by elastic moduli that measures the ratio of stress to strain (Barnes, 2000). An ideal elastic solid following Hooke's law exhibits a full recovery after deformation (MenJivar, 1990). This *Hookean solid* has linear elastic behavior so that strain γ is directly proportional to the applied stress σ (Barnes, 2000). As a result, a material experiencing shear deformation has the elastic modulus $G = \sigma/\gamma$ with units of pascal (Pa) (Barnes, 2000; MenJivar, 1990).

2.1.1.2. Introduction of Dough Rheological Properties

In terms of fundamental rheological principles, dough is unlike a purely viscous *Newtonian fluid* or fully recoverable *Hookean solid*, and thus it exhibits partially the viscous behavior of a *non-Newtonian fluid* and partially the elastic behavior of a *Hookean elastic solid* (Faubion & Hoseney, 1990; MenJivar, 1990). Therefore, dough rheological properties can be investigated by characterizing the viscoelastic behavior of dough. Dough viscoelastic behavior is defined as a combination of viscosity (ratio of stress to strain rate) and elasticity (ratio of stress to strain).

In a creep and recovery test, the viscoelastic behavior of bread dough can be defined by compliance (ratio of strain to stress). Due to being a viscoelastic material, as opposed to a fully

recoverable *Hookean solid*, bread dough is able to only partially recover from the deformation (strain) induced by the stress applied to the dough. When the dough is subjected to a stress, the resultant strain is not proportional to the stress, indicating a nonlinear relationship between strain and stress (Steffe, 1996).

To describe the viscoelastic behavior of bread dough in simple terms, several basic rheological models, such as Maxwell, Kelvin-Voigt, Burgers and power-law gel models (Figure 2.1), need to be considered. The rheological models (Figure 2.1) are represented by various combinations of linear viscous η (*i.e.*, dashpot) and elastic G (*i.e.*, spring) elements (Barnes, 2000), providing parameters that directly indicate changes in the rheological properties of doughs over a range of formulation and processing conditions.

Figure 2.1: (a) Maxwell, (b) Kelvin-Voigt, (c) Burgers and (d) power-law gel models. G, G_1 and G_2 represent spring (elastic) elements, whereas η, η_1 and η_2 represent dashpot (viscous) elements.

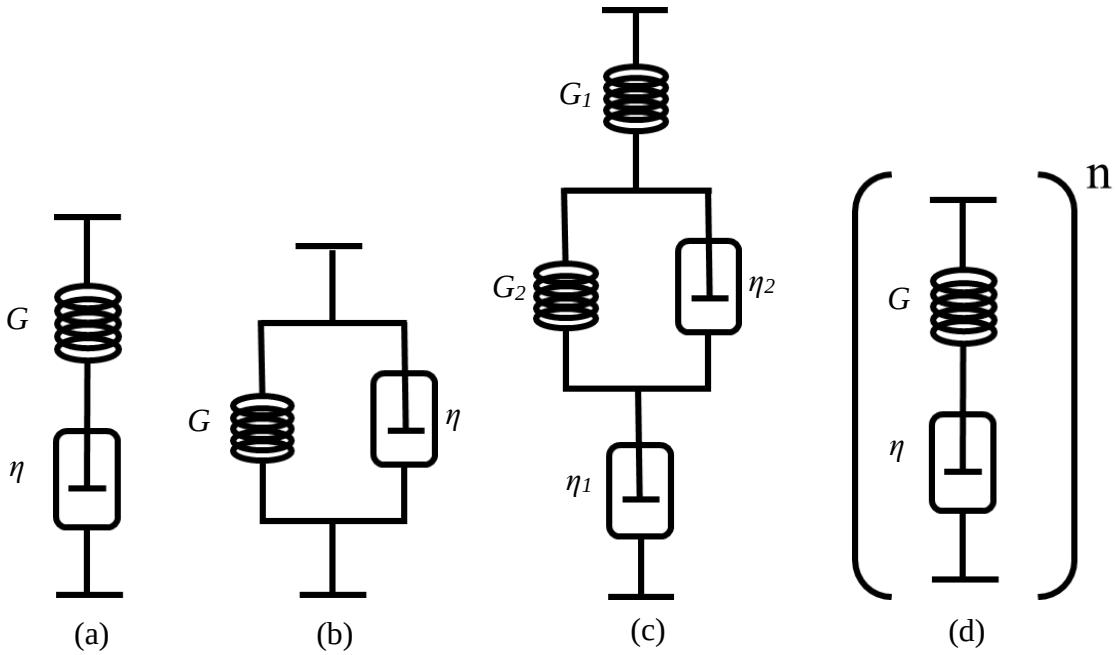

The Maxwell and Kelvin-Voigt models both consist of one dashpot and one spring. The dashpot and spring are arranged in series for the Maxwell model (Figure 2.1a) and in parallel for the Kelvin-Voigt model (Figure 2.1b). The Maxwell model represents an ideal viscoelastic liquid that flows when the slightest force is applied (Muller, 1973). The Kelvin-Voigt model represents an ideal viscoelastic solid that eventually completely recovers after the force is removed (Muller, 1973). According to differences in arrangement of the elements (*i.e.*, dashpot and spring), the Maxwell model has a total strain from adding up the strain of each element and it has equal stress for each element (Muller, 1973). However, the Kelvin-Voigt model has a total stress by summing up the stress on each element and it has equal strain for each element (Muller, 1973).

As bread dough behaves like both a viscous liquid and an elastic solid, a combined use of Maxwell and Kelvin-Voigt models is suggested to describe its rheological properties. A Burgers model (Figure 2.1c) consists of a Maxwell model and a Kelvin-Voigt model in series, and thus it has four elements representing an instantaneous elastic response G_1, a retarded elastic response (G_2, η_2), and a steady-state viscous response η_1 (Barnes, 2000). Previous studies have used the Burgers model to determine dough viscoelastic behavior from creep and recovery tests (Beck et al., 2012a; Campos et al., 1997; Lazaridou et al., 2007; Meerts et al., 2017; Skendi et al., 2010; Tronsmo, Magnus, Færgestad, & Schofield, 2003; Tronsmo, Magnus, Baardseth, et al., 2003; Van Bockstaele et al., 2011). A power-law gel model (Figure 2.1d) consists of a combination of Maxwell models in a continuous series, and this has also been used to describe dough viscoelasticity (Leroy, Pitura, Scanlon, & Page, 2010; Ng, McKinley, & Padmanabhan, 2006; Ng, 2008). Investigations of dough rheological properties using the Burgers and power-law gel models will be introduced in more detail in the section small-deformation measurements of dough (2.1.2.2).

Empirical rheological methods, such as the farinograph and mixograph, are usually used in combination with fundamental rheological methods, such as dynamic oscillatory rheometry and creep recovery tests, in comprehensive studies of how dough rheological properties are affected by formulation and processing. For example, a combination of farinograph and dynamic oscillatory rheometry was used to examine the effects of water content and mixing time on the rheological properties of wheat flour dough (Létang et al., 1999). The rheological properties of wheat flour dough were also measured by the mixograph and dynamic oscillatory rheometry to show that dough viscoelastic properties were affected by mixing time (Gómez et al., 2011). Furthermore, farinograph and mixograph parameters of wheat flour dough were found to be correlated with dough's creep and recovery strain measured by the creep recovery test (Wang & Sun, 2002), indicating a direct relationship between empirical and fundamental rheological studies. Compared to separately conducting empirical and fundamental rheological methods, a combined use of them has a better ability to define dough rheological properties.

2.1.1.3. Relationship of Dough Rheology and Bread Quality

The rheological properties of wheat flour dough, due to the breadmaking strength of a given wheat cultivar, are important factors for determining the quality of the resultant breads (Dobraszczyk & Morgenstern, 2003; Khatkar, Bell, & Schofield, 1996). Compared to doughs made from weaker cultivars, those made from stronger cultivars entrained a lower volume of bubbles during mixing (Campbell, Rielly, Fryer, & Sadd, 1993). Doughs that are too strong cannot develop bubbles appropriately, leading to loaves which are small in volume, dense, and unpalatable (Belton, 2012). However, doughs that are too weak are not able to hold the bubbles and lead to the collapse of the loaf or the formation of large holes in the loaf (Belton, 2012).

The aim of determining dough rheology is to quantitatively describe the mechanical properties of dough, to figure out the correlation of dough rheology to its molecular structure and composition, to characterize and imitate the processing performance of dough, and to control and predict the quality of the resultant products (Dobraszczyk & Morgenstern, 2003; Song & Zheng, 2007). Previous empirical rheological studies have reported a positive correlation of crumb uniformity to dough extensigraph parameters, *i.e.*, maximum resistance to extension and the ratio of resistance to extensibility (Horvat, Magdić, Simić, Dvojković, & Drezner, 2008; Janssen et al., 1996). Dough extensibility positively correlated with the loaf volume (Janssen et al., 1996). Fundamental rheological studies have shown that there is an inverse and nonlinear correlation of loaf volume to dough dynamic rheological parameters, *i.e.*, storage modulus G' ($r^2 = 0.75$) and loss modulus G'' ($r^2 = 0.72$) (Van Bockstaele et al., 2008b). On the contrary, Khatkar and Schofield (2002) found that the G' of wheat flour dough was not able to predict loaf volume due to their weak correlation ($r^2 = 0.16$). But they found that the G' of gluten significantly correlated with the loaf volume of breads baked from gluten-flour blended doughs ($r^2 = 0.73$), indicating that gluten elasticity is an important factor affecting the breadmaking performance of dough. Loaf volume has been seen to correlate with creep-recovery measurement parameters also. For example, the instantaneous recovery compliance positively correlated with loaf volume ($r^2 = 0.66$). Van Bockstaele et al. (2008a) found that a combination of the maximum recovery strain and one empirical rheological parameter (*i.e.*, farinograph water absorption or alveograph deformation energy) provided a better prediction of loaf volume compared to a use of maximum recovery strain alone (Van Bockstaele et al., 2011).

2.1.2. Determination of Dough Rheological Properties

In terms of the magnitude of the exerted deformation on dough, testing can be categorized as large- and small-deformation rheological measurements (Dobraszczyk & Morgenstern, 2003). Empirical rheological measurements are commonly conducted at large deformations. These measurements are able to determine the properties of dough during the mixing process and after fermentation (Faubion, 1987), while they are not sufficient for a determination of fundamental rheological behavior of dough (Song & Zheng, 2007). At small deformations, the storage and loss modulus (G' and G''), indicative of the elastic and viscous properties of a material (Rao, 2007), have been measured to define the fundamental rheological behavior of dough (Hardt, Boom, & van der Goot, 2014; Jekle & Becker, 2011, 2012; Mastromatteo et al., 2013; Miller & Hoseney, 1999; Skendi et al., 2010; Yovchev et al., 2017a, 2017b).

From dynamic oscillatory rheometry measurements, the storage and loss modulus as a function of angular frequency (ω), shown as $G'(\omega)$ and $G''(\omega)$, of wheat flour doughs show a linear viscoelastic behavior if a small amplitude of shear strain, *i.e.*, $\gamma \leq 0.2\%$, is applied (Leroy et al., 2010; Navickis et al., 1982). With increasing the strain amplitude higher than 0.2%, G' and G'' display non-linear viscoelastic behavior (Berland & Launay, 1995b). During the measurements of G' and G'', the applied amplitude of shear strain needs to be considered for a determination of dough viscoelasticity in the linear or non-linear region.

The compliance $J(t)$, a measure of the strain undergone by a material as a function of time, t, when the material is subjected to a constant stress (Steffe, 1996), has also been measured to characterize dough viscoelastic behavior (Edwards, Peressini, Dexter, & Mulvaney, 2001; Skendi et al., 2010; Tronsmo, Magnus, Færgestad, et al., 2003; Tronsmo, Magnus, Baardseth, et al., 2003; Yovchev et al., 2017a, 2017b). In creep-recovery tests, when applying a small magnitude of shear

stress (σ = 1, 6, 8, 16 and 20 Pa), *J(t)* was determined for a long time (*i.e.*, *t* = 12 and 46 h) to show the linear viscoelastic behavior of wheat flour dough (Lefebvre & Mahmoudi, 2007; Lefebvre, 2006, 2009). However, non-linear viscoelastic behavior of wheat flour dough was seen from *J(t)* measurements if the shear stress was large (σ = 100, 250 and 280 Pa) (Lefebvre, 2009; Van Bockstaele et al., 2011). As such, the applied magnitude of shear stress during creep-recovery tests needs to be considered when characterizing the linearity or non-linearity of dough's viscoelastic behavior.

2.1.2.1. Large-Deformation Measurements of Dough

Large-deformation measurements, *i.e.*, farinograph and mixograph, have been widely used to investigate the rheological properties of wheat flour dough in order to predict baking behavior (Oliver & Allen, 1992), screen wheat cultivars suitable for breadmaking (Gélinas & Mckinnon, 2013; Martinant et al., 1998), and optimize breadmaking processes (Zounis & Quail, 1997). When the wheat flour is mixed using a farinograph, its farinogram identifies four mixing periods, *i.e.*, hydration, development, plateau and breakdown (Oliver & Allen, 1992). While the dough is under-mixed during hydration period, it is overmixed during the breakdown period. The optimal loaf volume was achieved if the dough was mixed until the end of the plateau period in the farinogram (Oliver & Allen, 1992). Wheat cultivars over a range of gluten strengths were investigated and screened by a farinograph (Gélinas & Mckinnon, 2013), suggesting that the farinograph parameter dough stability was an indicator of a cultivar's breadmaking performance.

Mixograph parameters, *i.e.*, peak height and bandwidth, strongly correlated with gluten protein composition (Martinant et al., 1998), suggesting that the mixograph could be used to determine the breadmaking performance of wheat cultivars (Khatkar et al., 1996). A good bread quality, including loaf volume, external appearance, crumb color and texture, was obtained when

the dough was mixed for the optimal bakery mixing time (Zounis & Quail, 1997). The optimal mixing time of dough measured by a mixograph was significantly correlated with that measured by a bakery pin mixer (Zounis & Quail, 1997). Therefore, the mixograph is a good tool when used to prepare the dough for breadmaking.

2.1.2.1.1. Farinograph

The farinograph is a widely used instrument to investigate the physical properties of wheat flour dough by measuring the resistance (torque, Tq) the dough exerts on the mixing paddles during a relatively gentle mixing action (Shuey, 1972; Zounis & Quail, 1997). The approach of a farinograph study is to mix the wheat flour with a sufficient content of water (farinograph water absorption, FAB) so that a viscous dough with a consistency of 500 Brabender Unit (B.U.), shown as the peak torque, is produced (AACC International, 2011; Oliver & Allen, 1992; Shuey, 1972). FAB, referred to as the optimal water absorption of a given wheat flour, has been determined as the water content used for producing baked goods (Linko, Härkönen, & Linko, 1984; Oliver & Allen, 1992; Salovaara, 1982; Yovchev et al., 2017b; Zounis & Quail, 1997).

At the maximum dough consistency of 500 B.U., the farinograph parameters dough development time (DDT, min), dough stability (STA, min), and mixing tolerance index (MTI, B.U.) have been determined to indicate changes in dough strength with its formulation, *e.g.*, wheat flour and salt content (Galal, Varriano-Marston, & Johnson, 1978; Gélinas & Mckinnon, 2013; Horvat et al., 2008; Linko et al., 1984; Preston, 1989; Puppo, Calvelo, & Añón, 2005; Salovaara, 1982; Wehrle, Grau, & Arendt, 1997). The farinograph has also been used to investigate the variation in dough consistency induced by the formulation (Hardt et al., 2014; Hlynka, 1962; Manohar & Rao, 1999; Tanaka, Furukawa, & Matsumoto, 1967; Tkachuk & Hlynka, 1968).

Farinograph measurements have been used to demonstrate how dough rheological properties are affected by the type of wheat flour, and the content of water and salt in the dough. For example, doughs made from stronger wheat cultivars had a higher DDT and STA (Horvat et al., 2008; Puppo et al., 2005), which was attributed to a higher ratio of glutenin to gliadin for the stronger wheat cultivars (Puppo et al., 2005). With increasing water content, dough consistency decreased and DDT increased (Hardt et al., 2014; Hlynka, 1962; Manohar & Rao, 1999), indicating that increased water content delays optimal dough development. Salt reduction led to an increase in dough consistency and a decrease in DDT (Galal et al., 1978; Linko et al., 1984; Tanaka et al., 1967; Tkachuk & Hlynka, 1968; Wehrle et al., 1997), indicating that dough development becomes faster with salt reduction. Salt reduction also resulted in an increase in MTI and a decrease in STA (Galal et al., 1978; Gélinas & Mckinnon, 2013; Linko et al., 1984; Tkachuk & Hlynka, 1968; Wehrle et al., 1997), indicating that reduced-salt conditions produce doughs with lower tolerance to overmixing.

2.1.2.1.2. Mixograph

Similar to the farinograph, the mixograph is a mixing instrument widely used for dough preparation. Compared to the farinograph where there is a Z-arm mixer, the mixograph is a pin mixer that measures the resistance (torque, Tq) the dough exerts on the mixer pins as a function of mixing time (Haraszi, Larroque, Butow, Gale, & Bekes, 2008; Shuey, 1972; Zounis & Quail, 1997). Compared to the farinograph, the mixograph appears to have a higher rate of mixing work input and better capacity to develop a dough that is fitting for modern bakery production (Zounis & Quail, 1997). Accordingly, when doughs are mixed by a Z-arm mixer and a mixograph at their optimal development times as assessed by the peak in their mixing curves, the degree of dough development differs according to the mixer type (Haraszi et al., 2008).

The mixograph parameters, mixing development time (min, optimal mixing time), peak height (Tq, maximum dough resistance), peak bandwidth (Tq, bandwidth at maximum dough resistance), and work input (Tq × min, incorporated energy at maximum dough resistance) have been measured to screen wheat cultivars according to their breadmaking strengths (Gras & O'Brien, 1992; Khatkar, Bell, & Schofield, 1995; Khatkar et al., 1996; Martinant et al., 1998). Stronger wheat cultivars were seen to produce doughs with larger values for the mixograph parameters defined above (Khatkar et al., 1996). From mixograph measurements, the breadmaking strength of wheat cultivars has been shown to relate to the content and composition of gluten proteins (*i.e.*, glutenins and gliadins) (Khatkar et al., 1995, 1996; Martinant et al., 1998).

The mixograph has been used to investigate the effects of water and salt content on dough rheological properties (Gras & O'Brien, 1992; Lang, Neises, & Walker, 1992; Singh et al., 2003). With increasing water content in the dough, the mixing development time increased, whereas peak height, peak bandwidth and work input decreased (Baig & Hoseney, 1977; Gras, Carpenter, & Anderssen, 2000; Lang et al., 1992), indicating that increased water content prolongs optimal dough development and increases dough softness. With salt reduction in the dough, the mixing development time, peak height and peak bandwidth decreased (Danno & Hoseney, 1982a; He, Roach, & Hoseney, 1992; Lang et al., 1992; Singh et al., 2003), indicating that salt reduction leads to a weakening effect on wheat flour dough. In addition to the salt content, the type of salt was also seen to affect the mixograph parameters associated with dough strength (He et al., 1992).

2.1.2.2. Small-Deformation Measurements of Dough

Small-deformation measurements, *e.g.*, dynamic oscillatory rheometry and creep-recovery tests, have been used to investigate fundamental rheological properties (*i.e.*, viscosity and elasticity) of wheat flour doughs for various ingredient and processing conditions, *i.e.*, the strength of a wheat

cultivar, the content of water and salt, as well as the mixing condition (*i.e.*, optimal- *vs.* over-mixing) (Beck et al., 2012a; Edwards, Dexter, Scanlon, & Cenkowski, 1999; Hardt et al., 2014; Meerts et al., 2017; Skendi et al., 2010; Yovchev et al., 2017b). Compared to large-deformation measurements where dough samples undergo destruction or large structural changes, small-deformation measurements are non-destructive for dough samples subjected to a relatively small force (Tietze, Jekle, & Becker, 2016). Results from dynamic oscillatory rheometry and creep-recovery tests have verified that there is a relationship of dough viscoelastic properties to the quality of the resultant breads baked from it (*e.g.*, loaf volume and crumb cell structure) (Khatkar & Schofield, 2002; Lynch et al., 2009; Mani et al., 1992; Mastromatteo et al., 2013; McCann & Day, 2013; Van Bockstaele et al., 2008a; Wang & Sun, 2002; Yovchev et al., 2017b).

2.1.2.2.1. Dynamic Oscillatory Rheometry

Dynamic oscillatory rheometry has been used to measure the storage (elastic) modulus G' and loss (viscous) modulus G'' for the characterization of the viscoelastic behavior of wheat flour dough as a function of angular frequency (ω) (Berland & Launay, 1995a; Bohlin & Carlson, 1980; Dreese, Faubion, & Hoseney, 1990; Georgopoulos, Larsson, & Eliasson, 2004; Hardt et al., 2014; Hibberd, 1970; Khatkar & Schofield, 2002; Larsson, Eliasson, Johansson, & Svensson, 2000; Leroy et al., 2010; Létang et al., 1999; Masi, Cavella, & Sepe, 1998; Mastromatteo et al., 2013; McCann & Day, 2013; Miller & Hoseney, 1999; Navickis et al., 1982; Peressini, Sensidoni, Pollini, & Cindio, 2000; Salvador, Sanz, & Fiszman, 2006; Upadhyay, Ghosal, & Mehra, 2012). The viscoelastic properties of wheat flour doughs have been investigated over a range of dough formulations. For example, the strength of wheat cultivar (Khatkar & Schofield, 2002; Miller & Hoseney, 1999), water concentration (Berland & Launay, 1995a; Dreese et al., 1988; Létang et al., 1999; Mani & Trligardh, 1992; Masi et al., 1998; Navickis et al., 1982; Upadhyay et al., 2012), as

well as salt concentration (Larsson, 2002; Lynch et al., 2009; McCann & Day, 2013; Peressini et al., 2000; Salvador et al., 2006; Wehrle et al., 1997).

Compared to weaker cultivars, stronger cultivars produced doughs with higher values for the storage and loss modulus $G'(\omega)$ and $G''(\omega)$ and lower values for the loss tan δ ($G''(\omega)/G'(\omega)$) over a frequency range of 0.1 to 1000 rad.s^{-1} (Miller & Hoseney, 1999). Therefore, they concluded that doughs made from stronger cultivars were relatively more elastic. In contrast, higher values of $G'(\omega)$ over the frequency of 0.06 to 62.8 rad.s^{-1} were seen for weaker flour doughs rather than the stronger ones (Khatkar & Schofield, 2002). Since weaker cultivars have a lower ratio of protein to starch, this finding has been interpreted by Khatkar & Schofield (2002) that protein-starch and starch-starch interactions predominate over protein-protein interactions in small strain tests.

With increasing water content in the dough, both $G'(\omega)$ and $G''(\omega)$ significantly decreased (Berland & Launay, 1995a; Dreese et al., 1988; Létang et al., 1999; Mani & Trligardh, 1992; Masi et al., 1998; Navickis et al., 1982; Upadhyay et al., 2012). This water-induced decrease in $G'(\omega)$ and $G''(\omega)$ is attributed to the role of water as a mobility enhancer in the dough system. Increased water content accelerates the relaxation dynamics of dough, resulting in dough that behaves more like a liquid material, lowering its $G'(\omega)$ and $G''(\omega)$ (Masi et al., 1998).

With salt reduction in the dough, both $G'(\omega)$ and $G''(\omega)$ decreased (Lynch et al., 2009; McCann & Day, 2013; Salvador et al., 2006). This phenomenon has been interpreted as due to an decrease in inter-protein hydrophobic interactions with salt reduction that reduces protein aggregations and this in turn decreases dough elasticity (Preston, 1989; Salvador et al., 2006). In a contrasting study, an increase in the $G'(\omega)$ of a dough was seen with salt reduction (Larsson, 2002). These contradictory results may be explained as arising from the salt-induced response of $G'(\omega)$ and $G''(\omega)$ of the dough being dependent on the quantity and quality of proteins in the wheat

flour (Peressini et al., 2000; Wu et al., 2006). With salt reduction from 3% to 0%, $G'(\omega)$ decreased for lower-protein doughs and it increased for higher-protein doughs (Wu et al., 2006).

Over a certain range of frequency, the frequency-dependent increase in storage modulus $G'(\omega)$ and loss modulus $G''(\omega)$ were seen to follow a power-law model, shown in Eqs. [1] and [2] (Bohlin & Carlson, 1980; Georgopoulos et al., 2004; Peressini et al., 2000; Upadhyay et al., 2012):

$$G'(\omega) = G_0' \, \omega^{n'} \quad [1]$$

$$G''(\omega) = G_0'' \, \omega^{n''} \quad [2]$$

where G_0' and G_0'' are the intercepts of the power-law modeling of $G'(\omega)$ and $G''(\omega)$, whereas n' and n'' are the corresponding slopes (exponents) indicative of the frequency dependency of $G'(\omega)$ and $G''(\omega)$.

For wheat flour doughs, n' and n'' increased with increasing water content (Georgopoulos et al., 2004; Masi et al., 1998; Navickis et al., 1982), indicating that $G'(\omega)$ and $G''(\omega)$ were more frequency dependent for higher water content doughs. In contrast, Hibberd (1970) found that the frequency dependence of $G'(\omega)$ and $G''(\omega)$ was independent of water content in the dough, whereas it increased with increasing the ratio of protein to starch content in the dough (Hibberd, 1970). In agreement, $G'(\omega)$ and $G''(\omega)$ were more responsive to frequency change for doughs higher in protein content (Smith, Smith, & Tschoegl, 1970), or lower in starch content (Larsson et al., 2000).

In a dough system, the frequency dependency of $G'(\omega)$ and $G''(\omega)$ increased from the low to high frequency region (Larsson et al., 2000; Salvador et al., 2006). This finding agrees with observation of a linear relationship of log $G'(\omega)$, log $G''(\omega)$ *vs.* log ω in the high frequency region (Bohlin & Carlson, 1980). They also emphasized that $G'(\omega)$ and $G''(\omega)$ data should be evaluated at higher frequencies because the data at lower frequencies was less accurate. Over a wide range of frequencies (*i.e.*, 10^{-2} to 10^{7} rad s^{-1}), the linear viscoelastic behavior of dough was investigated

by a power-law gel model fitting of log $G'(\omega)$, $G''(\omega)$ *vs.* log ω (Leroy et al., 2010). The power-law gel model is expressed in Eqs. [3] and [4] (Ng, McKinley, & Ewoldt, 2011; Ng et al., 2006; Ng, 2008):

$$G'(\omega) = \Gamma(1-n)\cos\frac{n\pi}{2}S\omega^n \quad [3]$$

$$G''(\omega) = \Gamma(1-n)\sin\frac{n\pi}{2}S\omega^n \quad [4]$$

where n is the gel exponent, $\Gamma(1-n)$ is the gamma function for $1-n$, and S is the gel strength. Wheat flour dough is deemed to be a critical gel-like material that undergoes a transition from liquid to solid and also follows a continuous power-law relaxation time spectrum (Horst & Winter, 2000; Izuka, Winter, & Hashimoto, 1994; Mours & Winter, 1996). Therefore, the power-law gel model with the parameters gel exponent and strength characterizes linear dough viscoelasticity and can indicate dough strength (Gabriele, De Cindio, & D'Antona, 2001; Ng et al., 2006).

2.1.2.2.2. Creep-Recovery Test

In creep-recovery tests applying a constant shear stress σ_0, dough viscoelastic behavior is described by measuring the strain (γ, %) or compliance (J, Pa^{-1}) of the dough as a function of creep and recovery time (t, s), shown as the creep-recovery strain $\gamma(t)$ or compliance $J(t) = \gamma(t) / \sigma_0$ (Campos et al., 1997; Edwards et al., 1999, 2001; Jekle & Becker, 2011; Laguna, Hernández, Salvador, & Sanz, 2013; Mastromatteo et al., 2013; Meerts et al., 2017; Pedersen, Kaack, Bergsøe, & Adler-Nissen, 2004; Tronsmo, Magnus, Færgestad, et al., 2003; Tronsmo, Magnus, Baardseth, et al., 2003; Van Bockstaele et al., 2011). A representative creep-recovery test curve is shown in Figure 2.2.

In a creep-recovery curve for dough, the creep phase shows dough experiencing three types of deformation, *i.e.*, instantaneous elastic deformation (Figure 2.2a), retarded elastic deformation

(Figure 2.2b), and viscous deformation (Figure 2.2c) (Beck et al., 2012a; Van Bockstaele et al., 2011). At the end of the creep phase, the maximum creep strain $\gamma_{c,\,max}$ or compliance $J_{c,\,max}$ (Figure 2.2d) is determined (Mastromatteo et al., 2013; Van Bockstaele et al., 2011). After the shear stress is removed ($\sigma_0 = 0$), the dough starts to recover the elastic part of the deformation over time, and this is comprised of two parts: 1) the instantaneous strain or compliance; and 2) the retarded strain or compliance (Jekle & Becker, 2011; Van Bockstaele et al., 2011). The recovery phase consists of two types of recovery, *i.e.*, the instantaneous elastic recovery (Figure 2.2e), and the retarded elastic recovery (Figure 2.2f) (Van Bockstaele et al., 2011). The maximum recovery strain $\gamma_{r,\,max}$ or compliance $J_{r,\,max}$ (Figure 2.2g) is determined at the end of the recovery phase (Mastromatteo et al., 2013; Van Bockstaele et al., 2011). A lower $\gamma(t)$ or compliance $J(t)$ was indicative of a stronger dough with a higher resistance to flow (Campos et al., 1997; Edwards et al., 1999, 2001; Laguna et al., 2013; Mastromatteo et al., 2013; Meerts et al., 2017).

Figure 2.2: A representative creep-recovery test curve. The creep phase includes (a) instantaneous elastic deformation, (b) retarded elastic deformation, (c) viscous deformation, and (d) maximum creep compliance ($J_{c,\,max}$), whereas the recovery phase includes (e) instantaneous elastic recovery, (f) retarded elastic recovery, and (g) maximum recovery compliance ($J_{r,\,max}$).

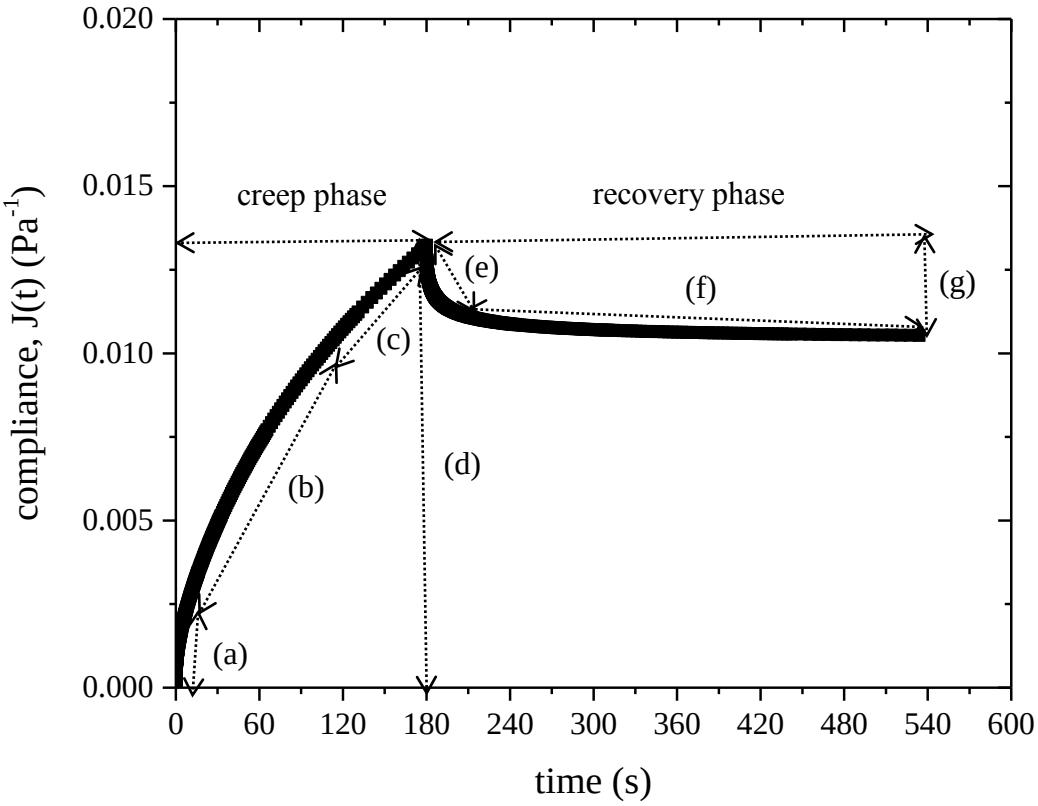

To quantify these deformations of doughs in creep-recovery tests, the creep compliance $J_c(t)$ and recovery compliance $J_r(t)$ have been modeled using a four-parameter Burgers model (Beck et al., 2012a; Laguna et al., 2013; Lazaridou et al., 2007; Skendi et al., 2010; Van Bockstaele et al., 2011) or a six-parameter Burgers model (Campos et al., 1997; Edwards et al., 2001; Meerts et al., 2017; Tronsmo, Magnus, Færgestad, et al., 2003; Tronsmo, Magnus, Baardseth, et al., 2003; Van Bockstaele et al., 2011). The four-parameter Burgers model is expressed in Eq. [5] for creep and in Eq. [6] for recovery (Beck et al., 2012a; Lazaridou et al., 2007; Skendi et al., 2010).

$$J_c(t) = J_0^c + J_1^c \left[1 - exp\left(-\frac{t}{\lambda_1^c}\right)\right] + \frac{t}{\eta_0^c} \quad [5]$$

$$J_r(t) = J_{c,\,max} - J_0^r - J_1^r \left[1 - exp\left(-\frac{t}{\lambda_1^r}\right)\right] \quad [6]$$

where J_0^c is the instantaneous compliance (Pa^{-1}), J_1^c is the retarded compliance (Pa^{-1}), λ_1^c is the retardation time (s), and η_0^c is the zero shear viscosity (Pa·s), for modeling of $J_c(t)$. J_0^r, J_1^r, and λ_1^r are the counterparts for modeling of $J_r(t)$. $J_{c,\,max}$ is the maximum creep compliance obtained at the end of the creep phase. The six-parameter Burgers model is expressed in Eq. [7] for creep and in Eq. [8] for recovery (Campos et al., 1997; Meerts et al., 2017; Van Bockstaele et al., 2011).

$$J_c(t) = J_0^c + J_1^c \left[1 - exp\left(-\frac{t}{\lambda_1^c}\right)\right] + J_2^c \left[1 - exp\left(-\frac{t}{\lambda_2^c}\right)\right] + \frac{t}{\eta_0^c} \quad [7]$$

$$J_r(t) = J_0^r + J_1^r \left[1 - exp\left(-\frac{t}{\lambda_1^r}\right)\right] + J_2^r \left[1 - exp\left(-\frac{t}{\lambda_2^r}\right)\right] \quad [8]$$

where J_2^c is the retarded compliance (Pa^{-1}) and λ_2^c is the retardation time (s) for modeling of $J_c(t)$. J_2^r and λ_2^r are the counterparts for modeling of $J_r(t)$.

The various parameters from the Burgers model have been shown to characterize the non-linear viscoelastic properties of doughs well over a range of formulations, *i.e.*, wheat cultivar (Edwards et al., 2001; Yovchev et al., 2017b), water content (Jekle & Becker, 2011; Meerts et al., 2017; Skendi et al., 2010; Yovchev et al., 2017a) and salt content (Beck et al., 2012a). Doughs made from stronger wheat cultivars had higher η_0^c and lower creep compliances, *i.e.*, J_0^c, J_1^c and J_2^c (Edwards et al., 2001) as well as lower $J_{c,\,max}$ (Yovchev et al., 2017b), indicating that stronger doughs have larger values for their viscosity and elasticity. Increased water content led to an increase in $J_{c,\,max}$ (Jekle & Becker, 2011; Yovchev et al., 2017a), and a decrease in η_0^c, λ_2^c and λ_2^r of the dough (Meerts et al., 2017; Skendi et al., 2010). This finding indicates a weakening effect of water that results in a lower elasticity and viscosity as well as a faster relaxation of the dough

(Meerts et al., 2017). With increasing salt content in the dough, J_0^c and J_1^c increased, whereas η_0^c and λ_1^c decreased (Beck et al., 2012a), indicating that the creep response of dough to increased salt content was similar to that of increased water content (Meerts et al., 2017). This has been interpreted as due to the added salt in a dough system occupying the sites on the surface of the gluten proteins, and thus decreasing the sites available for water to interact with; the increased amount of free water resulted in a weaker dough (Bushuk & Hlynka, 1964; Jekle & Becker, 2012).

2.1.3. Effects of Basic Ingredients on Dough Rheological Properties

Wheat flour dough (not containing yeast) primarily consists of wheat flour, water and salt. Each of those basic ingredients plays a variety of roles in the dough system to affect dough rheological properties and the quality of the final products. For example, the quality of a wheat flour directly determines the rheological properties of wheat flour dough (Khatkar et al., 1996; Lukie, 2001). Water exerts a softening effect on wheat flour dough due to its function as a mobility enhancer in a dough system (Baig & Hoseney, 1977; Farahnaky & Hill, 2007; Lang et al., 1992). Salt has an important effect on the rheological properties of dough due to the changes in gluten structure induced by salt addition (Belton, 2012; Eliasson & Larsson, 1993).

2.1.3.1. The Effect of Flour Quality on Dough Rheology

Wheat flour is the primary ingredient in a dough system. The rheological properties of wheat flour dough differed according to flour strength (Huang, Yun, Quail, & Moss, 1996; Miller & Hoseney, 1999; Pedersen et al., 2004). Flour strength parameters measured by a mixograph have been reported as indicators for breadmaking qualities of wheat flour (Khatkar et al., 1996). As such, the strength of the wheat flour demonstrates its applicability for breadmaking (Horvat et al., 2008; Kokelaar et al., 1996). For breadmaking, flours with suitable strength contribute to the development of doughs with good handling properties, which in turn produces breads with

desirable qualities, *i.e.*, fine crumb structure, high loaf height and volume (Tipples, Preston, & Kilborn, 1982). Due to the superior ability of stronger cultivars to produce good-quality breads (Huang et al., 1996), cultivar-dependent dough strength is important to consider for breadmaking (Edwards et al., 1999, 2001; Khatkar et al., 1996).

The viscoelastic behavior of gluten in wheat flour is indicative of the flour quality (Khatkar et al., 1995). Gluten is composed of glutenins and gliadins and these function in different ways to affect dough viscoelastic properties. Glutenins are responsible for dough elasticity (Bushuk, 1987; Khatkar et al., 1995; Spies, 1990), while gliadins are responsible for dough viscosity (Spies, 1990; Uthayakumaran, Gras, Stoddard, & Bekes, 1999). Therefore, a good balance of elasticity and viscosity of the dough depends on the ratio of glutenins to gliadins in the wheat flour. Unlike the gliadins that exist as monomers, glutenins are present as polymers bonded by disulfide crosslinks (Shewry & Jones, 2012). Glutenins consist of high molecular weight (HMW) and low molecular weight (LMW) subunits (Payne & Corfield, 1979; Shewry & Jones, 2012). HMW glutenin subunits play an important role in determining the breadmaking performance (*i.e.*, the strength and mixing properties) of a wheat flour (Bushuk, 1987; Shewry & Jones, 2012).

2.1.3.2. The Effect of Water Content on Dough Rheology

Wheat flour is mixed with water to form a dough. Water has a variety of functions in a dough system. For instance, water is a common solvent for salt, a medium for redox and enzymatic reactions, and a determinant of the conformation of proteins due to hydrogen bonding between water and proteins (Hoseney, 1986). As the dough is a polymeric system, water, due to a relatively higher mobility, performs as a mobility enhancer that is incorporated into the dough polymers to increase their extensibility, flexibility, or workability (Masi et al., 1998). With increasing water content, the average molecular weight of the polymer (*i.e.*, dough)-water mixture decreases, and

the mobility of this mixture increases (Ferry, 1961). Therefore, water has a positive effect on the mobility of dough polymeric system, leading to a decrease in dough's viscosity and resistance to mixing (Ferry, 1961; Masi et al., 1998). As such, the content of water in a dough exerts significant effects on dough rheology (Kamman, 1970).

An optimally-developed dough requires a certain amount of water that is dependent on the strength and the moisture content of the wheat flour (Kilborn & Tipples, 1981). This finding agrees with the observation that the amount of water added into a dough varies according to the quantity and quality of proteins in the wheat flour (Bushuk & Hlynka, 1964). Wheat flours with finer particle sizes required a greater amount of water to form a fully-developed dough, indicating that flour particle size was also a determinant of water addition to the dough (Bushuk & Hlynka, 1964). The optimal content of water for dough development is also determined by the content of salt in the dough system due to the interactions of proteins, water and salt in the dough (Bushuk & Hlynka, 1964; Spies, 1990). The farinograph has been used to determine the optimal water absorption of wheat flour (Gómez et al., 2011), *i.e.*, the amount of water required for a given weight of flour to form a dough with definite consistency, defined as the dough's farinograph absorption (FAB, % flour weight) (AACC International, 2011; Shuey, 1972). At a constant consistency of doughs, a higher FAB was seen for doughs mixed at a higher speed (Hlynka, 1962).

Water content in the dough has significant effects on dough rheological properties. As the water content was increased, dough resistance was seen to decrease from extensigraph measurements (Casutt et al., 1984), indicating a softening effect of water on dough. Water addition also led to a decrease in dough consistency measured by a farinograph, which is due to water-induced changes in the level of gluten hydration as well as the time required for all flour particles to be hydrated (Létang et al., 1999). In agreement with this study, a farinograph study on wheat

flour dough showed that increased water content from 50% to 74% softened the dough and prolonged the development time of dough (Farahnaky & Hill, 2007).

With an increase in water content from 42% to 47% in the dough, the *G'* and *G"* of dough decreased (Mani & Trligardh, 1992), indicating that water addition weakens wheat flour doughs. The weakening effect of water on dough is ascribed to the dual functions of water, *i.e.*, an inert component proportionally lowering the dough elasticity, and a lubricant promoting the relaxation of the flour-water system (Masi et al., 1998). An increased water content of 3% in the dough was seen to increase dough compliance by 13% (Manohar & Rao, 1999).

2.1.3.3. The Effect of Salt Content on Dough Rheology

Salt is an important ingredient for breadmaking. Not only is salt considered as a flavor enhancer for the final product, but also it affects the gas retention, increases the optimum mixing time and the stability of the dough (Eliasson & Larsson, 1993). An increase of salt (NaCl) content enhances the strength of gluten proteins (Belton, 2012). At higher NaCl conditions (0.5-1.0M), a higher charge density of the metal ion Na^+ promotes a water structure that is greatly oriented by the ion, which in turn retards the interactions between water and gluten and enhances the hydrophobic interactions between gluten proteins (Belton, 2012; Preston, 1985, 1989). The dough system has a pH of 5.5-6.0, which is below the average isoelectric point of gluten proteins (pH 7.5) (Miller & Hoseney, 2008). Accordingly, the gluten proteins have a net positive charge with a low charge density in this mildly acidic dough system. Adding NaCl to the dough system, due to the presence of the anion Cl^-, neutralizes the positively charged amino acids (*i.e.*, Lys, Arg, and His) on the surface of gluten proteins. This results in stronger hydrophobic interactions between gluten proteins (Preston, 1989) and in turn protein aggregation (Kim & Bushuk, 1995), and thus NaCl may strengthen the gluten network to some extent.

The salt-induced aggregation behavior of gluten is determined by polymeric gluten proteins, *i.e.*, glutenins (Arakawa & Yonezawa, 1975). As the content and molecular size distribution of glutenins determine the strength of gluten proteins exacted from different wheat cultivars (Gupta, Khan, & Macritchie, 1993; Isaak, 2019; Uthayakumaran et al., 1999), the sensitivity of gluten to NaCl addition is cultivar-dependent (Arakawa & Yonezawa, 1975; Huebner, 1970). Recently, it has been shown that the presence of NaCl during mixograph measurements helps discriminate wheat cultivars according to their gluten strengths (Isaak, Sapirstein, Wu, & Graf, 2019), suggesting the application of NaCl for better screening wheat cultivars according to their breadmaking strengths. However, it was also argued by Isaak et al. (2019) that salt's effects on dough strength of different cultivar samples during mixograph measurements were somewhat "unpredictable".

Hydrogen bonding between water and gluten proteins is believed to play an important role in determining dough strength as evinced by extensigraph studies of the effects of H_2O, D_2O, and NaCl on the maximum resistance (R_{max}, B.U.) of wheat flour dough (Tkachuk & Hlynka, 1968). From measurements on the "dough strength" parameter R_{max}, the change in R_{max} was seen with dough formulation, shown as D_2O+NaCl>D_2O>H_2O+NaCl>H_2O (Tkachuk & Hlynka, 1968). The increase in dough strength was attributed to a stronger hydrogen bonding induced by a combined addition of D_2O and NaCl in the dough (Tkachuk & Hlynka, 1968). In terms of the effects of NaCl on water-protein interactions as above, it indicates that NaCl interacts with water to affect dough strength.

2.1.4. Effects of Mixing on Dough Rheological Properties

An optimally-mixed dough has the following characteristics: 1) a homogenous mixture of flour and water; 2) a three-dimensional gluten network with a good capacity for gas retention; and 3) an appropriate incorporation of gas bubbles into the dough (Baig & Hoseney, 1977; Campos et al., 1997; Kilborn & Tipples, 1972; Larsen, 1964; Lee et al., 2001; Paredes-Lopez & Bushuk, 1982; Seabourn, Xie, & Chung, 2008). Mixing process parameters, *i.e.*, mixing time and work input, play important roles in the determination of dough rheology.

2.1.4.1. The Effect of Mixing Time on Dough Rheology

In the process of dough mixing, the shear and normal forces exerted on the dough make the gluten polymer partially unfold, resulting in changes in gluten structure and this in turn affects dough rheological properties (Lee et al., 2001). Before reaching the optimal development for the dough, increased mixing time is believed to strengthen the interactions between gluten proteins, leading to an increase in dough strength and maximum resistance to extension (Létang et al., 1999). After optimal dough development, longer mixing time was seen to decrease the molecular weight of glutenin polymers (Skerritt et al., 1999), contributing to a depolymerization process where the crosslinks (*i.e.*, disulfide bonds) of glutenin polymers break down with overmixing (Létang et al., 1999; Skerritt et al., 1999). In agreement, a lower viscosity was seen for the wheat proteins extracted from overmixed doughs due to the depolymerization of wheat proteins induced by overmixing (Danno & Hoseney, 1982b). From farinograph measurements, doughs made from stronger wheat flours exhibited a higher tolerance to overmixing compared to those made from weaker ones (Kilborn & Tipples, 1972).

Dynamic oscillatory rheometry and creep-recovery tests have been widely used for investigations of dough viscoelasticity with mixing time (Amemiya & Menjivar, 1992; Bohlin &

Carlson, 1980; Dreese et al., 1988; Gómez et al., 2011; Larsson et al., 2000; Lee et al., 2001; Létang et al., 1999; Mani et al., 1992; Mani & Trligardh, 1992; Meerts et al., 2017; Wehrle et al., 1997). With increasing mixing time before reaching the optimal development time, dough viscoelastic parameters increased, *i.e.*, storage modulus G' (Bohlin & Carlson, 1980; Gómez et al., 2011; Larsson et al., 2000), loss modulus G'' (Bohlin & Carlson, 1980), and complex modulus $G^* = (G'^2 + G''^2)^{1/2}$ (Amemiya & Menjivar, 1992; Lee et al., 2001). This phenomenon has been interpreted as gluten proteins becoming more evenly distributed during mixing until reaching optimal dough development, and this leads to stronger interactions between gluten proteins resulting in more elastic doughs (Amemiya & Menjivar, 1992). After reaching optimal dough development, further increases in mixing time led to a decrease in G' (Dreese et al., 1988; Mani et al., 1992; Mani & Trligardh, 1992) and G^* (Wehrle et al., 1997), but to an increase in tan δ (Létang et al., 1999; Mani et al., 1992; Mani & Trligardh, 1992). As such, overmixing increases dough softness and decreases dough elasticity (Mani et al., 1992; Mani & Trligardh, 1992; Wehrle et al., 1997). This finding may be attributed to the decrease in water-binding capacity of gluten with overmixing the dough, increasing the amount of released water that is responsible for a softer and less elastic dough (Dreese et al., 1988). In creep-recovery tests, overmixed doughs were determined to have a larger maximum recovery compliance and a longer retardation time (Meerts et al., 2017), indicating that overmixing causes the dough to be less elastic and relax slower.

2.1.4.2. The Effect of Mixing Work Input on Dough Rheology

The optimal development of a dough requires that the work input incorporated into the dough during mixing is greater than a minimum critical level (Kilborn & Tipples, 1972). To achieve optimal dough development, stronger wheat flours require a higher level of mixing work input compared to weaker ones (Kilborn & Tipples, 1972; Wilson, Wooding, & Morgenstern, 1997;

Zheng, Morgenstern, Campanella, & Larsen, 2000). Before reaching the critical level of work input for optimal dough development, increased mixing work input led to an increase in dough resistance to extension (Belton, 1999, 2012), indicating a strengthening effect of mixing work input on the dough. In agreement, a higher work input applied during dough mixing led to an increase in dough consistency measured by a farinograph (Skeggs & Kingswood, 1981). Regardless of the mixer type, the work input applied during dough mixing showed good correlations with farinograph parameters, *i.e.*, dough development time and dough stability (Wilson et al., 1997). After passing the critical level of work input for optimal dough development, increased mixing work input resulted in a decrease in dough resistance to extension (Belton, 2012; Peighambardoust, van der Goot, Boom, & Hamer, 2006), indicating a weakening effect on the dough induced by overmixing.

2.2. Studies on Gas Bubble Entrainment and Evolution in Bread Dough

2.2.1. The Rationale for Studying Dough's Gas Phase during Breadmaking

Gas bubbles play an important role in breadmaking (Chevallier, Zúñiga, & Le-Bail, 2012; Romano, Cavella, Toraldo, & Masi, 2013; Romano, Toraldo, Cavella, & Masi, 2007) as they contribute to approximately 9-20% of bread dough's total volume at the end of mixing (Marsh, 1998; Whitworth & Alava, 1999). Subdivision of gas bubbles that are entrained during mixing occurs throughout later breadmaking processes, *i.e.*, punching, sheeting and molding (Baker & Mize, 1941), leading to changes in the number and distribution of gas bubbles. The contribution of these bubbles to total gas volume increases towards the end of breadmaking, accounting for 70-75% at the end of proving, due to bubble inflation from CO_2 production by yeast (Campbell & Shah, 1999; Sroan, Bean, & MacRitchie, 2009). During baking, as temperature increases, gas in

the bubbles expands resulting in a final baked loaf containing 75-85% gas by volume (Campbell & Shah, 1999; Sroan et al., 2009).

The involvement of the gas phase in the mixing process of dough can be identified as three concurrent stages: gas entrainment, gas disentrainment and bubble break-up (Campbell et al., 1993; Campbell & Shah, 1999). A balance between entrainment and disentrainment of gas bubbles during mixing affects the volume of gas in the dough, *i.e.*, dough's void fraction (VF) (Campbell & Mougeot, 1999; Campbell & Shah, 1999), whereas bubble break-up together with entrainment and disentrainment affect the size distribution of bubbles in the dough (Chin, Martin, & Campbell, 2004; Martin, Chin, Campbell, & Morrant, 2004; Trinh, Lowe, Campbell, Withers, & Martin, 2013). Entrainment is defined as the process that entraps a certain volume of gas into the dough when surfaces of the dough approach each other and adjoin during mixing (Chin et al., 2004), indicating that there is a positive relationship between entrainment and VF. Disentrainment leads to the removal of gas in the dough, and thus it has a negative relationship with VF (Campbell & Mougeot, 1999; Chin et al., 2004).

In addition to their contribution to the dough volume, the presence of gas bubbles in dough also affects the volume, appearance, taste and texture of bread (Cauvain, Whitworth, & Alava, 1999; Demirkesen, Kelkar, Campanella, & Sumnu, 2014; Scanlon & Zghal, 2001). Obtaining an appealing cell structure in the bread crumb, *i.e.*, small cells (1 to 2 mm) within the crumb, requires not only a homogenous mixture of ingredients within the dough, but also an incorporation and subdivision of small-sized bubbles into the dough (Cauvain et al., 1999; Cauvain, 1998). During proving and baking, the growth and coalescence of gas bubbles cause further changes in the size distribution of bubbles and the total VF, and this in turn affects the cell structure of the resulting bread crumb (Babin et al., 2008; Scanlon & Zghal, 2001; Whitworth, 2008).

2.2.2. The Entrainment of Gas Bubbles in Dough during Mixing

Gas bubbles are entrained into the dough during the process of mixing (Baker & Mize, 1941). The rate of bubble entrainment varies at different mixing stages (Baker & Mize, 1946). During early stages of mixing, the entrainment of gas bubbles is relatively slow because the dough is still hydrating. Then the rate of bubble entrainment greatly increases until the dough reaches its maximum resistance to mixing (optimal development of gluten proteins). After maximum dough resistance to mixing is reached, the bubble entrainment rate decreases.

The final VF at the end of mixing is affected by mixing process parameters, *i.e.*, mixing speed, work input, mixer headspace pressure, and mixing time. For example, the VF of dough increases with increasing the mixing speed and work input (Chin & Campbell, 2005b), and with increasing the mixer headspace pressure (Campbell, Herrero-Sanchez, Payo-Rodriguez, & Merchan, 2001). It has also been shown that an increase in mixing time leads to an increase in VF as measured by dough density (Junge, Hoseney, & Varriano-Marston, 1981; Koksel & Scanlon, 2012; Mehta et al., 2009), ultrasonic studies (Mehta et al., 2009) as well as fluorescence fingerprint imaging analyses (Kokawa et al., 2012).

Entrainment of gas bubbles into a dough is also affected by ingredients (*e.g.*, flour type, and thus "dough strength", water and salt content). According to dough density measurements, doughs made from a stronger flour have higher density and thus a lower volume of gas bubbles entrained (Campbell et al., 2001). Dough density was also observed to increase with increasing water content in the dough (Koksel & Scanlon, 2012), indicating that higher water content doughs had a lower volume of gas bubbles entrained during mixing (Peighambardoust, Fallah, Hamer, & van der Goot, 2010). In terms of VF measurements, salt (NaCl) reduction leads to a higher volume of gas bubbles entrained into the dough (Bellido et al., 2006; Koksel et al., 2014).

The VF of dough, and how it is affected by mixing speed, mixing time, and ingredients, etc., influence dough's rheological properties (Chin et al., 2005b; Elmehdi, Page, & Scanlon, 2004), and the quality of products baked from it (Sapirstein, Roller, & Bushuk, 1994; Scanlon & Zghal, 2001; Zghal, Scanlon, & Sapirstein, 1999). Decreases in its elastic modulus and dough's resistance to extension were observed with increased VF, as measured by low-intensity ultrasonic (Elmehdi et al., 2004) and large-deformation biaxial extension (Chin et al., 2005a) measurement, respectively. The resistance of dough to biaxial extension positively correlated with the breadmaking performance of dough (Kokelaar et al., 1996), suggesting that a lower volume of gas bubbles entrained into the dough favors better bread quality. In line with these findings, excessive entrainment of gas bubbles into the dough was also reported to cause a poor cell structure within the bread crumb (Williams, 1975).

Bread dough has been characterized as a soft material consisting of three phases: 1) the hydrated semi-solid phase of the gluten-starch matrix; 2) the liquid phase that consists of free water and surface active materials (*e.g.*, soluble proteins); and 3) the gas phase (Gan et al., 1990; Gan, Ellis, & Schofield, 1995). By the end of mixing, individual small bubbles are entrained into the continuous network of gluten-starch matrix and the liquid phase of the dough (MacRitchie, 1976). During its early stages and until the end of proving, the gas bubbles are surrounded by both the gluten-starch matrix and the liquid phase. If the gluten-starch matrix has good extensibility, it reinforces the liquid phase so that bubble stability is increased (Bloksma, 1990a; Gan et al., 1990; MacRitchie, 1976). Towards the end of proving, the growth of gas bubbles results in discontinuous areas in the hydrated gluten-starch matrix leaving only the liquid phase as 'films' between growing bubbles (Gan et al., 1995). Although the original gluten-starch matrix around a given bubble may no longer be intact at the end of proving and the early stages of baking, the liquid films at the gas-

dough matrix interfaces are able to retain the integrity of gas bubbles (Gan et al., 1990, 1995). This allows release of gas from the dough to the surrounding atmosphere only at a critical point during baking (Mills, Wilde, Salt, & Skeggs, 2003), contributing to a bread loaf with a good volume and a uniform crumb cell structure (Gan et al., 1995; Hayman, Hoseney, & Faubion, 1998).

2.2.3. Factors Affecting Gas Bubble Stabilization

During breadmaking, any factor which affects the stability of gas bubbles in turn determines the cell structure of the resulting bread crumb (Hayman et al., 1998; Mills et al., 2003; Zghal et al., 1999). The stability of gas bubbles is affected by certain processes, *i.e.*, disproportionation, bubble growth and coalescence (Mills et al., 2003; Shah, Campbell, McKee, & Rielly, 1998; van Vliet, Janssen, Bloksma, & Walstra, 1992; van Vliet, 2008). Disproportionation is defined as the pressure-driven diffusion of gas from smaller-sized to larger-sized bubbles, causing larger-sized bubbles with smaller inner pressures to grow as the smaller-sized bubbles with higher inner pressures are consumed (Stevenson, 2010; van Vliet et al., 1992) (further explained in section 2.2.3.1). During breadmaking, bubble disproportionation starts right after mixing and continues during the early stages of proving (Mills et al., 2003; van Vliet et al., 1992). During proving and the early stages of baking, bubble growth occurs due to diffusion of CO_2 from the surrounding dough matrix into the bubbles and expansion of gas in the bubbles arising from increased temperature (Bloksma, 1990a, 1990b; Shah et al., 1998). During later stages of proving and baking, bubbles coalesce due to the rupture of the liquid films between bubbles (van Vliet et al., 1992; van Vliet, 2008).

2.2.3.1. Disproportionation

Disproportionation is a coarsening process arising from inter-bubble gas diffusion (Stevenson, 2010) as gas moves from smaller-sized to larger-sized bubbles (Mills et al., 2003).

The Young-Laplace equation (Eq. [9]) defines the pressure difference (ΔP) across a curved spherical surface (*i.e.*, between the inside and outside of a bubble) as:

$$\Delta P = \frac{2\gamma_s}{R} \quad [9]$$

where γ_s is the surface tension of the gas-dough matrix interface, and R is the bubble radius (Garrett, 1993; Mills et al., 2003; Stevenson, 2010). Compared to a larger-sized bubble, a smaller-sized bubble has a higher pressure difference between the inside and outside of the bubble, indicating that smaller-sized bubbles have higher inner pressures (Lemlich, 1978; Murray & Ettelaie, 2004).

According to Henry's law, the higher pressure in smaller-sized bubbles promotes a higher concentration of gas dissolved into the interfacial volume of dough around them, resulting in additional dissolved gas in the liquid phase of the dough. This concentration gradient leads to the diffusion of gas through the liquid phase of dough to regions of lower concentration that will be present in the environs of the larger-sized bubbles (van Vliet, 1999). As a result of gas diffusion, larger-sized bubbles keep growing, whereas smaller-sized bubbles shrink and ultimately disappear (Shimiya & Yano, 1987; Venerus, Yala, & Bernstein, 1998; Venerus & Yala, 1997). As such, disproportionation results in changes in the size and number of bubbles (Lemlich, 1978).

In a dough system, a significant reduction in the number of bubbles occurs due to disproportionation immediately after mixing (van Vliet et al., 1992). To maintain a sufficient number of bubbles in the dough during breadmaking processes, disproportionation needs to be prevented or retarded (Kokelaar et al., 1996; van Vliet, 2008). In a bread dough, at a constant strain rate (*i.e.*, bubble sizes increase constantly), as the strain increases (*i.e.*, a bubble grows in size), the stress required to deform the dough stretched around a bubble will be much larger than that required to deform a non-stretched dough, due to a phenomenon called strain hardening (Kindelspire, Glover, Caffé-Treml, & Krishnan, 2015; van Vliet et al., 1992; van Vliet, 1999).

This indicates that the stress around a growing larger-sized bubble would be greater than that around a smaller-sized bubble, limiting the further growth of bubbles that are stretched substantially (Dobraszczyk & Roberts, 1994; Kokelaar et al., 1996). This in turn decreases the driving force for gas transport between different sized bubbles (van Vliet, 1999, 2008), leading to slower disproportionation and increased bubble stability during breadmaking (Kokelaar et al., 1996; van Vliet & Kokelaar, 1994; van Vliet, 1999). Biaxial extension tests have been conducted showing that doughs made from stronger wheat cultivars and lower water content have higher strain hardening values against disproportionation (Janssen et al., 1996; Kokelaar et al., 1996; Sliwinski, Kolster, & van Vliet, 2004).

Increasing the concentration of surface active materials (*e.g.*, proteins and lipids) in a dough formulation has been observed to decrease the rate of gas diffusion between bubbles (Lucassen, 1981; Quoc, Zitha, & Currie, 2002) and thus slow down disproportionation, through their role in reducing surface tension at a bubble interface (Kokelaar & Prins, 1995). Proteins are able to form macromolecular films at the bubble-protein interfaces. Due to a relatively high viscosity and elasticity of these films, proteins are considered good examples of surface active materials that form a strong interfacial network (Martin, Grolle, Bos, Cohen Stuart, & Van Vliet, 2002; Walstra, 2003) and increase bubble stability against disproportionation (Murray & Ettelaie, 2004). However, it should be pointed out that disproportionation in such a situation is retarded only if the decrease in bubble surface tension is greater than the reduction in bubble radius (Lucassen, 1981; Meinders & Van Vliet, 2004; van Vliet et al., 1992).

2.2.3.2. Bubble Growth

In yeasted doughs, bubble growth is induced by yeast fermentation. As yeast produces CO_2, the concentration of CO_2 in the dough matrix increases (Mills et al., 2003; Shah et al., 1998). Since

no new bubbles are entrained after mixing , according to Henry's law, CO_2 solubilized in the liquid phase of the dough diffuses through to the bubble-dough matrix interface, and desorbs to cause an increase in the partial pressure of CO_2 inside the bubbles (Amon & Denson, 1984). To achieve mechanical equilibrium between the inside and outside of the bubbles, bubbles grow in size (Amon & Denson, 1984).

One of the factors that affects this CO_2 diffusion-induced bubble growth is dough rheology around a growing bubble (Shimiya & Yano, 1987; Venerus et al., 1998; Venerus & Yala, 1997; Venerus, 2001, 2015). By taking the biaxial extensional properties of dough into account, a gas bubble growth model has been developed to predict the increase in dough volume during proving (Huang & Kokini, 1999). Higher biaxial extensional viscosity of dough increases the resistance of bubbles to grow (Huang & Kokini, 1999). Dough's strain hardening properties has also been reported to play an important role during bubble growth (Huang & Kokini, 1999; van Vliet & Kokelaar, 1994), *i.e.*, doughs with higher strain hardening values have shown lower bubble growth rates (Kokelaar et al., 1996).

The rate of bubble growth is also affected by yeast concentration (Chiotellis & Campbell, 2003a, 2003b; Shah et al., 1998). Changes in the bubble size distribution (BSD) was modeled to show an increase in the rate of bubble growth with increasing the yeast concentration in the dough (Chiotellis & Campbell, 2003a). Increased yeast concentration increases the concentration of CO_2 that is dissolved in the dough liquid phase surrounding the bubbles, which promotes the mass transport of CO_2 into the bubbles and increases bubble growth rate during proving (Chiotellis & Campbell, 2003b).

2.2.3.3. Coalescence

Due to increased concentration of CO_2 by yeast activity and increased desorption of water vapor due to the temperature rise, bubbles expand more rapidly during the early stages of baking (Mills et al., 2003). Meanwhile, gas volume fraction in the dough increases and thus bubbles become polyhedral with their surfaces separated by only thin layers of liquid films (Gan et al., 1990, 1995). As the liquid film between two bubbles thins further, the distance between the two bubbles decreases; while the attractive van der Waals forces between the two bubble-liquid interfaces increase, steric and electrostatic repulsive forces between the two bubble-liquid interfaces decrease (Örnebro, Nylander, & Eliasson, 2000; Walstra, 1989). When the repulsive forces are no longer able to maintain separation between the two bubbles and the liquid film fails to maintain its expansion rate the same as the bubble growth rate, this film ruptures so that the two bubbles coalesce (Babin et al., 2006; Örnebro et al., 2000; Shehzad et al., 2010; van Vliet et al., 1992).

As a result of bubble coalescence at the surface of the dough, some gas is lost to the atmosphere during breadmaking, resulting in a lower loaf volume (van Vliet et al., 1992). Extensive coalescence of bubbles in the interior of the dough results in a broad and uneven distribution of gas cells within the bread crumb (Hayman et al., 1998; Scanlon & Zghal, 2001; van Vliet et al., 1992; Zghal, 2001). Accordingly, for a good loaf volume with an even crumb structure, bubble coalescence needs to be prevented. One way to prevent bubble coalescence, and to increase bubble stability, is to improve the properties of the film at the bubble-dough matrix interface (Mills et al., 2003), through manipulation of bulk or surface rheological properties (Dobraszczyk & Roberts, 1994; Kokelaar & Prins, 1995; Kokelaar et al., 1996; van Vliet et al., 1992). A higher strain hardening value of the dough (Dobraszczyk & Roberts, 1994; Kokelaar et al., 1996; van

Vliet et al., 1992) and higher concentration of surface active materials in the dough (Hu, Nienow, & Pacek, 2003; Örnebro et al., 2000) have been reported to increase bubble stability against coalescence.

2.2.4. Evolution of Gas Bubbles in Dough during Breadmaking

Evolution of gas bubbles in dough, both their size and number, is affected by the concentrations of water, yeast and endogenous lipids in the flour (Sahi, 1994; Sroan et al., 2009; Upadhyay et al., 2012). A decrease in water content leads to a decrease in the size of bubbles (Upadhyay et al., 2012). During proving and baking, the expansion of bubbles is delayed for doughs made from the wheat cultivar with a higher content of endogenous lipids (Sahi, 1994). An increased content of added lipids has been reported to reinforce the dough liquid film around bubbles, contributing to the stabilization of expanding bubbles and the improvement in dough's breadmaking performance (Sroan et al., 2009). Evolution of gas bubbles, and the resulting loaf volume and crumb cell structure in parallel, is affected by wheat cultivar (Campbell et al., 2001; He & Hoseney, 1991; Whitworth & Alava, 1999). For example, doughs made from a stronger wheat flour are better at retaining the gas during breadmaking so that a higher volume of loaf is produced (He & Hoseney, 1991; Zghal, Scanlon, & Sapirstein, 2001).

2.2.5. Bubble Size Distribution (BSD) and its Evolution in Bread Dough

As the gas phase of the dough at the end of mixing, and how it evolves during later breadmaking processes, directly influences crumb cell structure and loaf volume (Gan et al., 1995; Mills et al., 2003), investigations of the BSD and its evolution in bread dough is of utmost importance to provide strategies for improvement of the quality of bakery products (Lim & Barigou, 2004; Örnebro et al., 2000; Scanlon & Zghal, 2001). Changes in the gas phase of the dough during breadmaking can be studied by investigations of the gas void fraction (VF) of the

dough and the BSD (Campbell, Rielly, Fryer, & Sadd, 1991; Örnebro et al., 2000; van Vliet, 2008). The VF of dough can easily be determined from dough density measurements (Campbell et al., 2001; Leroy et al., 2008). However, the BSD of dough is much more challenging to obtain due to the fragility and opacity of dough (Bellido et al., 2006; Campbell et al., 1991).

2.2.5.1. Definition of BSD

The number distribution of bubbles in dough per unit volume, *i.e.*, the BSD, can be expressed using two parameters, *i.e.*, the mean bubble diameter (D'), and the standard deviation (s) of the distribution, *i.e.*, the spread of bubble sizes in the dough (Campbell et al., 1991; Monsalve & Schechter, 1984):

$$D' = \frac{\sum_{i=1}^{c} N_v(i) D_{mi}}{N_v} \quad [10]$$

$$s = \frac{\sum_{i=1}^{c} N_v(i)(D_{mi} - D')^2}{N_v} \quad [11]$$

where i is a bubble size class from 1 to c, c is the total number of bubble size classes, N_v is the total number of bubbles per unit volume of the dough, $N_v(i)$ is the number of bubbles at the i^{th} size class per unit volume of the dough, D_{mi} is the average of D_{i-1} (the smallest bubble diameter in the bubble size class of i) and D_i (the largest bubble diameter in the bubble size class of i). Although these two parameters provide information on the average bubble size and the dispersion of bubble sizes compared to the mean (Campbell et al., 1991), they are not able to sufficiently characterize the numbers and sizes of bubbles in dough. In order to fully describe the BSD over a wide range of size classes, the use of a statistical function (*i.e.*, a probability density function) (Proussevitch, Sahagian, & Carlson, 2007b) secures the capture of all the experimental data. In the literature, both normal and lognormal probability density functions have been used to characterize the BSD in dough (Koksel, 2014).

2.2.5.1.1. Normal Distribution

To characterize the BSDs, the normal (Gaussian) distribution is the most widely used probability density function (Mathai & Pederzoli, 1977; Forbes, Evans, Hastings, & Peacock, 2017). For a normally distributed random variable y, the probability density function of y is

$$f(y) = \frac{1}{\sqrt{2\pi}\sigma_n} \exp\left[\frac{-(y-\mu)^2}{2\sigma_n^2}\right] \quad [12]$$

where μ is the mean, and σ_n is the standard deviation of the normal distribution (Mathai & Pederzoli, 1977).

2.2.5.1.2. Lognormal Distribution

The lognormal distribution has been commonly used for characterizing the size distribution of bubbles or cells in non-food materials, *i.e.*, vocanic rocks (Proussevitch, Sahagian, & Carlson, 2007a; Proussevitch et al., 2007b) and liquid foams (Lachaise, Sahnoun, Dicharry, Mendiboure, & Salager, 1991; Magrabi, Dlugogorski, & Jameson, 1999), and food materials, *i.e.*, cocoa press cakes (Limpert, Stahel, & Abbt, 2001). The lognormal distribution is defined as the distribution of a positive random variable x whose logarithm is normally distributed (Shimizu & Crow, 1988). As such, x is lognormally distributed if $y = \ln x$ is normally distributed with a mean μ and a standard deviation ε. For a lognormally distributed random variable x, the probability density function of x is (Shimuzu & Crow, 1988):

$$f(x) = \frac{1}{\sqrt{2\pi}\varepsilon x} \exp\left[\frac{-(\ln x - \mu)^2}{2\varepsilon^2}\right] \quad [13]$$

where $\exp \mu$ is equal to the median of the lognormally distributed x.

During dough mixing, a subdivision of gas bubbles makes their sizes geometrically proportional, resulting in a lognormal BSD (Bellido et al., 2006; Shimiya & Nakamura, 1997). For modeling the lognormal BSD in dough, the probability density function is expressed as:

$$f(R) = \frac{1}{\sqrt{2\pi}\varepsilon R} \exp\left(\frac{-\ln (R/R_0)^2}{2\varepsilon^2}\right) \quad [14]$$

where R is the bubble radius, R_0 is the median of the bubble radii, and ε is the width of the BSD (Bellido et al., 2006; Shimiya & Nakamura, 1997). This lognormal distribution function has been used to characterize the BSD in noodle doughs and non-yeasted doughs shortly after mixing (Guillermic et al., 2018; Koksel et al., 2016).

2.2.5.2. Determination of BSD in Bread Dough

Investigations of the BSD in bread dough have been conducted using various imaging techniques. For example, microscopy (Upadhyay et al., 2012), magnetic resonance imaging (MRI) (De Guio, Musse, Benoit-Cattin, Lucas, & Davenel, 2009; van Duynhoven et al., 2003), and X-ray microtomography (X-MT) (Babin et al., 2006; Bellido et al., 2006; Koksel et al., 2016; Shehzad et al., 2010; Trinh et al., 2013; Turbin-Orger et al., 2012, 2015).

2.2.5.2.1. Microscopy

Microscopy is a widely used imaging technique for investigations of food structure (Kaláb, Allan-Wojtas, & Miller, 1995). The BSD in bread dough has been investigated using microscopic techniques, including light microscopy (LM) (Campbell et al., 1991; Carlson & Bohlin, 1978; Shimiya & Nakamura, 1997), scanning electron microscopy (SEM) (Whitworth & Alava, 1999), and confocal laser scanning microscopy (CLSM) (Upadhyay et al., 2012). These microscopic techniques differ in their illumination source, *i.e.*, a beam of visible light for LM, a beam of electrons for SEM, and a laser beam for CLSM (Falcone et al., 2006). These techniques require an element that focuses the illumination source onto the tested sample, and an image generator that records the sample information (Falcone et al., 2006).

Light microscopy (LM) was used to study the BSD in dough slices (30 μm of thickness), the bubble diameters were measured (Carlson & Bohlin, 1978), and their distribution was fitted

using a function with one parameter, *i.e.*, the mean bubble diameter (Carlson & Bohlin, 1978). A mean bubble surface area of 41 cm^2 per cm^3 of the dough was reported (Carlson & Bohlin, 1978). However, bubbles with diameters smaller than 45 μm were not counted due to the limitation in the resolution of LM. When measuring the BSD in frozen dough slices (also 30 μm of thickness), LM was used to enable the measurement of bubbles corresponding to diameters as small as 39 μm (Campbell et al., 1991). This work provided a higher resolution for BSD determination compared to the work conducted by Carlson & Bohlin (1978). However, both studies were conducted on dough slices, resulting in damage to the dough structure and in turn changes to the fragile gas phase of dough.

Compared to previous studies of BSD in doughs (Campbell et al., 1991; Carlson & Bohlin, 1978), a LM with higher resolution was used to measure bubbles as small as 3 μm in diameter (Shimiya & Nakamura, 1997). The BSD was characterized with a lognormal distribution function using two parameters, *i.e.*, the median bubble size and the standard deviation of the distribution (Shimiya & Nakamura, 1997). Immediately after mixing unyeasted dough, the median bubble diameter was measured as 15 μm, whereas it increased to 38 μm due to disproporionation during 160 min resting of the dough (Shimiya & Nakamura, 1997). Over this period, the width of the BSD slightly decreased from 0.18 to 0.16 (Shimiya & Nakamura, 1997).

In addition to LM, scanning electron microscopy (SEM) and X-ray computerized tomography (X-CT) were used to measure the evolution of bubble sizes during breadmaking (Whitworth & Alava, 1999). A combined use of LM (bubble diameters of 20 to 1500 μm), SEM (bubble diameters of 20 to 1500 μm), and X-CT (bubble diameters larger than 1000 μm) aimed to investigate a wide range of bubble sizes due to their evolution throughout breadmaking processes (Whitworth & Alava, 1999). At the end of mixing, the entrained bubbles in dough were reported

to have a maximum diameter of 2500 μm (Whitworth & Alava, 1999). Due to considerable expansion of bubbles during proving, a doubling in the maximum bubble diameter was observed at the end of proving (Whitworth & Alava, 1999).

Confocal laser scanning microscopy (CLSM) was used to investigate the evolution of bubbles in yeasted doughs during breadmaking (Heertje, Vlist, Blonk, Hendrickx, & Brakenhoff, 1987). Bread dough was prepared by mixing wheat flour with water, yeast and a fluorescent die to label proteins and starch (Heertje et al., 1987). In the CLSM images, gas bubbles (darker color) were easily identified (qualitatively) in the protein-starch matrix (strong-faint fluorescence). The increase in dough volume was also observed as a result of bubble expansion during proving (Heertje et al., 1987). Unlike previous CLSM studies that did not quantify the size distribution of bubbles (Heertje et al., 1987; Thorvaldsson, Stading, Nilsson, Kidman, & Langton, 1999), Upadhyay et al. (2012) acquired the BSD by tabulating the frequency of bubble sizes in an ascending order of diameters, and then grouping them into 10 μm-wide size classes. Rather than using a normal or lognormal probability density function for fitting to the BSD, they calculated the average and standard deviation of bubble diameters in the dough, and used them for describing the BSD of the dough (Upadhyay et al., 2012).

2.2.5.2.2. Magnetic Resonance Imaging

Magnetic resonance imaging (MRI) is a non-destructive imaging technique that is widely used for medical diagnosis and analysis of food materials (Rouillé, Bonny, Della Valle, Devaux, & Renou, 2005; Takano, Ishida, Koizumi, & Kano, 2002). Using MRI, the internal structure of soft materials can be investigated (Takano et al., 2002). An MRI scanner takes advantage of radio frequency waves and strong magnetic fields. In a strong magnetic field, certain atomic nuclei, such as hydrogen atoms, absorb or emit energy at radio frequencies (van Duynhoven et al., 2003). As

hydrogen atoms are abundant in biological materials like bread dough, a density map of hydrogen atoms based on their alignment in the magnetic field, and their relaxation once the magnetic field is removed, is obtained (Falcone et al., 2006). This 2D density map of hydrogen atoms in bread dough can be used to depict the inner structure of the dough (Rouillé et al., 2005; Takano et al., 2002), *i.e.*, the gray level of a voxel in an MRI image can be used to quantify the volume of gas bubbles in the dough (Grenier, Lucas, Collewet, & Le Bail, 2003).

The MRI images of frozen and non-frozen doughs were used to depict the evolution of bubble sizes during proving, and to link the growth of bubble sizes with the development of the gluten network during punching and molding (Takano et al., 2002). A larger number of bubbles and a better developed gluten network have been observed in non-frozen doughs, and these favor bubble stability during dough expansion and a good crumb cell structure (Ishida et al., 2001; Takano et al., 2002). A combination of MRI and digital image analysis (DIA) was used to investigate the effect of flour components on the growth of gas bubbles in dough during proving and the crumb cell structure of the resultant breads (Rouillé et al., 2005). Bubble sizes in the dough and gas cell sizes in the crumb were quantified from 2D MRI images to confirm that with increasing the endogenous soluble fractions (*i.e.*, low-molecular-weight sugars, pentosans and soluble proteins like globulins and albumins in the flour) in the dough, the bubble growth rate increased and the crumb structure became coarser (Rouillé et al., 2005).

MRI combined with DIA was also used to show that molding and kneading processes produce a more homogeneous distribution of bubble sizes in the dough (van Duynhoven et al., 2003). BSDs in non-yeasted and yeasted doughs at the early stages of proving were seen to fit well to a normal distribution (De Guio et al., 2009). MRI was also used to investigate the effect of dough composition on the number and size evolution of bubbles during proving (Bonny et al.,

2004). The BSD in different doughs was determined during proving and larger bubble diameters were observed for defatted doughs when compared to regular doughs (Bonny et al., 2004). The time-dependent evolution of BSD in dough during proving was also determined using MRI and DIA (Bajd & Serša, 2011). As the proving time increased, the mean bubble size shifted towards the larger bubble sizes as expected (Bajd & Serša, 2011).

2.2.5.2.3. X-Ray Microtomography

X-ray microtomography is a non-destructive imaging technique that is widely used for medical diagnosis and biological material microstructure characterization (Fitzgerald, 2000; Gundogdu, Nirgianaki, Che Ismail, Jenneson, & Bradley, 2007; Karunakaran et al., 2015; Kashyap et al., 2008). During imaging by X-ray microtomography, the X-ray beam and radioscopic detector are located at opposite sides of the sample being tested (Falcone et al., 2006). The X-ray beam focuses on the sample located at a rotation stage and the radioscopic detector determines the attenuation of X-rays passing through the sample along various beam paths and directions as the sample is rotated (Barigou & Douaire, 2013; Lim & Barigou, 2004). Higher density materials attenuate X-rays to a higher degree, leading to brighter regions in the resultant X-ray radiograph (Falcone et al., 2006). A continuous series of 2D radiographs are produced for different viewing angles of the sample (Falcone et al., 2006). By mapping the X-ray attenuation, a reconstruction step using a computer converts the 2D radiographs into a 3D volume of interest in the sample (Barigou & Douaire, 2013; Falcone et al., 2006; Martz, Logan, Schneberk, & Shull, 2017).

The source of X-ray beam, *i.e.*, lab-scale X-ray source (Pinzer et al., 2012; Trater, Alavi, & Rizvi, 2005), *vs.* synchrotron X-ray source (Babin, Della Valle, Dendievel, Lourdin, & Salvo, 2007; Maire et al., 2003), determines the resolution limit of the images obtained by the X-ray microtomography (Barigou & Douaire, 2013; Falcone et al., 2006). A synchrotron is a type of

charged particle accelerator, which can accelerate electrons up to the speed of light (Martz et al., 2017). Compared to lab-scale sources, synchrotron radiation sources produce a much larger density of photon flux and thus substantially higher intensity and brightness of the X-rays (Babin et al., 2006, 2008; Falcone et al., 2006). As such, synchrotron X-ray microtomography provides higher-resolution (*i.e.*, smaller size of a pixel or voxel) images for a shorter scanning time.

Lab-scale X-ray microtomography has been used to investigate the evolution of gas bubbles in doughs during breadmaking (Bellido et al., 2006; Trinh et al., 2013; Whitworth, 2008). At a spatial resolution of 10 μm per pixel, the median diameter of lognormal BSD was determined as 100.00 ± 1.79 μm for a "stiff" dough formula of 63 % water and 2.4 % NaCl, flour weight basis and 109.30 ± 1.62 μm for a "slack" dough formula of 67.4 % water and 0.75 % NaCl, flour weight basis (Bellido et al., 2006). This indicates that increased water content and decreased salt content in the dough leads to a shift of the median of BSD towards larger bubble sizes.

The size distribution and connectivity of gas cells within bread crumb have been investigated using lab-scale X-ray microtomography (Demirkesen, Kelkar, Campanella, & Sumnu, 2014; Lampignano, Laverse, Mastromatteo, & Del Nobile, 2013; Wang, Austin, & Bell, 2011). A larger number of smaller-sized gas cells was associated with a finer crumb structure of gluten-free breads (Demirkesen et al., 2014) and a firmer texture of regular breads (Lampignano et al., 2013).

Due to its higher resolution than lab-scale X-ray microtomography, synchrotron X-ray microtomography has been used for qualitative and quantitative studies of the size distribution and rapid evolution of gas bubbles in the dough during breadmaking as well as the crumb cell structure of breads. BSDs in non-yeasted bread and noodle doughs were measured using synchrotron X-ray microtomography at a spatial resolution of 8.75 μm per pixel, and BSDs were fitted well to a lognormal distribution function (Guillermic et al., 2018; Koksel et al., 2016). With pixel

resolutions of 15 μm (Babin et al., 2006; Turbin-Orger et al., 2015) and 5 μm (Turbin-Orger et al., 2012, 2015), synchrotron X-ray microtomography was used to assess the growth of bubble sizes in dough during proving and show that there was an increase in bubble sizes as a function of proving time. The mean bubble diameter was seen to increase from 410 μm to 675 μm over 140 min (Turbin-Orger et al., 2012). With pixel resolutions of 14 μm (Falcone et al., 2004, 2005) and 10 μm (Babin et al., 2005; Lassoued et al., 2007), synchrotron X-ray microtomography has also been used to measure the size distribution of gas cells in bread crumb. As the mean gas cell diameter decreased from 1.47 to 1.12 mm due to the use of different dough formulations, the value of crumb fineness index (the higher the index, the higher the number of small cells in the crumb) increased (Lassoued et al., 2007). These results indicate that a distribution of smaller-sized bubbles in the dough favors a finer crumb in the bread.

2.2.6. Effects of Basic Ingredients on the Gas Phase of the Dough

In non-yeasted doughs, the number and size distribution of bubbles at the end of mixing depend on the type of wheat flour (Chin & Campbell, 2005b) and other ingredients, *i.e.*, the content of water and salt (Bellido et al., 2006; Chin, Campbell, et al., 2005; Koksel & Scanlon, 2012; Koksel et al., 2014; Thorvaldsson et al., 1999), and shortening (Mehta et al., 2009). During proving, the evolution of bubble sizes in dough not only depends on these basic ingredients, but also on leavening agents (Bellido, Scanlon, & Page, 2009), surface active materials (Campbell et al., 2001), and sugar (Shehzad et al., 2010; Turbin-Orger et al., 2012, 2015).

2.2.6.1. The Effect of Flour Quality on Gas Bubble Entrainment and Evolution

The effects of flour type on the entrainment of gas bubbles differ due to the difference in breadmaking strength between wheat cultivars (Campbell et al., 2001, 1993; Chin & Campbell, 2005b). From dough density measurements, doughs made from a stronger wheat cultivar have

been observed to entrain a higher volume of gas bubbles (Campbell et al., 2001, 1993; Chin & Campbell, 2005b). Increased gluten content in the dough was seen to increase dough's VF (Koksel & Scanlon, 2012). Thus, wheat flour with higher gluten content is considered to produce doughs with a higher volume of gas bubbles entrained.

Evolution of bubble sizes in the dough during breadmaking is also affected by the flour type. The baking performance of flour, that determines the gas retention ability of the dough and the volume of the resultant loaf, differs due to the wheat cultivar (He & Hoseney, 1991, 1992). The volume and height of dough have been determined during breadmaking to show that the rate of bubble expansion is increased if a wheat cultivar with better baking performance is used (He & Hoseney, 1991, 1992). Doughs made from wheat flours with better baking performance have also been shown to possess better strain hardening properties (Kokelaar et al., 1996). A higher strain hardening value of the dough contributes to bubble stability against disproportionation or coalescence during breadmaking (Dobraszczyk & Roberts, 1994), results in the equal growth of bubbles during proving, and produces a loaf with higher volume (Sroan et al., 2009).

The stability of gas bubbles is increased if the surface tension of the bubble interface is decreased (Kokelaar & Prins, 1995). A lower surface tension of bubbles has been observed in doughs made from wheat cultivars with a higher content of endogenous soluble proteins and lipids (Sahi, 1994), indicating that increased content of proteins and lipids in the dough increases bubble stability, and thus enhances dough's gas retention capacity during breadmaking. With increasing content of soluble proteins and/or increasing content of lipids, the specific volume of dough (*i.e.*, the reciprocal of density) increased due to a better gas retention capacity of dough and a higher rate of bubble growth during proving (Rouillé et al., 2005).

2.2.6.2. The Effect of Water Content on Gas Bubble Entrainment and Evolution

An increase in water content has been shown to cause an increase in dough development time (D'Appolonia & Gilles, 1971), resulting in a higher volume of gas bubbles entrained into the dough due to a longer time of mixing (Chin, Campbell, et al., 2005; Mastromatteo et al., 2013). In addition to the effect on initial bubble entrainment during mixing, water content has an effect on bubble growth during the later stages of breadmaking (Peighambardoust et al., 2010). When dough volume was measured as a function of proving time, increased water content from 50 to 54.5 % in wheat flour dough was seen to decrease the rate of bubble expansion at the later stages of proving (Peighambardoust et al., 2010). Throughout dough proving, the retarding effect of increased water content on bubble expansion was more noticeable for doughs made from flours with higher farinograph absorption (FAB) (Peighambardoust et al., 2010; Unbehend, Lindhauer, & Meuser, 2004), indicating that this water-induced decrease in bubble expansion rate is wheat flour dependent.

2.2.6.3. The Effect of Salt Content on Gas Bubble Entrainment and Evolution

Increased salt (NaCl) content in dough has been observed to increase dough density at the end of mixing (Chin, Campbell, et al., 2005; Koksel et al., 2014), indicating that increased salt content decreases the volume of gas bubbles entrained into the dough during mixing. The negative effect of increased salt content on gas bubble entrainment is attributed to NaCl-induced changes in the protein network (Beck et al., 2012b). The Na^+ and Cl^- ions shield the positive charges on the surface of the gluten proteins, reducing the repulsive forces between them (Beck et al., 2012b), so that increased salt content promotes hydrophobic interactions between gluten proteins, allowing them to approach each other (Miller & Hoseney, 2008; Preston, 1981). The increase in protein-protein interactions reduces the surface sites of gluten proteins available for water molecules to

interact with, and thus slows down flour hydration and results in longer mixing times to achieve optimal dough development (Farahnaky & Hill, 2007; Hlynka, 1962). When the mixing development time of dough is fixed (as opposed to mixing until optimal development), higher salt content doughs are relatively less developed, resulting in a lower volume of gas bubbles entrained (Koksel & Scanlon, 2012).

An ultrasonic transmission technique has been used to measure BSDs in doughs varying in formulation, and the BSDs have been fitted with a lognormal distribution (Koksel et al., 2014; Leroy et al., 2008). The evolution of BSD was investigated by measuring the median bubble size and the width of lognormal distribution function fitted to BSD (Koksel et al., 2014; Leroy et al., 2008). With increasing the salt content from 0.8 to 2.4%, the median bubble radius decreased and the width of the BSD increased for well-aged doughs (Koksel et al., 2014). This finding agrees with an observation by X-ray microtomography measurements that higher salt content results in a smaller median bubble diameter and larger width for the BSD in non-yeasted doughs (Bellido et al., 2006). This salt-induced decrease in median bubble size indicates that increased salt content retards or prevents disproportionation in the dough. This effect is attributed to a reduction in the surface tension and an increase in the stability of bubbles in the liquid phase of the dough (Salt et al., 2006).

The expansion and retention of gas bubbles in yeasted doughs have been investigated by examining the maximum dough height as a function of proofing time using a Chopin rheofermentometer (Lynch et al., 2009). Increased salt content (from 0, 0.3, 0.6, to 1.2% NaCl) has been shown to lower the maximum dough height (Lynch et al., 2009), indicating that increased salt content decreases the expansion rate of gas bubbles (Calderón-Domínguez, Farrera-Rebollo, Arana-Errasquín, & Mora-Escobedo, 2005). The retarding effect of increased salt content on

bubble expansion has been attributed to the salt-induced inhibition of yeast activity (Lynch et al., 2009; R. A. Miller & Hoseney, 2008). Increased NaCl content hinders the metabolic activity of yeast due to an increase in osmotic pressure that causes water loss in yeast cells (Hutton, 2002).

2.2.7. Effects of Mixing on Gas Bubble Entrainment in Bread Dough

The effect of mixing process parameters on gas entrainment in bread dough has been investigated using dough density measurements (Campbell et al., 2001, 1993; Chamberlain, Collins, & Redman, 1970; Chin & Campbell, 2005a, 2005b; Chiotellis & Campbell, 2003b) and ultrasonic studies (Elmehdi et al., 2004; Mehta et al., 2009). The mixing time and work input have been shown as two important factors that affect the volume of gas bubbles entrained into the dough.

2.2.7.1. The Effect of Mixing Time on Gas Bubble Entrainment

Increased mixing time has been observed to enhance the entrainment of gas bubbles into the dough (Koksel & Scanlon, 2012; Mehta et al., 2009), resulting in a higher gas volume fraction (VF) in doughs (Campbell et al., 1998; Koksel & Scanlon, 2012). This finding is also confirmed by low-frequency (50 kHz) ultrasonic investigations that showed an increase in the attenuation coefficient (indicative of an increase in VF) of dough is observed when a longer mixing time is used (Mehta et al., 2009).

Digital image analysis (DIA) has been used to determine the relationship between mixing time and the bubble volume fraction in the dough (Kokawa et al., 2012; Trinh et al., 2013). When doughs were prepared at mixing times of 1 min (under-mixing), 2 min 30 s (optimal-mixing) and 7 min (over-mixing), the ratio of total bubble area to total dough volume was ranked as: under- < optimal- < over-mixed doughs (Kokawa et al., 2012). The mean bubble size of the BSD was also shown to shift towards larger bubble sizes as dough's mixing condition changed from under- to

over-mixing (Kokawa et al., 2012). Using X-ray tomography, the volume of gas bubbles in the dough was seen to increase with increasing mixing time (Trinh et al., 2013).

The relationship between mixing time and the size distribution of gas cells in bread crumb has been investigated using DIA (Crowley, Grau, & Arendt, 2000). Compared to the over-mixed doughs, optimally-mixed doughs resulted in bread crumb with a higher number of smaller-sized gas cells (Crowley et al., 2000), suggesting that optimal mixing time favors a finer bread crumb.

2.2.7.2. The Effect of Mixing Work Input on Gas Bubble Entrainment

From dough density measurements, an increase in the volume of gas bubbles entrained into the dough has been observed if a higher level of mixing work input is used to mix the dough until its optimal development (Chin & Campbell, 2005b). Overmixing weakens the ability of dough to entrain gas bubbles and results in a lower gas volume fraction (VF) in the dough at the end of mixing (Chin & Campbell, 2005b). The response of dough's VF to mixing work input has been reported to differ according to the wheat cultivar (Chin & Campbell, 2005b).

Using DIA, the level of mixing work input has been observed to affect the BSD in the dough after mixing (Kansou et al., 2013) and the bubble stability during proving (Shehzad et al., 2010). The size distribution of gas bubbles in the dough was modeled to show that a higher level of mixing work input resulted in a larger number of smaller-sized bubbles entrained and a more homogenous distribution of bubble sizes (Kansou et al., 2013). As a result, increased mixing work input for dough preparation may increase bubble stability against disproportionation or coalescence in the dough (Shehzad et al., 2010). This finding is possibly due to a better development of the gluten network and a higher strain hardening value of the dough (Dobraszczyk & Roberts, 1994; van Vliet et al., 1992; van Vliet, 2008) that is induced by a higher level of mixing work input.

3. The Effects of Sodium Reduction on the Mechanical Properties of Doughs Made from a Range of Wheat Strengths using a Mixograph

X. Sun [*], F. Koksel, M. G. Scanlon, and M. T. Nickerson

(Recommended publication by Cereal Chemistry on Jun 26th, 2019)

**I conducted the experiments, wrote the manuscript, and coordinated with F. Koksel, M. G. Scanlon, and M. T. Nickerson and thus they provided intellectual input.*

3.1. Abstract

To meet Health Canada's target for reduced-sodium bread production, relationships between dough formula and dough mechanical properties were examined. A mixograph was used to investigate the interactions of wheat cultivar, water and NaCl content on the mechanical properties of doughs made from wheat cultivars with a range of breadmaking strengths. Mixograph parameters peak height (PKH) and energy to peak (ETP) were used to define the salt (NaCl)-induced change in dough properties for doughs made from various wheat cultivars and water contents. From ETP measurements, doughs became less responsive to salt reduction as water content was increased. The parameter ETP was a good indicator of the cultivar-dependent response of doughs to salt reduction, indicating that doughs made from the wheat cultivar Harvest had a good tolerance to salt reduction. Lower salt content conditions led to less differentiation between wheat cultivars according to their breadmaking strengths. Overall, both flour type and water content need to be considered when developing reduced-sodium bread formulas.

3.2. Introduction

Dough mechanical properties are reported to have a direct relation to breadmaking performance and loaf quality, justifying studies of the mechanical properties of bread dough prior to baking (Dobraszczyk & Morgenstern, 2003; Horvat et al., 2008). For this purpose, various empirical rheological methods such as the farinograph, mixograph and extensigraph have been employed (Gélinas & Mckinnon, 2013; Martinant et al., 1998; Oliver & Allen, 1992; Zounis & Quail, 1997). However, the mechanical behavior of bread dough is complex due to it being a mixture of a variety of interacting materials (Hoseney, 1994). In order to develop a dough so that it is optimized for breadmaking, it is essential to understand how wheat flour, water and NaCl affect dough mechanical properties.

The strength of the wheat cultivar directly determines the mechanical properties of wheat flour dough (Khatkar et al., 1996; Lukie, 2001). Nevertheless water, which is a key component in developing bread dough, influences the dough's mechanical properties by functioning as a mobility enhancer, softening the dough (Baig & Hoseney, 1977; Farahnaky & Hill, 2007; Lang et al., 1992). The mechanical properties of doughs made from various wheat cultivars indicated a cultivar-specific response of dough to water (Hoseney, 1986; Levine & Slade, 1990).

Similar to the effect of water addition, NaCl has been shown to have a cultivar-dependent effect on dough's mechanical properties as measured by mixograph and extensigraph tests (Butow et al., 2002). This differential sensitivity of wheat cultivars to NaCl can be attributed to NaCl effects on the gluten proteins, *i.e.*, glutenins and gliadins (Arakawa & Yonezawa, 1975; Huebner, 1970; Kim & Bushuk, 1995). On the basis of a protein extraction study of a strong and a very strong wheat cultivar, in terms of the proportion (%) of protein precipitated after NaCl addition, Kim & Bushuk (1995) showed that glutenins and gliadins extracted from the strongest wheat cultivar were more sensitive to NaCl addition, and this was attributed to molecular weight differences between the proteins of the two cultivars.

In contrast to water, NaCl affects the mechanical properties of bread dough by enhancing dough strength. This finding has been shown from various empirical rheological studies where parameters used to assess dough strength increased with increasing NaCl addition (Danno & Hoseney, 1982a; Galal et al., 1978; He et al., 1992; Hlynka, 1962; Lang et al., 1992; Preston, 1989). The strengthening effect of NaCl on dough is attributed to NaCl-induced changes in gluten structure (Belton, 1999, 2012; Eliasson & Larsson, 1993). NaCl addition is thought to promote hydrophobic interactions between gluten proteins, and to enhance the hydrogen bonding between water and gluten proteins, resulting in structural changes in gluten that improve the strength of the

dough (Belton, 1999, 2012; Melander & Horváth, 1977; Preston, 1981, 1989; Tkachuk & Hlynka, 1968).

In dough systems at a fixed farinograph water absorption, salt (NaCl) is believed to compete with confined water to occupy sites on the surface of the gluten proteins, which leads to a release of confined water, an increase of bulk water and dough mobility (reciprocal of maximum dough consistency measured by a farinograph, 1/B.U.) (Bushuk & Hlynka 1964; Hlyka 1962; Kontogiorgos, 2011). As such, NaCl and water both interact with gluten proteins to affect dough mechanical properties. Since gluten proteins vary across wheat cultivar, it is important to investigate the interactions of wheat cultivar, the content of water and the NaCl content on dough mechanical properties.

The mixograph is an instrument used to investigate the mechanical properties of dough by determining the resistance (torque, Tq) the dough exerts on the mixer pins as a function of mixing time. Dough mixograph parameters have been used to show how dough mechanical properties were affected by the wheat cultivar (Khatkar et al., 1996; Lukie, 2001) and by water content (Baig & Hoseney, 1977; Lang et al., 1992) and by NaCl content (Danno & Hoseney, 1982a; He et al., 1992; Lang et al., 1992). Water and NaCl exerted opposite effects on dough mixograph parameters except for mixing time, where "an enhancing effect" was seen with the addition of both water and NaCl (Baig & Hoseney, 1977; Danno & Hoseney, 1982a; He et al., 1992; Lang et al., 1992). Measurements of dough strength parameters, *i.e.*, peak height, peak bandwidth, and energy to peak, have shown a weakening response to added water and a strengthening response to added NaCl (Baig & Hoseney, 1977; Danno & Hoseney, 1982a; He et al., 1992; Lang et al., 1992).

Health Canada's Sodium Working Group recommends a maximum of 330 mg sodium/100 g bread, down from the typical value of 520 mg sodium/100g bread (Yovchev et al., 2017b).

Therefore, understanding the effects of reduced-sodium bread production on the mechanical properties of dough is important for devising strategies to overcome potential processing difficulties (Yovchev et al., 2015; Yovchev et al., 2017b). Therefore, this research examined the interaction of wheat cultivar, water content and reducing levels of sodium chloride to ascertain relationships between formula and dough mechanical properties for reduced-sodium bread production. In particular, for doughs made from hard red spring wheat cultivars with a range of breadmaking strengths, we wanted to determine which wheat cultivars had better tolerance to salt (NaCl) reduction as determined by dough mechanical properties evaluated by mixograph tests.

3.3. Materials and Methods

3.3.1. Wheat Flour Dough

Wheat flours (Grains Innovation Lab, University of Saskatchewan) used for this study were prepared from a Canada Western Red Spring (CWRS) wheat cultivar, *i.e.*, Roblin, and Canada Northern Hard Red (CNHR) wheat cultivars, *i.e.*, Pembina, McKenzie and Harvest, so that a range of breadmaking strengths was utilized. All four wheat cultivars were grown in the year of 2013 in one location at the University of Saskatchewan's Kernen Crop Research Farm (Yovchev et al., 2017b). For each cultivar, 14 kg flour was milled on a Buhler mill after tempering to 15.5% moisture. On a flour moisture basis (mb) of 14%, flour and dough properties are those reported in Table 3.1. A wide range in dough formulations was studied for their mixograph response for each cultivar. Doughs were created by mixing wheat flours with varying water content, relative to farinograph optimal water absorption (FAB), *i.e.*, FAB-4, FAB-2, FAB, FAB+2 and FAB+4 (% flour weight basis), and varying NaCl content, *i.e.*, 0, 0.4%, 0.8%, 0.25 mol L^{-1}, 1.5%, 2.0%, 2.5% and 3.0% (flour weight basis).

In order to prepare the doughs, the farinograph optimal water absorption (FAB) of each wheat flour was determined by method No. 54-21.02 (AACC International, 2011). The NaCl content of 1.5% flour weight was determined according to the optimized straight-dough breadmaking method (AACC International, 1999a). According to a moisture content of 38% in white bread, the sodium content of 330 mg per 100 g bread (Health Canada's target) converts into approximately 1.2 % NaCl content on a flour weight basis (Appendix 1a). When considering the moisture content and FAB of each cultivar, 1.2 % NaCl converts into approximately 0.25 mol L^{-1} NaCl in the water of doughs averaged for the four wheat cultivars (Appendix 1b). In order to attain an NaCl content of 0.25 mol L^{-1} for the various wheat cultivars and water contents, the salt content was varied when preparing the doughs (Appendix 1c).

Table 3.1: Flour and dough properties

Cultivar	Yield (%)	Protein (%, 14% mb)	Ash (%)	FAB (%, 14% mb)	DDT (min)	MTI (FU)	STA (min)
Harvest	72.4	13.2	0.45	65.5	3.9	41	4.9
McKenzie	69.6	13.2	0.46	64.1	4.6	29	6.5
Pembina	73.7	12.6	0.46	61.6	5.7	30	7.8
Roblin	71.7	13.8	0.40	65.0	6.0	6	16.6

mb: moisture basis. FAB: farinograph water absorption; DDT: dough development time; MTI: mixing tolerance index; STA: dough stability.

3.3.2. Mixograph Measurements

A strain gauge 10-g mixograph (Dynamic Machine Corporation, Winnipeg, MB, Canada) equipped with a torque reading software Power to Mixer, *i.e.*, P2M(UT) by RAR Software Systems (Winnipeg, MB, Canada) was used to measure the mixograph parameters, including mixing

development time (MDT, min), peak height (PKH, %Tq), peak bandwidth (PBW, %Tq), energy to peak (%Tq*min), and first minute slope (FMS, % Tq/min) (AACC International, 1999b; Pon, Lukow, & Buckley, 1988). Each dough sample was mixed for 10 min on the mixograph.

3.3.3. Experimental Design and Statistical Analysis

A completely randomized factorial design of four wheat cultivars (*i.e.*, Pembina, Roblin, McKenzie and Harvest), five water contents (*i.e.*, FAB-4%, FAB-2%, FAB, FAB+2% and FAB+4%) and eight NaCl contents (*i.e.*, 0, 0.4%, 0.8%, 0.25 mol L^{-1}, 1.5%, 2.0%, 2.5% and 3.0%) was used with three replications for each treatment. Analysis of variance (ANOVA) using Statistical Application Systems (SAS) software was used for analysis. A three-way ANOVA was conducted to evaluate the effects of wheat cultivar, water and NaCl on the mixograph characteristics of the various doughs (Appendix 4a and 5). For various wheat cultivars and water contents, the difference in the slopes or intercepts of linear fits of dough mixograph parameter *vs.* NaCl content were analyzed by the F-test (linear fit comparison of parameters in Origin graphing and analysis software, version 2016, Originlab Corporation, Northampton, MA, U.S.A.).

3.4. Results and Discussion

3.4.1. Interactions of Wheat Cultivar, Water and NaCl on Dough Mixograph Characteristics

All the mixograph parameters (Table 3.2) were significantly affected by wheat cultivar, water and NaCl ($P < 0.05$), indicating significant effects of formulation on dough mechanical properties. The interactive effects between wheat cultivar, water and NaCl varied according to the mixograph parameter (Table 3.2). Two-way interactive effects differed for the seven mixograph parameters except for PKH and STP and for PBW and FMS, where the two-way interactions were the same (Table 3.2). A three-way interaction of wheat cultivar, water and NaCl was observed for PKH and marginally for PBW (Table 3.2); these are two parameters that are associated with dough

resistance to mixing (Lukie, 2001; Pon et al., 1988). Therefore, the response of dough strength to salt (NaCl) reduction depends on both cultivar and water content.

Table 3.2: Effects of cultivar, water and NaCl on dough mixograph parameters

Effect	df	MDT	PKH	PBW	ETP	FMS	PBW/PKH
Cultivar	3	<.0001*	<.0001*	<.0001*	<.0001*	<.0001*	<.0063*
Water	4	<.0001*	<.0001*	<.0001*	0.0004*	<.0001*	<.0414*
NaCl	7	<.0001*	<.0001*	<.0001*	<.0001*	0.0015*	<.0001*
Cultivar×Water	12	<.0001*	0.0034*	0.0162*	0.6360ns	0.0001*	0.1303ns
Cultivar×NaCl	21	<.0001*	0.8942ns	0.0698ns	<.0001*	0.0712ns	0.3729ns
Water×NaCl	28	0.3192ns	0.0191*	0.2124ns	0.0008*	0.3890ns	0.0471*
Cultivar×Water×NaCl	84	0.6506ns	0.0069*	0.0411*	0.1355ns	0.1172ns	0.5676ns

df: degree of freedom. MDT: mixing development time; PKH: peak height; PBW: peak bandwidth; ETP: energy to peak; FMS: first minute slope. *P* values labeled by * = significant, 'ns'= not significant.

3.4.2. Effects of Water and NaCl on Dough Mixograph Characteristics

A significant interaction of water and NaCl was observed for dough strength parameters PKH and ETP (Table 3.2), indicating that the response of dough strength parameters to salt (NaCl) reduction depends on the water content in the dough. Therefore, it is essential to determine how changes in water content affect the interpretation of PKH changes with salt reduction in doughs made from different wheat cultivars.

With the reduction of NaCl from 3% to 0, the PKH of doughs decreased regardless of water content (Figure 3.1), indicating a negative effect of salt reduction on dough strength. Dough resistance to extension (indicative of dough strength) measured by an extensigraph was also shown

to decrease with NaCl reduction in the dough (Lynch et al., 2009). At a fixed water content, the PKH of dough showed a good linear relationship with NaCl reduction (Figure 3.1, r^2 values). The slope of PKH against NaCl content was not statistically differentiated according to water content in the dough (Figure 3.1, slope values in linear fit equations). Regardless of NaCl content, the PKH of doughs decreased as water content was increased (Figure 3.1, intercept values in linear fit equations). Therefore, it indicates a softening effect of water addition on wheat flour dough (Baig & Hoseney, 1977; Lang et al., 1992).

Figure 3.1: Effects of salt reduction and changes in water content on dough peak height (PKH) averaged for four red spring wheat cultivars. Water contents are FAB-4% (black squares), FAB-2% (red triangles), FAB (blue circles), FAB+2% (green rhombuses), and FAB+4% (purple stars). Linear fits (dashed lines): $y = 4.45^{a} x + 40.3^{A}$, $r^2 = 0.896$ (black), $y = 4.35^{a} x + 37.8^{B}$, $r^2 = 0.969$ (red), $y = 4.80^{a} x + 34.7^{C}$, $r^2 = 0.932$ (blue), $y = 4.37^{a} x + 33.5^{D}$, $r^2 = 0.906$ (green), $y = 4.66^{a} x + 30.9^{E}$, $r^2 = 0.979$ (purple). For the slope or intercept of the linear fits, values labeled by the same letter are not significantly different ($P < 0.05$).

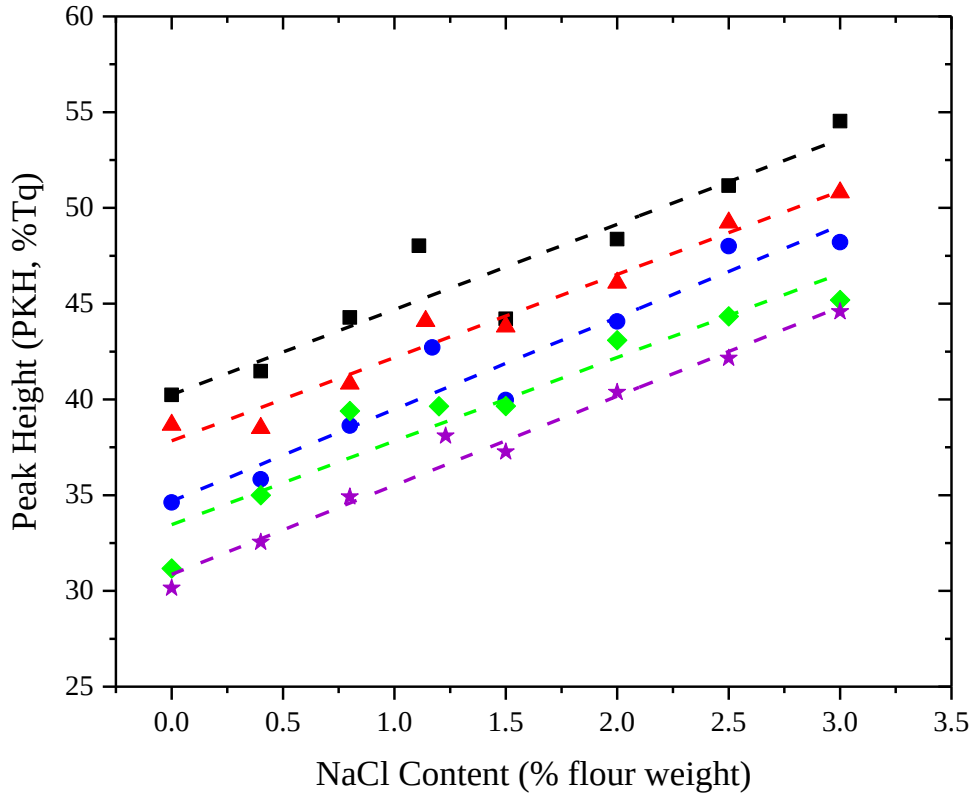

NaCl has a similar effect on the "dough strength" parameter ETP as it does on PKH. Lowering NaCl lowers ETP (Figure 3.2). However, unlike PKH, ETP did not clearly indicate the water-induced increase in dough softness (Figure 3.2, intercept values in linear fit equations). This outcome can be attributed to water exerting opposite effects on MDT and PKH (Lang et al., 1992), so that the two determinants of ETP, cancel each other out. Although some slopes of ETP against

NaCl reduction were not statistically different between water contents, higher water content doughs did show a lower slope of ETP for the reduction in NaCl content (Figure 3.2, slope values in linear fit equations). This possibly indicates that increasing water content decreased the sensitivity of wheat flour dough to salt reduction. This finding agrees with farinograph studies that have shown that the consistency (B.U.) of higher water content doughs was less responsive to NaCl reduction (Hlynka, 1962).

Figure 3.2: Effects of salt reduction and changes in water content on dough energy to peak (ETP) averaged for four red spring wheat cultivars. Water contents are FAB-4% (black squares), FAB-2% (red triangles), FAB (blue circles), FAB+2% (green rhombuses), and FAB+4% (purple stars). Linear fits (dashed lines): $y = 19.0^{a} x + 57.0^{A}$, $r^2 = 0.918$ (black), $y = 18.2^{a} x + 56.0^{A}$, $r^2 = 0.985$ (red), $y = 14.4^{b} x + 59.3^{A}$, $r^2 = 0.955$ (blue), $y = 14.2^{b} x + 59.3^{A}$, $r^2 = 0.945$ (green), $y = 13.5^{b} x + 59.3^{A}$, $r^2 = 0.943$ (purple). For the slope or intercept of the linear fits, value labeled by the same letter are not significantly different ($P < 0.05$).

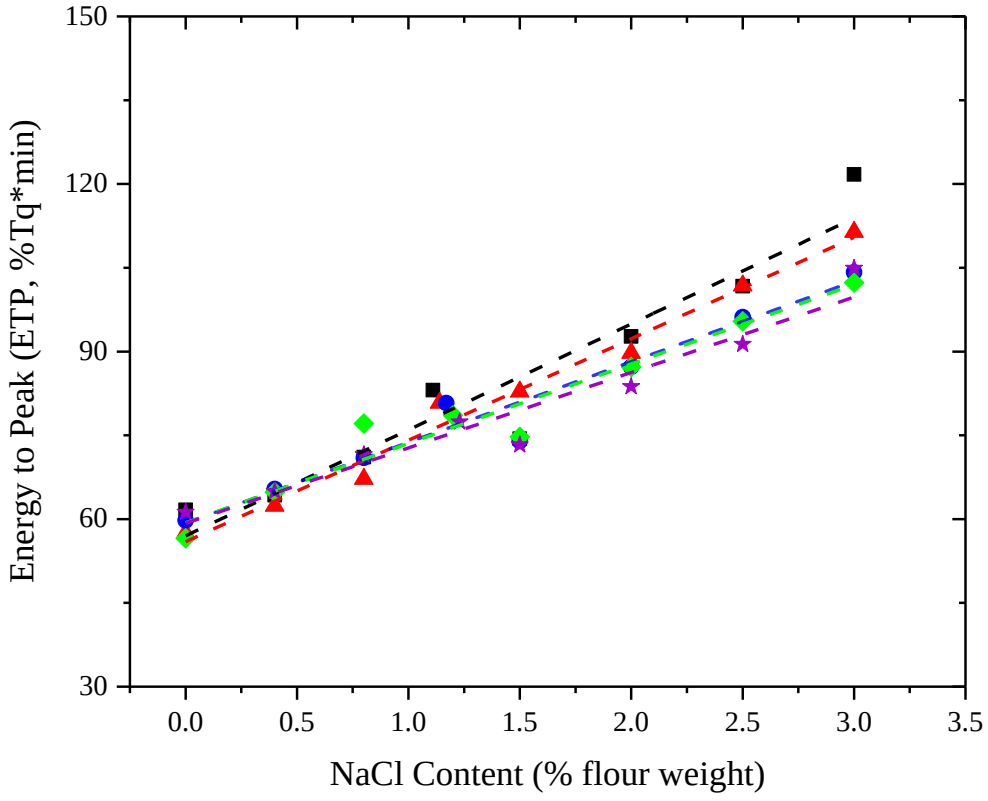

3.4.3. Effects of Wheat Cultivar and NaCl on Dough Mixograph Characteristics

The interactive effects of wheat cultivar and NaCl were observed for MDT and ETP (Table 3.2), two classic determinants of dough strength, indicating that how NaCl affects dough strength is dependent on the wheat cultivar used for dough preparation. The ETP values of doughs made from the four wheat cultivars were compared by averaging for five water conditions (Figure 3.3). For doughs made from the four wheat cultivars, the ETP had a good linear relationship with NaCl reduction (Figure 3.3, r^2 values). The slope of ETP against NaCl content significantly varied according to wheat cultivar (Figure 3.3, slope values in linear fit equations), indicating a potential use of ETP to discriminate the tolerance of dough made from a specific flour to salt reduction. Since gluten proteins vary in their molecular weight and subunit composition across wheat cultivars, the response of gluten proteins to NaCl-induced precipitation (*i.e.*, the proportion of protein precipitated with NaCl addition) depends on wheat cultivar (Arakawa & Yonezawa, 1975; Huebner, 1970; Kim & Bushuk, 1995). As a result, the response of dough strength to salt reduction is cultivar dependent.

Figure 3.3: Effects of salt reduction and wheat cultivar on dough energy to peak (ETP) averaged for five water contents. Wheat cultivars are Pembina (black squares), Roblin (red triangles), McKenzie (blue circles), Harvest (green rhombuses). Linear fits (dashed lines): $y = 22.6^{a} x + 69.4^{A}$, $r^2 = 0.962$ (black), $y = 15.1^{b} x + 70.5^{A}$, $r^2 = 0.964$ (red), $y = 15.3^{b} x + 47.5^{B}$, $r^2 = 0.959$ (blue), $y = 10.5^{c} x + 45.5^{B}$, $r^2 = 0.951$ (green). For the slope or intercept of the linear fits, values labeled by the same letter are not significantly different ($P < 0.05$).

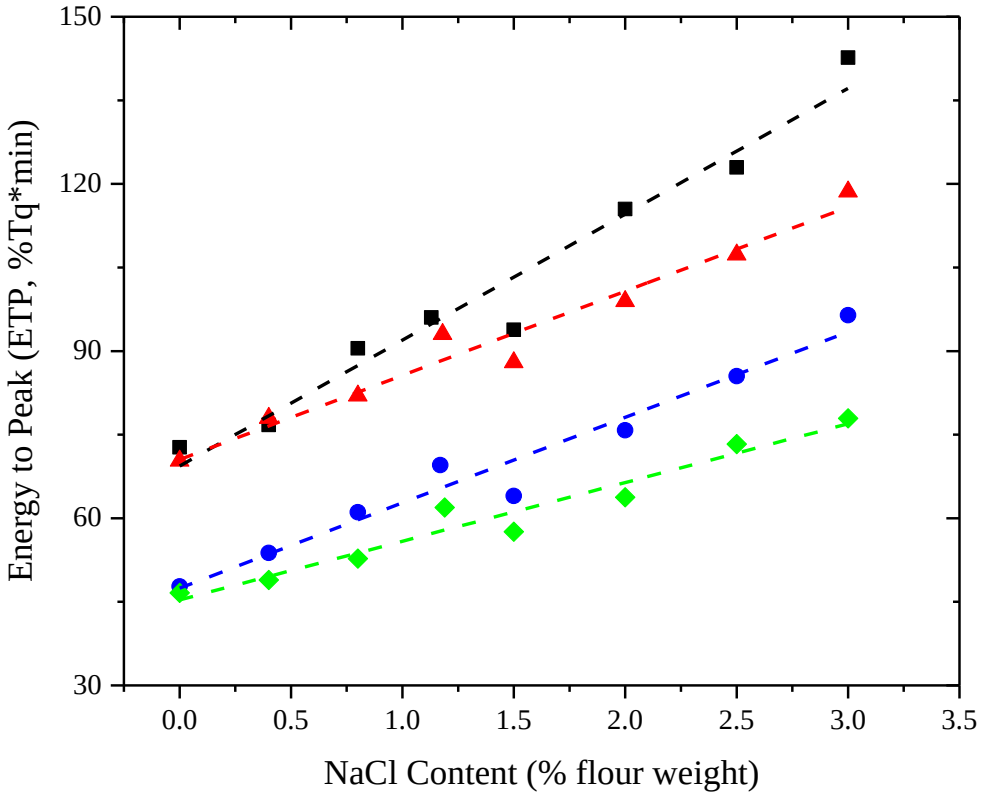

By comparing the slopes of ETP against NaCl content over all four wheat cultivars, an ascending order of cultivar sensitivity to NaCl reduction was Harvest < Roblin ~ McKenzie < Pembina (Figure 3.3, slope values in linear fit equations). A rank of breadmaking strengths (from weak to strong) was shown as Harvest < McKenzie < Pembina < Roblin (Table 3.1, DDT and STA), and this ranking according to ETP was essentially observed as Harvest < McKenzie < Roblin < Pembina at higher NaCl content (Figure 3.3). The lowest sensitivity to NaCl reduction

was seen for the weakest cultivar Harvest. Even though it is weaker, because it has good tolerance to salt reduction, Harvest may be a cultivar of choice when developing a reduced-salt bread formula.

NaCl reduction decreased the difference in ETP values between wheat cultivars (Figure 3.3). This indicates that the breadmaking strength of wheat cultivars is less obvious at reduced salt content conditions compared to a regular formula. This finding is probably attributable to hydrophobic interactions between gluten proteins being predominant at higher salt conditions (Huebner & Wall, 1980; Preston, 1981, 1984). As such, differences in gluten strength (arising from enhanced protein-protein interactions) are more pronounced at higher salt conditions. Therefore, when using a mixograph, higher NaCl content is better for screening wheat cultivars according to their breadmaking strengths.

One means of normalizing the mixograph results was to divide PBW by PKH, *i.e.*, PBW/PKH (the ratio of peak bandwidth to peak height), this essentially eliminated water effects and interaction effects (Table 3.2). Therefore, this parameter was plotted to show how it responded to NaCl reduction. The values of PBW/PKH of doughs made from the four wheat cultivars were compared by averaging for the five water conditions (Figure 3.4).

Figure 3.4: Effects of salt reduction and wheat cultivar on dough peak bandwidth/peak height (PBW/PKH) averaged for five water contents. Wheat cultivars are Pembina (black squares), Roblin (red triangles), McKenzie (blue circles), Harvest (green rhombuses). Linear fits (dashed lines) over lower salt contents (NaCl content of 0 to 1.5%): $y = 0.025^{b} x + 0.410^{A}$, $r^2 = 0.702$ (black), $y = 0.017^{b} x + 0.402^{B}$, $r^2 = 0.836$ (red), $y = 0.033^{a} x + 0.391^{B}$, $r^2 = 0.978$ (blue), $y = 0.021^{b} x + 0.402^{B}$, $r^2 = 0.938$ (green). For the slope or intercept of the linear fits, values labeled by the same letter are not significantly different ($P < 0.05$).

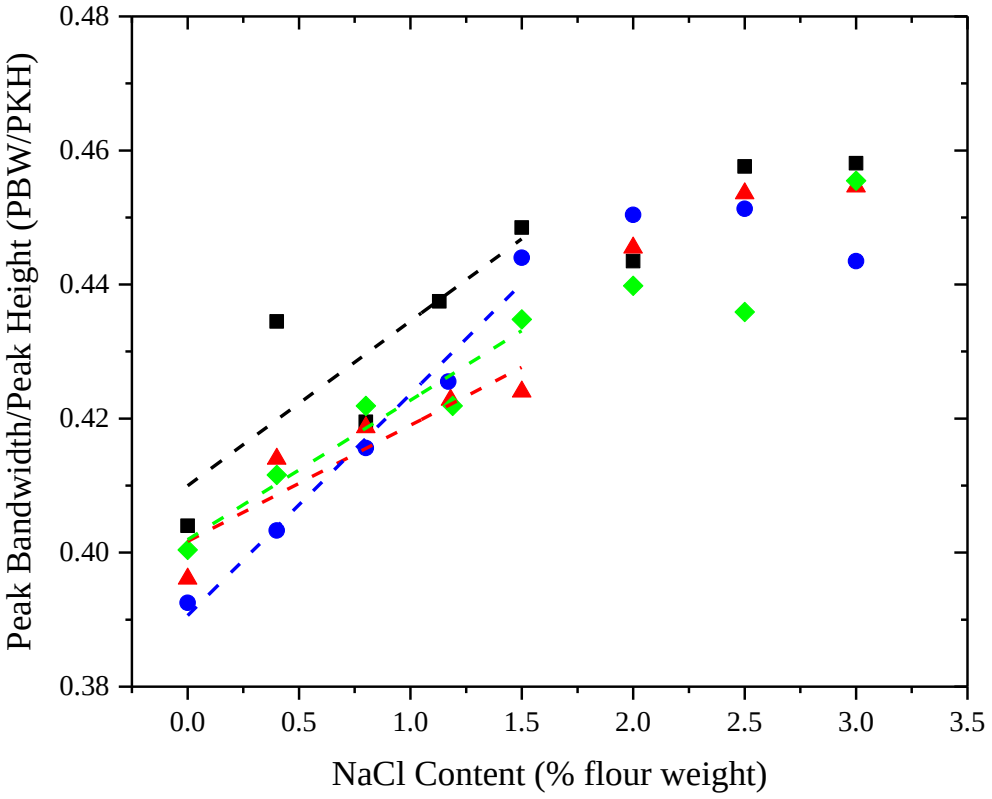

Although the effect of wheat cultivar on PBW/PKH was significant (Table 3.2), it was difficult to discern a consistent cultivar effect other than the tendency of Pembina doughs to have a higher PBW/PKH value at most NaCl contents (Figure 3.4). At a fixed NaCl condition, the mixing and extension properties of doughs were observed to correlate with the strength of wheat cultivar (Khatkar et al., 1996; Suchy, Lukow, & Ingelin, 2000). For doughs made from the four

wheat cultivars, a reasonably good linear fit of PBW/PKH against low NaCl contents (0 to 1.5% flour weight) was observed (Figure 3.4, r^2 values). The decrease in PBW/PKH with decreases in NaCl content at these lower contents is quite noticeable compared to at the higher NaCl contents. Changes in dough properties are therefore more susceptible to decreases in salt content below approximately 1.5% flour weight basis. Due to a higher slope value of PBW/PKH against NaCl reduction from 1.5% to 0 (Figure 3.4, slope values in linear fit equations), doughs made from the cultivar McKenzie were more responsive to salt reduction compared to those made from other three cultivars.

3.5. Conclusions

The mixograph is a practical and effective tool that provides useful parameters to show how doughs made from a wide range of formulations respond to salt (NaCl) reduction. Wheat flour dough becomes less responsive to salt reduction as water content is increased. The parameter ETP is a good indicator to show that dough's response to salt reduction differs according to wheat cultivar. By observing the slope of ETP against NaCl reduction across wheat cultivars, Harvest exhibited a better tolerance to salt reduction compared to three other cultivars. As such, incorporation of wheat flour from Harvest into reduced-sodium bread formulas is a potential dough handling improvement strategy. Breadmaking strength was less discriminated at lower salt contents compared to a regular formula. Overall, to meet Health Canada's target for bread production at reduced sodium content, the flour type (associated with wheat cultivar) and water addition both need to be considered when developing reduced-salt doughs with good handling properties.

3.6. Acknowledgements

The authors acknowledge the financial support provided by Canada Bread Corp. (Toronto, Canada), the Saskatchewan Agricultural Development Fund, the Western Grains Research Foundation, and through a joint NSERC (Natural Sciences and Engineering Research Council of Canada)-CIHR (Canadian Institute of Health Research) Institute of Nutrition, Metabolism and Diabetes Funding Initiative for Sodium Reduction in the Canadian Food Supply, and CSC (China Scholarship Council). The authors would like to thank Dr. Nancy Ames, and Mr. Dave Niziol from Agriculture and Agri-Food Canada (Winnipeg, MB, Canada) for their technical support.

3.7. Bridge between Chapters 3 and 4

In terms of mixograph studies (Chapter 3), the rheological properties of doughs were less responsive to salt (NaCl) reduction when the doughs were prepared using certain wheat cultivars (*i.e.*, Harvest and Roblin) and increased water contents. Therefore, wheat flour doughs made from Harvest and Roblin with reduced salt contents were selected for rheological modeling studies (Chapter 4). For a wide range of dough strengths and formulations, results from mixograph (Chapter 3) and rheological modeling studies (Chapter 4) are expected to provide a comprehensive understanding of dough rheological properties at both large and small strains.

4. Modeling the Viscoelastic Behavior of Wheat Flour Dough Prepared from a Wide Range of Formulations

X. Sun [*], F. Koksel, M. T. Nickerson, and M. G. Scanlon

(Published in Food Hydrocolloids 98 (2020) 105129. doi.org/10.1016/j.foodhyd.2019.05.030)

**I conducted the experiments, wrote the manuscript, and coordinated with F. Koksel, M. T. Nickerson, and M. G. Scanlon and thus they provided intellectual input.*

4.1. Abstract

The viscoelastic behavior of wheat flour dough has been characterized using constitutive models of varying degrees of complexity. Modeling characterizations of the viscoelasticity of dough have not always demonstrated the general applicability of their models to a wide range of dough strengths and formulations. Therefore, the objective of this study was to use two extrema in viscoelastic rheological models (*i.e.*, a power-law gel and the four-element Burgers models) to characterize the linear and non-linear shear behavior of wheat flour doughs. A wide range of breadmaking strength and formulations were employed, particularly those with varying salt (NaCl) content (to ascertain model applicability to strategies to reduce sodium in bread). The power-law gel model fitted all the experimental data well for oscillatory rheometry and creep-recovery tests. The power-law gel model was better at describing the linear viscoelasticity of wheat flour dough compared to the Burgers model, but was poorer at characterization of the recovery phase. Gel strength parameters derived from power-law gel models are recommended for defining the effects of changes in wheat cultivar, water and salt content on both the linear and non-linear viscoelasticity of dough rheology.

4.2. Introduction

Wheat flour dough is a viscoelastic material that combines the properties of a non-Newtonian viscous fluid and a Hookean elastic solid (Faubion & Hoseney, 1990). It has a small linear viscoelastic region. When the shear strain amplitude is increased beyond approximately 0.2%, non-linear viscoelastic behavior is evident (Berland & Launay, 1995b). Dough's viscoelastic properties have been characterized using shear tests at both small strain and in the non-linear viscoelastic region (Hardt et al., 2014; Jekle & Becker, 2011, 2012; Lefebvre & Mahmoudi, 2007; Lefebvre, 2009; Mastromatteo et al., 2013; Ng et al., 2006; Ng, 2008; Skendi et al., 2010; Yovchev

et al., 2017a, 2017c). A definition of the mechanical properties of this complex viscoelastic material is not only useful from a materials' perspective, but also because these properties correlate well with the handling performance of the dough and the properties of the bread baked from it (Autio et al., 2001; Khatkar & Schofield, 2002; Lynch et al., 2009; McCann & Day, 2013; Stojceska, Butler, Gallagher, & Keehan, 2007; Van Bockstaele et al., 2008b; Yovchev et al., 2017b). A good characterization of dough's viscoelastic behavior is therefore useful for optimizing dough formulation and processing to improve the breadmaking process.

However, one cannot portray dough as a single material with a restricted range of rheological properties. When formulation changes, the rheology of dough changes (Berland & Launay, 1995a; Dreese et al., 1988; Hardt et al., 2014; Larsson et al., 2000; Larsson, 2002; Létang et al., 1999; Masi et al., 1998). This is especially true as formulation changes are made to dough in response to consumer or regulatory pressures, such as when sodium reduction strategies for baked goods are introduced (Beck et al., 2012a; Jekle & Becker, 2012; McCann & Day, 2013; Yovchev et al., 2017b, 2017c). As a result, any rheological models used to characterize dough properties need to be sufficiently robust that they can broadly cover changes in rheology brought about by reformulations and process line innovations.

Constitutive models of varying degrees of complexity have been previously used to define dough properties. Depending on its formulation, dough has been characterized as a viscoelastic solid (Faubion & Hoseney, 1990) and as a viscoelastic liquid (Leroy et al., 2010; Ng et al., 2011, 2006; Ng, 2008). As a viscoelastic liquid, dough has been frequently cast as a Burgers model or as a Maxwell fluid (Steffe, 1996). The Burgers model consists of Maxwell elements (a spring lined up with a dashpot) in series with Kelvin-Voigt elements (a spring in parallel with a dashpot). The model is frequently used to describe the creep-recovery response of viscoelastic materials (Halim

& Shoemaker, 1990; Paredes, Rao, & Bourne, 1989; Steffe, 1996). According to the composition of mechanical elements, the simplest Burgers model is a four-element Burgers model that includes one Maxwell element and one Kelvin-Voigt element (Paredes et al., 1989; Steffe, 1996). The four-element Burgers model has been used to describe the shear creep and recovery of dough (Beck et al., 2012a; Lazaridou et al., 2007; Skendi et al., 2010).

Additional elements can be added to better model the mechanical properties of dough. The six-element Burgers model includes one Maxwell element and two Kelvin-Voigt elements (Halim & Shoemaker, 1990; Steffe, 1996), and this has been used to characterize the shear creep and recovery compliance of wheat flour doughs (Campos et al., 1997; Tronsmo, Magnus, Baardseth, et al., 2003; Van Bockstaele et al., 2011). Additional Kelvin-Voigt elements have been added to further reconcile model and experimental shear creep and recovery compliances (Meerts et al., 2017; Tronsmo, Magnus, Færgestad, et al., 2003).

Characterizing dough as a Maxwell fluid has been the focus of a number of studies using small strain shear evaluations (Beck et al., 2012a; Masi et al., 1998; Navickis et al., 1982) and shear creep-recovery compliances (Lefebvre & Mahmoudi, 2007; Lefebvre, 2006, 2009). Multiple Maxwell elements have been found necessary to adequately model dough's frequency response at small strains (Leroy et al., 2010; Ng et al., 2006; Sofou, Muliawan, Hatzikiriakos, & Mitsoulis, 2008) and its time-dependent response at large strains (Ng, 2008). One means of dispensing with the need for multiple sets of relaxation times is to define dough as a power-law gel material (Leroy et al., 2010; Ng, 2008).

As a power-law gel material, wheat flour dough is a critical gel-like material with a broad distribution of relaxation times that follows a power-law model (Gabriele et al., 2001; Ng et al., 2006). Two parameters suffice to describe the linear viscoelastic behavior of wheat flour dough

(Ng et al., 2006), and this model has been used to characterize the frequency-dependent shear modulus, of dough over a very wide frequency range (Leroy et al., 2010). In addition, the power-law gel model can be used to describe dough properties in the non-linear viscoelastic region (Ng, 2008).

Frequently, modeling studies of the linear and non-linear viscoelasticity of wheat flour doughs have not demonstrated the general applicability of their models to a *wide* range of flour strength and formulations. Therefore, the objectives and novelty of this research were: 1) the use of two extremes in viscoelastic rheological models (*i.e.*, the power-law gel and the four-element Burgers model) to characterize the linear and non-linear shear behavior of wheat flour doughs made from a wide range of breadmaking strength and formulations, particularly those with varying salt content; 2) determine relationships between the model parameters that are derived from characterization of these doughs' linear and non-linear rheology to acquire novel insights into the effects of formulation changes; 3) evaluate the effects of water and salt content on the rheological modeling parameters of dough made from wheat cultivars of contrasting strengths.

4.3. Materials and Methods

4.3.1. Wheat Flour Dough

Doughs were prepared for all rheological measurements by mixing flour milled from two hard red spring wheat cultivars Harvest and Roblin (the same source of flour samples that was used in Chapter 3), water and salt (NaCl) in a moving bowl 10-g mixograph instrument (National MFG. CO., Lincoln, NE, U.S.A.) equipped with Mixsmart computer software (v. 3.80). Treatments were water content (*i.e.*, FAB-4%, FAB-2%, FAB, FAB+2% and FAB+4%, expressed as a % of flour weight) and NaCl content (*i.e.*, 0, 0.25M and 2.5%, flour weight basis). FAB is the optimal farinograph water absorption of the wheat flour. The FAB was determined (AACC

International, 2011) as 65.5% for Harvest and 65% for Roblin. The addition of 0.25M NaCl was determined based on the water content of the dough and the amount of salt required to meet Health Canada's sodium reduction recommendation of 330 mg sodium/100 g bread. According to a moisture content of 38% in white bread, the sodium content of 330 mg per 100 g bread converts into approximately 1.2% NaCl content on a flour weight basis. When considering the FAB of each cultivar, 1.2% NaCl converts approximately into an NaCl molarity of 0.25 mol/L in the water used to make the dough. The 0.25 mol/L NaCl was held constant to prepare the doughs with various water contents, which results in varying the amount of NaCl used to formulate these doughs. All doughs were mixed for their optimal time according to the mixogram. The optimal mixing time of dough was determined by the mixograph (AACC International, 1999b) with an average coefficient of variation of 7%. All doughs were prepared and measured in triplicate.

4.3.2. Rheological Measurements

The dynamic rheological properties of dough samples were analyzed using an AR 1000 Advanced Rheometer (TA instruments, New Castle, DE, U.S.A.) with a Peltier plate temperature-controlled system (T = 30 °C) and a 40 mm diameter smooth parallel plate geometry (Yovchev et al., 2017c). Approximately 5 g of dough was loaded onto the bottom plate and the top plate lowered to a gap of 2 mm. Excess dough was trimmed off and removed from the outer edge of the top plate geometry, and then the dough residue at the bottom plate of the rheometer was cleaned up. Paraffin oil was then added to the outer edge of the dough to prevent drying during measurement, and the dough was allowed to rest for a 10 min equilibration period. For each dough sample, a dynamic oscillatory frequency sweep was conducted at a constant strain amplitude ($\gamma = 0.1\%$) within the linear viscoelastic regime, followed immediately by a creep-recovery test (Yovchev et al., 2017c).

Oscillatory frequency sweeps were carried out to measure the dynamic storage modulus (G', Pa) and loss modulus (G", Pa) as a function of angular frequency (ω) from 0.628 to 628 rad.s^{-1}. The G'(ω) and G"(ω) were then modeled to determine the linear viscoelastic behavior of wheat flour doughs for the full range of dough formulations.

A creep recovery test was performed by applying a constant shear stress, σ_0, of 250 Pa to the dough for 180 s, after which the stress was removed ($\sigma_0 = 0$) and the shear recovery was measured for 360 s (Jekle & Becker, 2011). Deformation and recovery were measured as a function of time, and reported in terms of compliance:

$$J(t)=\frac{\gamma(t)}{\sigma_0} \quad [1]$$

where J(t) is the compliance (J, Pa^{-1}) over time (t, s), and γ(t) is the strain over time. Creep compliance was defined as $J_c(t)$ over the creep time (from 0 to 180 s, the end time of the creep phase t_c = 180 s), and the recovery compliance was defined as $J_r(t)$ for the recovery time (from 180 to 540s, the end time of the recovery phase t_r = 540 s). Both $J_c(t)$ and $J_r(t)$ were then modeled to characterize the non-linear viscoelastic behavior of wheat flour doughs of various strengths.

4.3.3. Rheological Models and Model Fitting

The frequency-dependent moduli of the oscillatory testing and the time-dependent compliance of the creep-recovery tests were determined in triplicate for each treatment. For each replicate, the appropriate model was fitted to the experimental data using Origin 2016 graphing and analysis software. The user defined expressions (Eqs. [2] to [7], [9] and [10]) were created using the fitting function builder (Origin 2016).

According to the power-law gel model from Ng (2008), the data curves of G'(ω) and G"(ω) against frequency were fitted to the relevant model expression (using Eq. [2] and [3]), respectively.

The power-law gel model parameters, the gel strength (S) and exponent (n), were derived from the best fit to the data (Origin 2016).

$$G'(\omega)=\Gamma(1-n)\cos\frac{n\pi}{2}S\omega^n \quad [2]$$

$$G''(\omega)=\Gamma(1-n)\sin\frac{n\pi}{2}S\omega^n \quad [3]$$

where Γ(1-n) is the gamma function for 1-n. Although a single *S* and *n* have been used to define both the storage and loss modulus for power-law materials (Bohlin & Carlson, 1980; Gabriele et al., 2001; Ng, 2008), in accordance with alternative outcomes from stress relaxation and creep studies on gluten gels (Kontogiorgos, 2017), we made no a priori assumptions on this. Accordingly, S' and n' were used as the gel strength and exponent, respectively, for modeling of G'(ω), and S" and n" were the counterparts for modeling of G"(ω).

The time-dependent characterization of the creep and recovery curves of the doughs as power-law materials was conducted in a similar fashion. The creep compliance $J_c(t)$ of each replicate dough was modeled by Eq. [4] (Ng, 2008), with the gel strength (S^c) and exponent (n^c) for the creep phase obtained from the best fit to the data (Origin 2016).

$$J_c(t)=\frac{t^{n^c}}{S^c\Gamma(1-n^c)\Gamma(1+n^c)} \quad [4]$$

For modeling of the recovery compliance, $J_r(t)$, with a power-law response, we used an expression of the fractional Maxwell model (FMM) given by Jaishankar & McKinley (2014) on the grounds that as the number of Maxwell elements gets extremely large, the FMM model is equivalent to the power-law gel model (Papoulia, Panoskaltsis, Kurup, & Korovajchuk, 2010). The gel strength (S^r) and exponent (n^r) for the recovery phase were derived from the best fit to the data.

$$J_r(t)=\frac{t^{n^r}-(t-t_c)^{n^r}}{S^r\Gamma(1-n^r)\Gamma(1+n^r)} \quad [5]$$

At the other extreme from characterization of dough using an infinite number of relaxation times, the four-element Burgers model has been used (Lazaridou et al., 2007; Skendi et al., 2010). In this case, the creep and recovery compliances of the dough samples as a function of time were modeled for each replicate using expressions [6] and [7], respectively, using the nomenclature of Yannas (2004). The Burgers model parameters were derived from the best fit to the data (Origin 2016), with the exception of the dashpot (viscous) constant from the Maxwell model (η_1^r) in the recovery phase, which was calculated from Eq. [8].

$$J_c(t)=\frac{1}{R_1^c}+\frac{1}{R_2^c}\left[1-\exp\left(-\frac{R_2^c t}{\eta_2^c}\right)\right]+\frac{t}{\eta_1^c} \quad [6]$$

$$J_r(t)=J_{max}-\frac{1}{R_1^r}-\frac{1}{R_2^r}\left[1-\exp\left(-\frac{R_2^c(t-t_c)}{\eta_2^c}\right)\right] \quad [7]$$

The spring (elastic) constants from the Maxwell and Kelvin-Voigt models are R_1 and R_2, respectively, while η_1 and η_2 are the dashpot (viscous) constants from the Maxwell and Kelvin-Voigt models, respectively. J_{max} is the maximum creep compliance obtained at the end of the creep phase.

When a sufficiently long time has been allowed for full recovery of the viscoelastic strain in the sample ($t\rightarrow\infty$), the $J_r(t)$ depends only on the compliance arising from the Maxwell model. Infinite time in this study is represented as the end time of the recovery phase (t_r = 540 s), and t_c is the end time of the creep phase (t_c = 180 s). Therefore, the dashpot (viscous) constant from the Maxwell model (η_1^r, Pa.s) in the recovery phase, was determined using Eq. [8].

$$\eta_1^r=\frac{180}{J_r(t)\big|_{t=540}} \quad [8]$$

The four-parameter Burgers model can also be fitted to the frequency-dependent data in the linear viscoelastic region using Eqs. [9] and [10] (Yannas, 2004):

$$G'(\omega)=\frac{\left(\frac{\eta_1'}{R_1'}+\frac{\eta_1'}{R_2'}+\frac{\eta_2'}{R_2'}\right)\eta_1'\omega^2-\frac{\eta_1'\eta_2'}{R_2'}\omega^2\left(1-\frac{\eta_1'\eta_2'}{R_1'R_2'}\omega^2\right)}{\left(\frac{\eta_1'}{R_1'}+\frac{\eta_1'}{R_2'}+\frac{\eta_2'}{R_2'}\right)^2\omega^2+\left(1-\frac{\eta_1'\eta_2'}{R_1'R_2'}\omega^2\right)^2} \quad [9]$$

$$G''(\omega)=\frac{\left(\frac{\eta_1''}{R_1''}+\frac{\eta_1''}{R_2''}+\frac{\eta_2''}{R_2''}\right)\frac{\eta_1''\eta_2''}{R_2''}\omega^2+\eta_1''\omega\left(1-\frac{\eta_1''\eta_2''}{R_1''R_2''}\omega^2\right)}{\left(\frac{\eta_1''}{R_1''}+\frac{\eta_1''}{R_2''}+\frac{\eta_2''}{R_2''}\right)^2\omega^2+\left(1-\frac{\eta_1''\eta_2''}{R_1''R_2''}\omega^2\right)^2} \quad [10]$$

where R_1', R_2', η_1' and η_2' are derived from modeling of G'(ω), and R_1'', R_2'' η_1'' and η_2'' are the counterparts for modeling of G"(ω). Our G'(ω) and G"(ω) data were fitted independently by Origin 2016 to the four-parameter model expressions. The modeling parameters were derived from the best fit to the data for each replicate (Origin 2016).

4.3.4. Statistical Analysis

Analysis of variance (ANOVA) using the Statistical Analysis Systems (SAS) software version 9.4 was conducted to determine differences in the rheological model parameters for wheat flour doughs created by different treatments ($P < 0.05$, Appendix 4b and 6). Differences between means of variables were analyzed by the Tukey test ($P < 0.05$, SAS 9.4, Appendix 4c and 6). The Pearson correlation coefficients (r) were calculated to show the relationships between different rheological model parameters ($P < 0.05$, SAS 9.4, Appendix 4d).

4.4. Results and Discussion

4.4.1. Linear Viscoelastic Behavior of Dough

The linear viscoelastic behavior of the wheat flour dough formulations is illustrated in Figure 4.1, using mean values of four treatments, according to a putative ranking of dough strength,

(a) > (b) > (c) > (d). The dough formulations are: (a) Roblin flour mixed with FAB-4% water and 2.5% NaCl; (b) Roblin flour mixed with FAB water and 0.25M NaCl; (c) Harvest flour mixed with FAB water and 0.25M NaCl; (d) Harvest flour mixed with FAB+4% water and 0% NaCl. In many cases experimental error bars are smaller than symbol size.

Figure 4.1: The storage (G', filled symbols ■) and loss (G", unfilled symbols □) shear moduli as a function of angular frequency (ω) for wheat flour doughs over a range of breadmaking strengths. Wheat flour doughs (a), (b), (c) and (d) are shown according to a decrease in breadmaking strength. Red lines are the power-law gel model fitting for the G'(ω) (solid line) and G"(ω) (dashed line) of doughs with Eqs. [2] and [3], respectively. Blue lines are the Burgers model fitting for the G'(ω) (solid line) and G"(ω) (dashed line) of doughs with Eqs. [9] and [10], respectively. Error bars show ± 1 SD, n = 3.

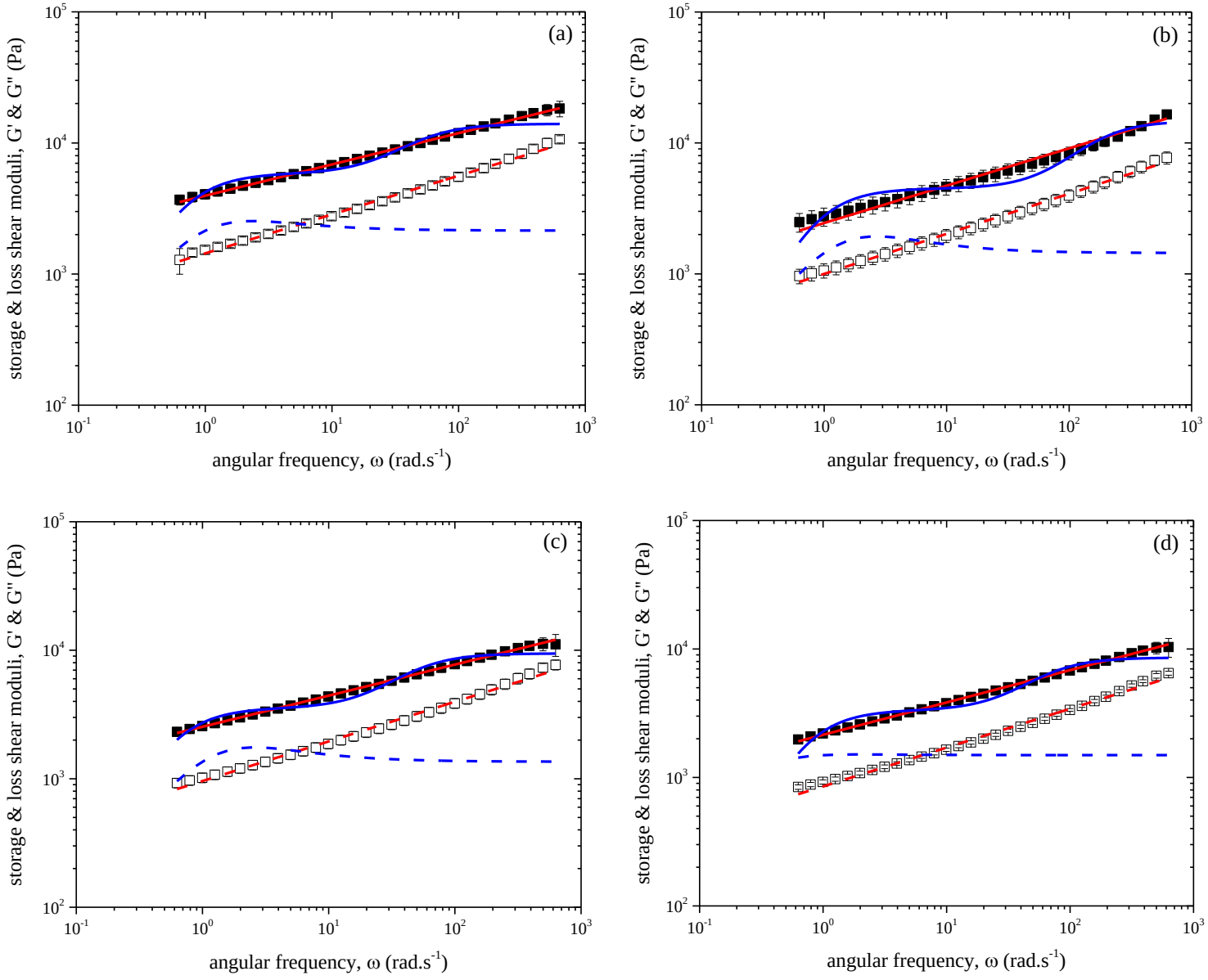

Table 4.1: Comparison of single modeling of G'(ω) and G"(ω) using one value for S and n vs independent modeling for G'(ω) and G"(ω)

Parameters	Wheat flour dough			
model fit	(a)	(b)	(c)	(d)
S (Pa.s^n)	2467 ± 132^b	1729 ± 241^b	1746 ± 288^{ab}	1610 ± 160^a
S' (Pa.s^n)	3472 ± 83^a	2196 ± 409^a	2103 ± 253^a	1829 ± 330^a
S" (Pa.s^n)	1956 ± 120^c	1347 ± 192^b	1196 ± 107^b	1142 ± 25^b
n	0.294 ± 0.003^b	0.293 ± 0.004^a	0.289 ± 0.017^b	0.284 ± 0.007^{ab}
n'	0.242 ± 0.008^c	0.297 ± 0.027^a	0.239 ± 0.031^b	0.250 ± 0.033^b
n"	0.323 ± 0.002^a	0.331 ± 0.005^a	0.341 ± 0.001^a	0.330 ± 0.002^a
'r^2	0.9386 ± 0.0193	0.9314 ± 0.0320	0.9152 ± 0.0327	0.9448 ± 0.0151
"r^2	0.9800 ± 0.0036	0.9302 ± 0.0466	0.9333 ± 0.0649	0.9572 ± 0.0034
r$^{2'}$	0.9968 ± 0.0020	0.9854 ± 0.0031	0.9861 ± 0.0084	0.9925 ± 0.0011
r$^{2"}$	0.9955 ± 0.0005	0.9956 ± 0.0002	0.9950 ± 0.0005	0.9950 ± 0.0007

Wheat flour doughs (a), (b), (c) and (d) are as Figure 4.1. Parameters gel strength S and exponent n were derived by fitting both G'(ω) and G"(ω) data to the power-law gel model, with goodness of fit of 'r^2 and "r^2 (mean ± SD, n = 3) for G'(ω) and G"(ω), respectively. Gel strength S' and exponent n' were derived by fitting the G'(ω) data to the power-law gel model, with goodness of fit of r$^{2'}$ (mean ± SD, n = 3). Gel strength S" and exponent n" were derived by fitting and G"(ω) data to the power-law gel model, with goodness of fit of r$^{2"}$(mean ± SD, n = 3). For the same parameter in

each column, values are mean ± SD, n = 3; means labelled by the same letter are not significantly different ($P < 0.05$).

For fitting of the power-law gel model (Eqs. [2] and [3]) and the Burgers model (Eqs. [9] and [10]), independent fits of G'(ω) and G"(ω) were conducted for each replicate. It can be seen that despite the wide range in dough strength, the power-law gel model with two parameters, gel strength (S) and exponent (n), provided an excellent fit to the G'(ω) and G"(ω) data, Figure 4.1 red lines. Over all 30 treatments the range in mean G' values at 1 Hz was from 2940 to 6940 Pa, while there was a two-fold increase in G", and so these 30 treatments clearly cover a large dough strength response (Masi et al., 1998; Skendi et al., 2010; Van Bockstaele et al., 2008b; Yovchev et al., 2017a). However, in contrast to previous studies on dough (Leroy et al., 2010; Ng et al., 2006; Ng, 2008), the use of single values of *S* and *n* for both G'(ω) and G"(ω) for this wide range of dough properties is not appropriate. This is illustrated in Table 4.1 for the four treatments of Figure 4.1. It can be seen that the slopes for storage and loss moduli differ substantially (Table 4.1). For single value fits of *S* and *n* to the data, r^2 values ranged from 0.92 to 0.98, whereas fits improved to r^2 values of 0.985 to 0.997 when the storage and loss moduli were fitted separately to their own *S* and *n* values. This finding is consistent with studies on gluten gels at different temperatures, where n" was consistently larger than n' (Kontogiorgos, 2017). Accordingly, in an evaluation of how wheat cultivar, water and salt affected linear viscoelastic dough properties, as characterized by the power-law gel model, we used S', S", n' and n".

For our wide range of dough strengths, the four-parameter Burgers model was able to fit the G'(ω) data reasonably well, except at the high frequency end (Figure 4.1, blue solid lines), but it was unable to fit the G"(ω) data (Figure 4.1, blue dashed lines). Compared to the Burgers model, the power-law gel model had a better fit for the G'(ω) data (Figure 4.1, red and blue solid lines).

Therefore, the power-law gel model with two parameters is better at characterizing dough's linear viscoelasticity compared to the four-parameter Burgers model. Because of the poor fit of Eq. [10], no further analysis of the loss modulus using the Burgers model was conducted.

4.4.2. Non-Linear Viscoelastic Behavior of Dough

To investigate the non-linear viscoelastic behavior of wheat flour dough, the shear creep compliance $J_c(t)$ and recovery compliance $J_r(t)$ were determined. To illustrate the range in rheological behavior, the creep-recovery response of the same dough formulations of Figure 4.1 are shown in Figure 4.2. As expected (Hardt et al., 2014; Yovchev et al., 2017a, 2017c), the $J_c(t)$ and $J_r(t)$ were larger for the weaker dough formulations (Figure 4.2).

Figure 4.2: The compliance (J(t), symbols ■) as a function of time (t) for wheat flour doughs over a range of breadmaking strengths. Wheat flour doughs (a), (b), (c) and (d) are as Figure 4.1. Red lines are the power-law gel model fitting for the creep compliance $J_c(t)$ (solid line) and recovery compliance $J_r(t)$ (dashed line) of doughs with Eqs. [4] and [5], respectively. Blue lines are the Burgers model fitting for the creep compliance $J_c(t)$ (solid line) and recovery compliance $J_r(t)$ (dashed line) of doughs with Eqs. [6] and [7], respectively. Error bars show ± 1 SD, n = 3.

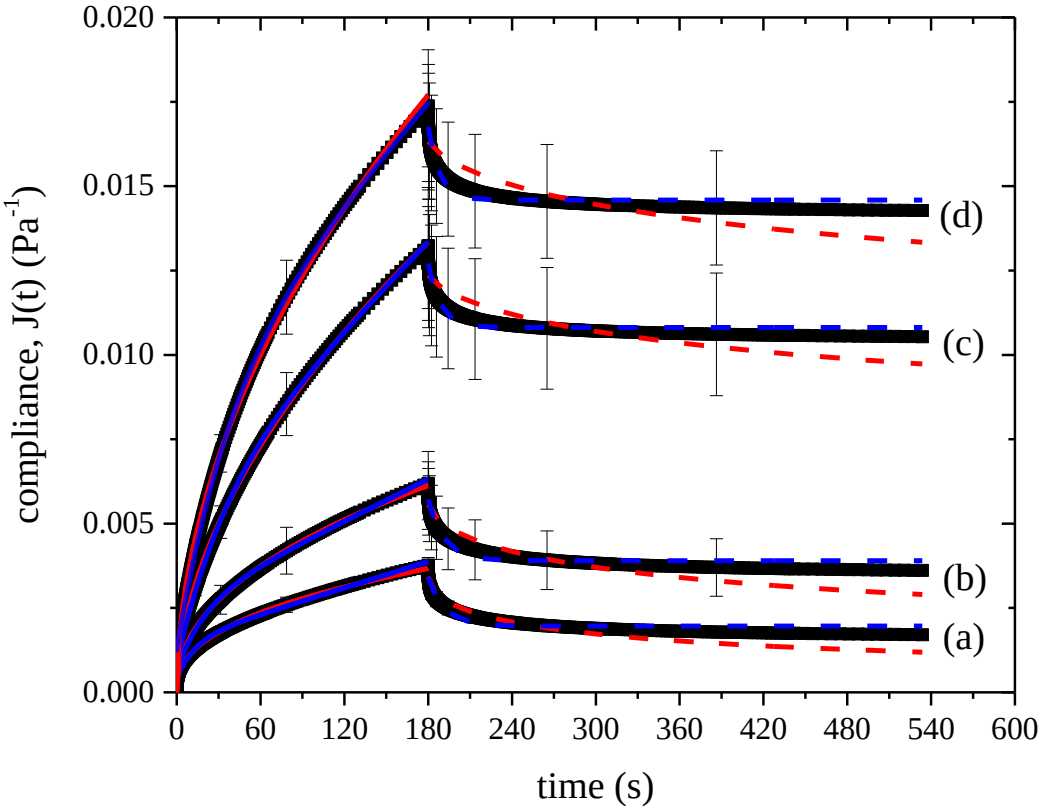

The $J_c(t)$ and $J_r(t)$ data were fitted to the power-law gel model (Eqs. [4] and [5]), respectively (Figure 4.2, red lines), i.e., the creep and recovery data were fitted independently. Attempts to model both sets of non-linear viscoelastic data with a single S and n provided poor fits ($r^2 \sim 0.75$) to either the recovery data or both creep and recovery data. As a result, the parameters derived in the creep phase were not equivalent to those derived in the recovery phase, an outcome

also reported by Lazaridou et al. (2007). The $J_c(t)$ data were well modeled by the power-law gel model despite the wide range of dough strengths analyzed (Figure 4.2, red solid lines) with r^2 values being 0.997 or greater. The recovery data were not modeled as well by the power-law gel model, particularly at long times where the model that was comprised of multiple relaxation times implied recovery that was not evident in the experimental data for any of the formulations.

The $J_c(t)$ and $J_r(t)$ were also independently fitted to the four-element Burgers model, Eqs. [6] and [7]. Over a wide range of dough strengths, the simple Burgers model fitted the $J_c(t)$ data very well (Figure 4.2, blue solid lines), $r^2 > 0.993$. For the recovery phase, very good fits were obtained except at long times (Figure 4.2, blue dashed lines). For the Burgers modeling at long times, the opposite effect was observed compared to the power-law gel model: the dough is modeled as experiencing its full recovery, whereas experimentally it continues to demonstrate shear recovery some 360 s after removal of the stress (Meerts et al., 2017; Van Bockstaele et al., 2011). This is not surprising when one examines the Burgers model parameters for the four dough formulations in Figure 4.2. The best-fit to the data predicts the retardation time ($\lambda^r = \eta^r_2/R^r_2$) for the four treatments in Figure 4.2 to have values from 8.3 ± 0.3 to 13.4 ± 0.1s. Therefore, one minute after load removal, the Burgers model predicts that appreciable recovery is not possible.

4.4.3. Correlation of Rheological Model Parameters

The Pearson correlation coefficients (r) were calculated for all rheological model parameters of wheat flour doughs to examine the strength of relationships between the various constitutive parameters. Power-law gel model parameters derived from G'(ω) and G"(ω) indicated that the gel strength parameter S' was highly correlated with S" (r = 0.905), but the exponent n' was poorly correlated with n" (r = 0.165). The positive linear relationship between S' and S" is shown in Figure 4.3 for the wheat cultivars Harvest (r^2 = 0.871) and Roblin (r^2 = 0.933). The

overall slope was 1.7, indicative of a rheological response to "strengthening" parameters, such as increased salt and reduced water content that affect the elastic character of the dough more than its viscous nature.

Figure 4.3: The relationship between the gel strength parameters S', S" determined from G'(ω) and G"(ω) plots for various wheat flour dough formulations made from the cultivars Harvest (blue squares) and Roblin (red squares). Error bars show ± 1 SD, n = 3. Horizontal error bars are used for S'. Vertical error bars are used for S".

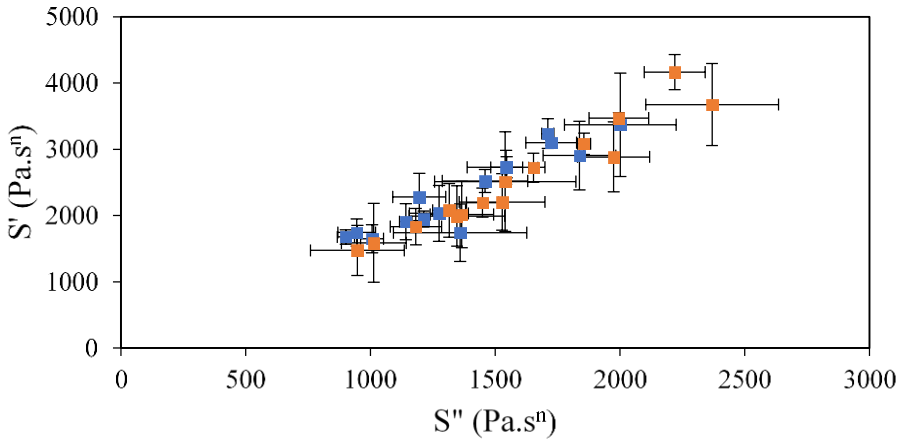

For the non-linear rheology, the gel strength parameter S^c derived from the creep data was strongly correlated with S^r derived from the recovery data (r = 0.956). Positive linear relationships were observed for doughs made from the wheat cultivars Harvest (r^2 = 0.980) and Roblin (r^2 = 0.875) (Figure 4.4a). The overall slope was 2.4, so that the formulation changes that weaken the dough are more effective at disrupting its recovery rather than its flow. The gel exponent n^c obtained from the creep phase was also highly positively correlated with n^r obtained from the recovery phase (Harvest, r^2 = 0.936 and Roblin, r^2 = 0.899) (Figure 4.4b). The overall slope from Figure 4.4b is 1.7, again indicative of more effective diminishment of the recovery process than the flow process as a result of formulation changes. From Gabriele et al. (2001):

$$G(t)=St^{-n} \qquad [11]$$

so we would expect an acceleration of stress relaxation processes with the formulation changes that weaken the dough since n is increased. Strong correlation of the maximum creep and recovery strain (r = 0.942) has been observed for doughs of a fixed salt content and various water contents made from durum wheat flours (Mastromatteo et al., 2013) and common wheat flours (Meerts et al., 2017).

Figure 4.4: The relationship between (a) the gel strength parameters S^c, S^r (b) exponent parameters n^c, n^r measured in creep and recovery for various wheat flour dough formulations made from the cultivars Harvest (blue squares) and Roblin (red squares). Error bars show ± 1 SD, n = 3. Horizontal error bars are used for (a) S^c, (b) n^c. Vertical error bars are used for (a) S^r, (b) n^r.

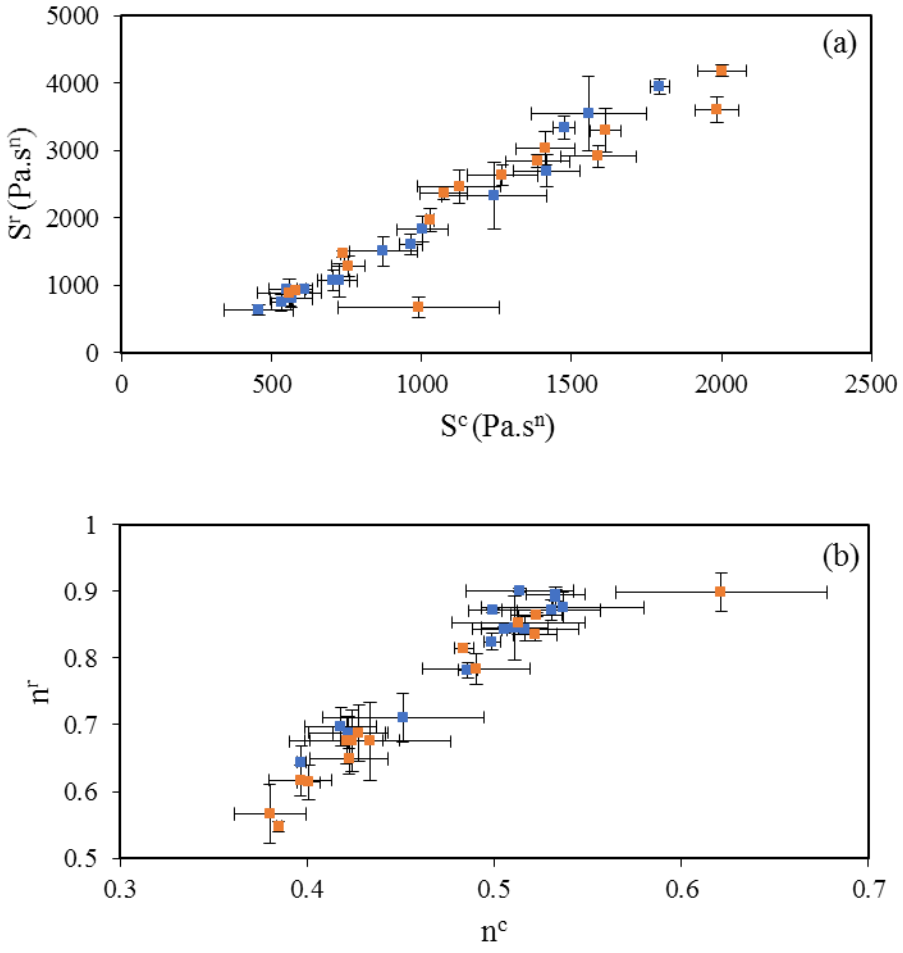

The correlations of power-law model parameters in the linear and non-linear viscoelastic region showed that the gel strength (*i.e.*, S' and S") from dynamic oscillatory rheometry tests at small strain were highly correlated with those (*i.e.*, S^c and S^r) from the creep-recovery tests (the four r values ranged from 0.781 to 0.918). However, poor correlations were observed for the gel exponent, with r values being as low as 0.086 to 0.429 between the linear (*i.e.*, n' and n") and non-linear (*i.e.*, n^c and n^r) viscoelastic tests. Therefore, gel strength parameters (S) from the power-law gel model are appropriate descriptors for both the linear and non-linear viscoelasticity of wheat flour doughs generated using a wide range of formulations.

As both power-law gel and Burgers models fitted the G'(ω) data, the power-law gel parameters also correlated with a number of the Burgers model parameters. In the linear elastic region, the gel strength S' was highly correlated with the spring (elastic) constant from the Kelvin-Voigt model R_2' (r = 0.911) and the dashpot (viscous) constant from the Maxwell model η_1' (r = 0.996). The creep characterizations were also well correlated between the two types of models of dough behavior. The parameter S^c was correlated to both R_1^c (0.956) and R_2^c (0.829); this was also seen in the recovery phase for S^r, but with correlations that were not as strong (0.779 for R_1^r and 0.766 for R_2^r). High positive correlations between the respective S parameter and the Burgers viscosity η_1 were also observed (0.938 in creep and 0.773 in recovery).

Parameters from the Burgers model were all positively correlated between the creep and recovery phases except for the retardation times, λ^c and λ^r, which had a negative correlation (r = -0.803). For instance, the elastic constant R_1^c in creep showed a strong linear relationship with R_1^r in recovery (Harvest, r^2 = 0.983 and Roblin, r^2 = 0.988) (Figure 4.5a), which corresponds to a good correlation for the elastic parameters between the creep and recovery phases, as previously observed by Jekle & Becker (2011). The inverse linear relationship between λ^c and λ^r (Harvest, r^2

= 0.889 and Roblin, $r^2 = 0.576$) (Figure 4.5b) contrasts with previous studies that showed a positive correlation of time constants between the creep and recovery phases (Lazaridou et al., 2007).

Figure 4.5: The relationship between Burgers model parameters (a) the elastic constant R_1^c, R_1^r (b) the retardation time λ^c, λ^r measured in creep and recovery for various wheat flour dough formulations made from the cultivars Harvest (blue squares) and Roblin (red squares). Error bars show ± 1 SD, n = 3. Horizontal error bars are used for (a) R_1^c, (b) λ^c. Vertical error bars are used for (a) R_1^r, (b) λ^r.

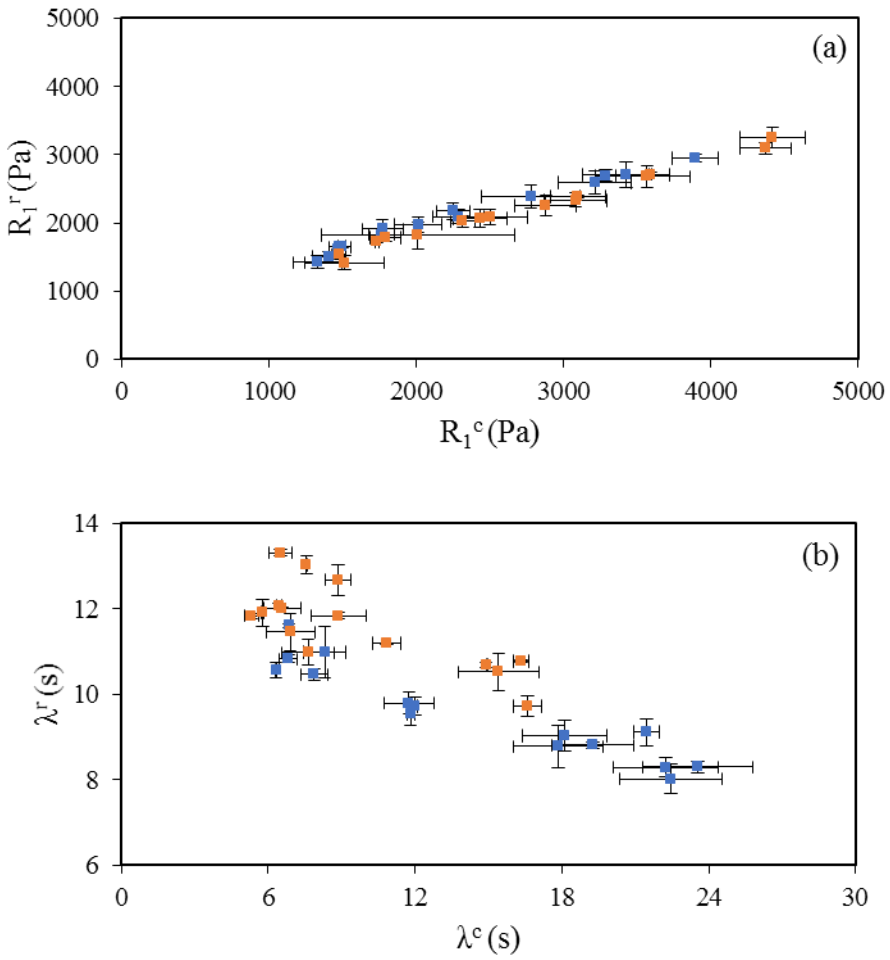

4.4.4. Effects of Wheat Cultivar, Water and Salt on Rheological Model Parameters of Dough

The model parameters which were useful for characterizing the rheology of the doughs were also examined by an analysis of variance to determine how definitions of dough strength were affected by variety, and by the influence of salt and water (Table 4.2). Only the Burgers model parameters for the non-linear rheological tests are shown in Table 2 due to the model's poor fit for the G"(ω) data. Greater values of the gel strength parameters were found for doughs made from the stronger wheat cultivar Roblin, although for S' the difference was not significant (Table 4.2). This indicates a positive relationship between gel strength parameters and dough strength (Ng, 2008). Therefore, gel strength can be considered as a "dough strength" parameter for both oscillatory and creep assessments of dough rheology. Differences in the power exponent n were observed between the two cultivars, although they were more manifest in the large strain test than in the linear viscoelastic test. The exponent was smaller for the stronger variety, implying that this dough took longer to relax.

Table 4.2: Effects of wheat cultivar, water and salt content on rheological model parameters of wheat flour doughs

Model	Wheat Cultivar		Water Content (%, flour weight)					Salt Content		
Parameters	Harvest	Roblin	FAB-4	FAB-2	FAB	FAB+2	FAB+4	0	0.25M	2.5%
S' (Pa.s^n)	2372^a	2527^a	3503^a	2627^b	2372^{bc}	2010^{cd}	1734^d	2732^a	2321^b	2294^b
S" (Pa.s^n)	1391^b	1584^a	2004^a	1647^b	1435^c	1299^c	1053^d	1702^a	1353^b	1408^b
S^c (Pa.s^n)	965^b	1207^a	1734^a	1315^b	1036^c	773^d	573^e	1227^a	1008^b	1023^b
S^r (Pa.s^n)	1823^b	2304^a	3592^a	2621^b	2046^c	1157^d	903^d	2408^a	1897^b	1887^c
n'	0.256^a	0.263^a	0.242^a	0.267^a	0.260^a	0.265^a	0.264^a	0.252^a	0.260^a	0.267^a
n"	0.331^a	0.324^b	0.319^b	0.327^{ab}	0.327^{ab}	0.330^{ab}	0.333^a	0.321^b	0.333^a	0.328^{ab}
n^c	0.490^a	0.456^b	0.4^c	0.452^b	0.469^b	0.528^a	0.517^a	0.474^a	0.476^a	0.471^a
n^r	0.814^a	0.716^b	0.623^d	0.718^c	0.764^b	0.851^a	0.87^a	0.765^{ab}	0.777^a	0.754^b
R_1^c (Pa)	2258^b	2719^a	3829^a	2965^b	2350^c	1780^d	1499^e	2784^a	2342^b	2339^b
R_1^r (Pa)	2077^b	2212^a	2897^a	2410^b	2088^c	1782^d	1546^e	2323^a	2065^b	2045^b
R_2^c (Pa)	485^b	946^a	1094^a	761a^b	537^{ab}	974^a	209^b	683^a	532^a	931^a
R_2^r (Pa)	727^a	590^a	815^a	653^b	571^a	830^a	424^a	650^a	572^a	754^a
λ^c (s)	14.1^a	9.7^b	6.3^d	8.1^d	11^c	16.1^b	18.2^a	11.5^b	13.2^a	11.1^b
λ^r (s)	9.6^b	11.6^a	11.7^a	11.4^b	10.7^c	9.9^d	9.4^e	10.6^b	10.2^c	11.1^a
η_1^c (kPa.s)	30.2^b	41.8^a	66.7^a	42.2^b	33.2^c	20.4^d	17.4^d	38.9^a	34.2^b	34.9^b
η_1^r (kPa.s)	36.6^b	51.3^a	87.4^a	50.5^b	36.9^b	30.7^{bc}	14.2^c	45.0^a	39.3^a	47.5^a

Gel strength (S^c, S^r) and exponent (n^c, n^r) were derived according to Eqs [4] and [5]. Spring (elastic) constants from the Maxwell (R_1^c, R_1^r) and Kelvin-Voigt (R_2^c, R_2^r) model, retardation time (λ^c, λ^r), and dashpot (viscous) constants from the Maxwell model (η_1^c, η_1^r) were derived according to Eqs

[6], [7] and [8]. To evaluate the effect of one of the three variables (*i.e.*, cultivar, water and salt content) by averaging the effects of the other two, values labelled by the same letter are not significantly different ($P < 0.05$).

With increasing water content, all four gel strength parameters (S', S'', S^c and S^r) of the doughs decreased. This corresponds with the results of Ng (2008) that gel strength responded strongly to water addition over a range of dough formulations. Due to its relative higher mobility, water performs as a mobility enhancer that is incorporated into the gluten polymers to increase the mobility and the flexibility of the gluten-water hydrocolloid (Ferry, 1961; Jekle & Becker, 2012). Therefore, the water-induced decrease in gel strength is due to the positive effect of water on the mobility of gluten polymeric system. The parameter S^c, strength measured in the creep test, was more responsive to the effect of water compared to the other three parameters (Table 4.2). These findings are consistent with previous studies that have shown a softening effect of water on dough from both empirical and fundamental rheological measurements (Berland & Launay, 1995a; Hardt et al., 2014; Jekle & Becker, 2012). The exponent's characterizations of changes in dough strength brought about by water addition were rather poor for the oscillatory tests, but discriminatory under creep and recovery testing. For the oscillatory tests, no significant change in the exponent was seen when varying the water content (Table 4.2, n' and n''), corresponding with findings by Ng (2008). With a decrease in water content, the exponent under creep and recovery decreased (Table 4.2, n^c and n^r).

Unlike the relatively straightforward effect of water on dough rheology (Meerts et al., 2017), the effect of salt on dough strength was more complex. Larger values of the gel strength parameters (S' and S'') were seen for no-salt doughs rather than salted doughs (Table 4.2), indicating that dough strength decreased with salt addition. This corresponds with previous studies

that have shown the complex modulus ($G^* = (G'^2 + G''^2)^{1/2}$) decreasing with addition of NaCl (Jekle & Becker, 2012). The authors argued that NaCl in the dough system neutralized the charged groups of the gluten proteins and inhibited the interaction of water molecules with the gluten proteins (Bushuk & Hlynka, 1964; Jekle & Becker, 2012). Weaker gluten-water interactions may lead to release of confined water molecules from nanoporous structures to the surrounding area of the gluten network, which in turn increases the amount of mobile water molecules surrounding the gluten network (Kontogiorgos, Shah, & Bills, 2016; Kontogiorgos, 2017). A weakening effect with 0.25M salt addition was also observed for the S parameter in both creep and recovery. Small changes in S were observed as the salt content was further increased to 2.5% (flour weight basis).

The parameters from the Burgers model also substantiated the conclusions drawn about the effects of cultivar, water and salt on dough strength. In creep and recovery, both moduli, R_1 and R_2, increased for Roblin compared to Harvest (although for R_2^r the cultivar-dependent difference was not significant, Table 4.2). Viscosities in both creep and recovery also were higher for Roblin. Larger η_1^c and η_1^r observed for doughs made from the stronger cultivar Roblin, corresponds with the positive correlation between the η_1^c and strength for doughs made from durum wheat cultivars with a wide range of gluten strength (Edwards et al., 2001). With increasing water content, both elastic parameters and the viscosity decreased, with the response being more manifest in the creep test (Table 4.2). This finding agrees with previous studies that showed water addition had a negative effect on the elasticity and viscosity of dough measured by creep-recovery parameters (Mastromatteo et al., 2013; Meerts et al., 2017; Yovchev et al., 2017a). The weakening effect of water on the elastic parameters is also found for gluten-free doughs (Lazaridou et al., 2007). The faster relaxation of doughs that are weaker, as predicted from the n values of the power-law gel model, is observed for Harvest, but only in the recovery test, and this is also seen as decreased

recovery relaxation times with increases in water content as the dough is weakened (Table 4.2). The perplexing negative correlation between relaxation times shown in Figure 4.5b is likely responsible for the creep phase result of Table 4.2 - relaxation times lengthening as the water content in the dough was increased. Burgers model parameters did not indicate a clear response of wheat flour dough to the addition of salt (Table 4.2), but the hydrocolloid network has less immediate elastic response in creep (R_1^c) and in recovery (R_1^r) when salt is added. This infers that salt directly alters the structure of the actively elastic protein network (Kontogiorgos, 2017).

4.5. Conclusions

Dough is an industrially important hydrocolloid whose mechanical properties are particularly sensitive to changes in water and salt content. Over a wide range of dough strength and formulations (particularly with reduced salt content), a power-law gel model fitted the experimental data well for linear viscoelasticity and creep-recovery tests. However, for this wide range of dough properties, separate gel strength and exponent parameters were required to attain good fits to the experimental data for both the linear and non-linear viscoelastic regions. Compared to the four-element Burgers model, the power-law gel model was better at describing the linear viscoelasticity of wheat flour dough, but was poorer at recovery test characterization.

Both gel strength and exponent derived from creep tests showed highly positive correlations with their counterparts in recovery. Changes in composition that weakened the dough hydrocolloids were more effective at diminishing dough elasticity rather than its flow. The highly positive correlations of gel strength parameters between the linear and non-linear viscoelastic tests showed the capacity of power-law gel models to describe the rheology of wheat flour doughs made from a wide range of formulations.

4.6. Acknowledgements

The authors would like to acknowledge the financial support provided by Canada Bread Corp. (Toronto, Canada), the Saskatchewan Agricultural Development Fund, the Western Grains Research Foundation, and through a joint NSERC (Natural Sciences and Engineering Research Council of Canada)-CIHR (Canadian Institute of Health Research) Institute of Nutrition, Metabolism and Diabetes Funding Initiative for Sodium Reduction in the Canadian Food Supply, and CSC (China Scholarship Council).

4.7. Bridge between Chapters 4 and 5

For a wide range of dough strengths and reduced salt (NaCl) formulations, the power-law gel model was able to characterize the linear and non-linear viscoelasticity of doughs well at small strains (Chapter 4). Using the power-law gel model, the best goodness of fit to the linear viscoelasitic parameters, *i.e.*, G'(ω) and G"(ω), were obtained when the G'(ω) and G"(ω) were independently fitted using their own gel strength (S) and exponent (n) (Chapter 4).

The formulation-induced changes in dough rheology characterized with S are expected to alter how bubbles are entrained into the dough during mixing. The size distribution of entrained bubbles by the end of mixing (Chapter 5) and how bubble sizes evolve with time (Chapter 5) will affect the crumb cell structure of bread baked from the dough. Therefore, bubble dynamics in the dough will be studied for a wide range of formulation and mixing conditions (Chapter 5). A combined investigation of dough rheology (Chapters 3 and 4) and dough's gas phase (Chapter 5) will provide a solid understanding of dough properties at both macroscopic and microscopic levels. Changes in rheological and gas phase parameters of reduced-salt doughs will provide insights into how to manipulate formulation and mixing conditions to produce doughs more tolerant to salt reduction (Chapters 4 and 5).

5. Investigation of the Effects of Sodium Reduction on Bubble Dynamics in Bread Dough using Synchrotron X-Ray Microtomography

5.1. Abstract

Although the bubble size distribution (BSD) in bread dough has been investigated during breadmaking processes, how dough formulation and processing conditions affect the BSD has not been clearly revealed yet. Therefore, the objective of this study was to use synchrotron X-ray microtomography to investigate the gas volume fraction, BSD and its evolution as a function of changes in formulation (*i.e.*, wheat cultivar, water and salt contents) and mixing conditions (under-, optimal- and over-mixing) for non-yeasted doughs. As Health Canada has targeted reducing sodium content in bread, this study aimed to develop processing strategies (*i.e.*, manipulate dough formulation and mixing time) for improving bubble stability in low-salt (NaCl) doughs. At the end of mixing, a higher gas volume was entrained into the doughs prepared from a weaker wheat cultivar, lower water content, higher salt content, and/or longer mixing time. The BSD in bread dough was well characterized by a lognormal distribution function fitting to the radius dependence of bubble volume fraction BVF(R). The median (R_0) and width (ε) of the distribution changed with time after mixing, and this was indicative of disproportionation. During the resting time after mixing, the rate of disproportionation increased if doughs were prepared at a higher water content, lower salt content, and/or longer mixing time. The loss of gas in the dough was a function of time after the end of mixing. The time-dependent gas loss was more observable for higher water content doughs. Based on how the content of salt and water interactively affect bubble dynamics in dough, disproportionation may be retarded by decreasing water content or increasing salt content. For low-sodium bread production, lower water content can be considered as a means of increasing bubble stability against disproportionation during breadmaking.

5.2. Introduction

During mixing, gas bubbles are entrained into the bread dough and subdivided into a range of smaller sizes (Baker & Mize, 1941, 1946). The number and size of gas bubbles in the dough at the end of mixing, *i.e.*, the bubble size distribution (BSD), has been reported to affect the rheological properties of dough (Upadhyay et al., 2012). Accordingly, the BSD at the end of mixing and how it evolves in the dough during breadmaking have a direct relationship with the crumb structure of the baked bread as well. For example, a higher number of smaller-sized and stable bubbles during breadmaking contributes to a finer crumb cell structure in the resultant bread loaf (Elmehdi et al., 2003; Hayman et al., 1998; Sapirstein et al., 1994; Scanlon & Zghal, 2001; Zghal et al., 1999, 2001; Zghal, Scanlon, & Sapirstein, 2002). Accordingly, to better control dough rheology during breadmaking and to manipulate bread crumb structure, it is essential to investigate the factors affecting the BSD and its evolution during breadmaking.

The entrainment of gas bubbles in the dough is a function of mixing conditions and dough formulation. A higher volume of gas bubbles are entrained into the dough with an increase in mixing pressure (Campbell et al., 1993; Chin & Campbell, 2005b; Elmehdi et al., 2004), mixing speed (Chin & Campbell, 2005a, 2005b; Chiotellis & Campbell, 2003b), mixing time (Kokawa et al., 2012; Koksel & Scanlon, 2012; Mehta et al., 2009; Trinh et al., 2013), and/or mixing work input (Chin & Campbell, 2005b). When these mixing conditions are fixed, a higher volume of gas bubbles are entrained into the dough with the use of weaker wheat cultivars (Campbell et al., 2001), higher water content (Chin et al., 2005a), and/or lower salt content (Chin et al., 2005a; Koksel et al., 2014). Such changes in formulation and how they affect bubble entrainment are critical to optimize loaf quality, especially for low-sodium formulations. For the bakery industry, Health Canada's Sodium Working Group recommends a reduction in sodium concentration in bread to

330 mg sodium /100 g bread (Yovchev et al., 2017b), in order to prevent or eliminate excessive sodium intake from bread products (Centers for Disease Control and Prevention, 2012).

In full-formula doughs before substantial yeast activity and in non-yeasted dough formulations, the evolution of bubbles with time is primarily attributed to disproportionation (van Vliet et al., 1992; van Vliet, 2008). Disproportionation is the pressure-driven diffusion of gas from smaller-sized to larger-sized bubbles (Garrett, 1993; Mills et al., 2003; Murray & Ettelaie, 2004; Stevenson, 2010), resulting in the growth of larger-sized bubbles and shrinkage (and even disappearance) of smaller-sized bubbles (Shimiya & Nakamura, 1997; Shimiya & Yano, 1987, 1988; Venerus et al., 1998; Venerus & Yala, 1997; Venerus, 2001, 2015). Accordingly, disproportionation shifts the mean bubble size towards larger bubble sizes (Bellido et al., 2006; De Guio et al., 2009; Koksel et al., 2014; Leroy et al., 2008) and may lead to a decrease in bubble numbers (van Vliet et al., 1992). Therefore, retarding or preventing disproportionation may contribute to retaining a higher number of smaller-sized bubbles in the dough, which ultimately favors a crumb structure with a uniform distribution of gas cells (Babin et al., 2006, 2005; Scanlon & Zghal, 2001).

Another phenomenon that slows down or prevents disproportionation is strain hardening (Kokelaar et al., 1996; van Vliet & Kokelaar, 1994; van Vliet, 1999). In a bread dough, at a constant strain rate (*i.e.*, bubble sizes increase constantly), as the strain increases (*i.e.*, a bubble grows in size), the stress required to deform a stretched dough will be much larger than that required to deform a non-stretched dough (Kindelspire et al., 2015; van Vliet et al., 1992; van Vliet, 1999). This indicates that the stress around a growing larger-sized bubble is greater than that around smaller-sized bubbles. Larger stress on a bubble surface limits the further growth of a larger-sized bubble (Dobraszczyk & Roberts, 1994; Kokelaar et al., 1996), which in turn decreases

the pressure difference between the larger- and smaller-sized bubbles (van Vliet, 1999, 2008). Due to a lower inter-bubble pressure difference, higher strain hardening properties of a dough matrix help to retard disproportionation and increase bubble stability during breadmaking (Dobraszczyk & Roberts, 1994; Sroan et al., 2009; van Vliet, 2008). The use of stronger wheat cultivars and lower water content have been shown to increase dough's strain hardening and favor bubble stabilization during breadmaking (Janssen et al., 1996; Kokelaar et al., 1996; Sliwinski et al., 2004). In other words, bubble stability decreases with increasing water content due to the diluting effect of water on the soluble proteins (a source of surfactants) in the dough's liquid phase (Salt et al., 2006). A lower protein concentration in dough's liquid phase causes an increase in surface tension and a decrease in bubble stability (Salt et al., 2006). An increase in salt content was reported to greatly reduce surface tension and thus increase bubble stability, possibly retarding disproportionation during breadmaking (Salt et al., 2006). This finding is due to the salt-induced improvement in the dispersion of endogenous lipids (a source of surfactants) in the dough's liquid phase (Salt et al., 2006).

The size distribution of bubbles in dough and its evolution can be described in terms of the number (Bellido, Scanlon, Sapirstein, & Page, 2008; Guillermic et al., 2018; Koksel et al., 2016) or the volume distribution of bubble sizes (Campbell et al., 1991; Koksel, 2014; Trinh et al., 2013). In both cases, bubbles are grouped into size classes from smallest to largest, and the selection of a number or volume basis affects the shape of the BSD. For example, bubbles at the smallest size class may provide a very large contribution to the size distribution on a number basis, whereas they may contribute very little to the size distribution on a volume basis (Koksel, 2014). In such a case, the smallest-sized bubbles no longer significantly affect the distribution if bubble distribution is presented on a volume basis.

A powerful technique to investigate the microstructure of soft solids is X-ray microtomography. X-ray microtomography has been used to investigate the gas volume fraction and size distribution of bubbles in non-yeasted doughs (Bellido et al., 2006; Guillermic et al., 2018; Koksel et al., 2016), as well as the time evolution of the BSD in yeasted doughs during breadmaking (Babin et al., 2006, 2008; Turbin-Orger et al., 2012, 2015) and to show how changes in the BSD during breadmaking links to the resultant bread crumb cell structure (Babin et al., 2005; Falcone et al., 2005). Although these studies proved that X-ray microtomography is very well suited to non-destructive studies of the BSD and its evolution in both yeasted and non-yeasted doughs, bubble dynamics in bread doughs varying in formulation and mixing conditions is yet to be identified.

The objective of this research is to investigate the gas volume fraction, the BSD and its evolution in bread doughs made from a wide range of formulations (*i.e.*, wheat cultivar, and water and salt contents) and mixing times, using synchrotron X-ray microtomography. In light of the changes in the gas phase of the dough, a second objective is to examine how formulation and mixing time can be manipulated to improve bubble stability in low-sodium bread doughs.

5.3. Material and Methods

5.3.1. Bread Dough Preparation

Bread doughs were prepared by mixing wheat flours with various concentrations of water (*i.e.*, at FAB (farinograph absorption), FAB-4%, and FAB+4%, flour weight basis) and salt (*i.e.*, 0 and 2% NaCl, flour weight basis) in a moving bowl 10-g mixograph (National MFG. CO., Lincoln, NE, U.S.A.) equipped with MixSmart software (version 3.80). The wheat flours (provided by Grains Innovation Lab, University of Saskatchewan) were milled from Canada Northern Hard Red (CNHR) wheat cultivars Harvest and Pembina grown in the year of 2016 in one location at

the University of Saskatchewan's Kernen Crop Research Farm (Yovchev et al., 2017b). For each cultivar, 14 kg flour was milled on a Buhler mill after tempering to 15.5% moisture. The FABs of the wheat flours Harvest and Pembina were determined as 65.5% and 61.6%, respectively, using a 50 g farinograph (C. W. Brabender Instruments, South Hackensack, NJ, U.S.A.) according to AACC International Approved Method No. 54-21.02 (AACC International, 2011). At no salt conditions, the optimal mixing time of flours was determined as 3 min 44 s for Harvest and 4 min 49 s for Pembina by the mixograph according to AACC International Approved Method 54-40.02 (AACC International, 1999b). At 2% salt conditions, the optimal mixing time of Harvest doughs was 5 min 14 s and that of Pembina doughs was 6 min 51 s. At FAB, Pembina dough were prepared at three different mixing conditions: 1. under-mixing (1 min); 2. optimal-mixing; 3. over-mixing (10 min). At FAB-4% and FAB+4%, Pembina doughs were prepared at the optimal mixing time.

All doughs were prepared in triplicates at the laboratory room of Canadian Light Source (Saskatoon, SK, Canada). For each replicate, a plastic spatula was used to remove the dough from the mixing bowl of the mixograph after mixing. A cylindrical subsample of approximately 3 mm height was cut away from the dough using the plastic spatula. The remaining dough was then kept in a sealed plastic container for density measurements.

5.3.2. Dough Density

The gas volume fraction from density measurements ($\varphi_{density}$) was determined according to Koksel & Scanlon (2012), shown in Eq. [1].

$$\varphi_{density} = 1 - \frac{\rho_{atm}}{\rho_{gf}} \quad [1]$$

where ρ_{atm} is the dough density measured at atmospheric pressure (P = 1 atm), ρ_{gf} is the gas-free dough density at zero pressure (P = 0 atm). ρ_{gf} was determined from dough density measurements conducted at two pressure conditions: atmospheric and reduced pressure (P ~ 0.04 atm) (Mehta et

al., 2009). Since dough density has an inverse linear relationship with the headspace pressure during mixing (Campbell et al., 1993), ρ_{gf} was determined from the y-axis intercept of the two-points line fitted to the dough density *vs.* mixer headspace pressure graph.

5.3.3. Synchrotron X-Ray Microtomography

To characterize the BSD and its evolution in bread dough, synchrotron X-ray microtomography experiments were conducted on the Biomedical Imaging and Therapy beamlines BMIT-BM 05B1-1 and BMIT-05ID-2 at the Canadian Light Source (Saskatoon, SK, Canada).

For the BMIT-BM 05B1-1 beamline, the X-ray beam had an energy range from 15 to 40 keV. Copper (thickness 0.05 mm) and molybdenum (thickness 0.076 mm) filters were used to filter the polychromatic X-ray beam. An AA40 beam monitor was the detector for the X-ray beams transmitted through the dough subsample. The cerium-doped gadolinium orthosilicate (GSO) scintillator (thickness of 10 μm) was used to convert the transmitted X-ray beams into visible light (Martz et al., 2017). The visible light was delivered to a Hamamatsu C11440-22CU (ORCA FLASH 4) charge-coupled device (CCD) camera. This CCD camera converted the visible light into digital images with a pixel size of 6.5 μm. Preliminary experiments were conducted to optimize the distance between the X-ray source and the dough subsample as 25 m, and the distance between the detector and the dough subsample as 0.15 m.

The BMIT-05ID-2 beamline employed a monochromatic X-ray beam with an energy of 25 keV. The X-ray beam was filtered using an aluminum filter with a thickness of 1 mm. The detector system consisted of an AA-60 beam-monitor, a Gadox (Gadolinium oxysulfide) scintillator with a thickness of 10 μm, and a Hamamatsu C9300-124 CCD camera. The pixel size of X-ray microtomography images obtained from the BMIT-05ID-2 beamline was 8.75 μm. According to preliminary experiments, the optimal distance between the X-ray source and the dough subsample

was 57 m, and the optimal distance between the detector and dough subsamples was 0.8 m (Guillermic et al., 2018).

For both beamlines BMIT-BM 05B1-1 and BMIT-05ID-2, two types of reference scans were sequentially performed to obtain: (1) the dark images (no transmission of X-ray beams, imaging shutter was closed, Figure 5.1a); (2) the flat images (transmission of X-ray beams only, dough subsample and sample holder were out of the X-ray beam, Figure 5.1b) (Koksel et al., 2016). The dark and flat images were used to correct the background of the CCD camera and eliminate noise effects induced by the X-ray source and all optical devices (*i.e.*, filters, scintillator and detector) (Guillermic et al., 2018; Koksel et al., 2016).

The dough subsample (3 mm height) was gently placed in the centre of a custom-made plastic holder, covered with parafilm to prevent drying, then placed in the correct spot within the experimental hutch of the beamline. In the BMIT-BM 05B1-1 beamline, 1001 projections were conducted with a rotation through 180º. The NRecon software, version 1.6.10.4 (Skyscan, U.S.A.), was used to reconstruct these projection images (Figure 5.1c). Each projection image consists of data coded in 299 rows which were rearranged to obtain 299 sinograms (Figure 5.1d). The dimension of each sinogram is 1800 × 300 pixels^2. All the sinograms were then backprojected to obtain 299 cross-sectional images (Fig. 1e), *i.e.*, slices of the dough subsample (dimension: 1800 × 1800 pixels^2/slice, height: 1 pixel/slice).

For the BMIT-05ID-2 beamline, 600 projections were conducted through a rotation of 180º. By using the same procedures of image reconstruction as the BMIT-BM 05B1-1 beamline, these projection images were arranged into 200 sinograms (dimension: 4000 × 248 pixels^2/sinogram). The sinograms were then reconstructed into 200 cross-sectional images of the dough subsample (dimension: 4000 × 4000 pixels^2/slice, height: 1 pixel/slice). Both BMIT-BM 05B1-1 and BMIT-

05ID-2 beamlines were used to monitor bubble dynamics in each dough subsample over a period of 45 min with a new scan every 5 or 10 min.

5.3.4. Image Analysis of Bubble Size Distribution (BSD)

For each dough subsample monitored using the BMIT-BM 05B1-1 beamline, 202 images out of the 299 backprojected 2D cross-sectional images (Figure 5.1e) were selected to avoid edge effects at the top and the bottom of the dough subsample. These 202 cross-sectional images were then divided into two stacks (101 slices/stack). For each stack (*i.e.*, s_1 or s_2), two different areas (*i.e.*, a_1 and a_2) of interest (191 pixels × 166 pixels each, pixel size = 6.5 μm) were selected. Therefore, four volumes (*i.e.*, a_1s_1, a_2s_1, a_1s_2, and a_2s_2) of interest ($191 \times 166 \times 101 \times (6.5)^3$ μm^3 each) were analyzed for determination of the BSD (the distribution of the number of bubbles per unit volume) and its evolution. For dough subsamples monitored on the BMIT-05ID-2 beamline, 196 images out of the 200 2D cross-sectional images were selected. These 196 cross-sectional images were then divided into two stacks (98 slices/stack). Two different areas of interest (101 pixels × 101 pixels each, pixel size = 8.75 μm) were then selected from each stack, resulting in four volumes of interest ($101 \times 101 \times 98 \times (8.75)^3$ μm^3 each) for the BSD analyses. Therefore, each selected volume (~ 0.8 mm^3) of interest was approximately equivalent between the two beamlines. All the selected areas of interest (yellow square, Figure 5.1e) were set away from the edges of the cross-sectional image. Using a custom-written MATLAB (version 7.12.0.635) code (Appendix 2), image intensity was enhanced by the 'histogram equalization' command. This procedure transforms the intensity values of an input image into a new range of intensity values, so that the resultant output image (Figure 5.1f) has a new uniformly distributed range of 64 intensity values.

Following this image intensity enhancement, a thresholding procedure was conducted to segment the bubbles from the background, *i.e.*, the dough matrix (Figure 5.1g). The gas volume fraction determined by density measurements ($\varphi_{density}$) was used to guide the calibration of image segmentation thresholding values (Koksel et al., 2016). The threshold of a stack of images was determined by matching the resultant gas volume fraction ($\varphi_{X\text{-}ray}$) to the $\varphi_{density}$ determined 0 min after mixing. The variation between $\varphi_{density}$ and $\varphi_{X\text{-}ray}$ (0 min) was less than 0.05% to ensure the accuracy of the threshold values. To determine the $\varphi_{X\text{-}ray}$ data as a function of time, *i.e.*, 10, 20, 30, 40, 45 min after mixing, the same threshold value was used. As a result of thresholding, all pixels in the input image that had larger intensity values than the threshold value were converted to white while rest of the pixels were converted to black in the output image. For each dough subsample, $\varphi_{X\text{-}ray}$ was reported as the average of gas volume fraction values derived from four volumes of interest of the dough.

The characterization of dough's 3D features over the stacks of 2D X-ray microtomography images was performed according to a 6-point neighboring 3D connectivity criterion (Kaufman, Cohen, & Yagel, 1993; Vu, Rangayyan, Deglint, & Boag, 2007). As such, bubbles in the dough (Figure 5.1h) are considered 'real', if their sizes are larger than 6 pixels and background noise otherwise (Koksel et al., 2016).

Figure 5.1: Procedures of X-ray microtomography image reconstruction and analysis: (a) a representative dark image; (b) a representative flat image; (c) a representative projection image; (d) a representative sinogram; (e) a representative 2D cross-sectional image; (f) a magnified 2D cross-sectional image after image intensity enhancement where bubbles are circled in white for ease of identification; (g) a 2D cross-sectional image after image segmentation where bubbles are white and dough matrix is black; (h) a representative 3D volume of interest converted from a stack of the segmented 2D cross-sectional images where bubbles are yellow-green.

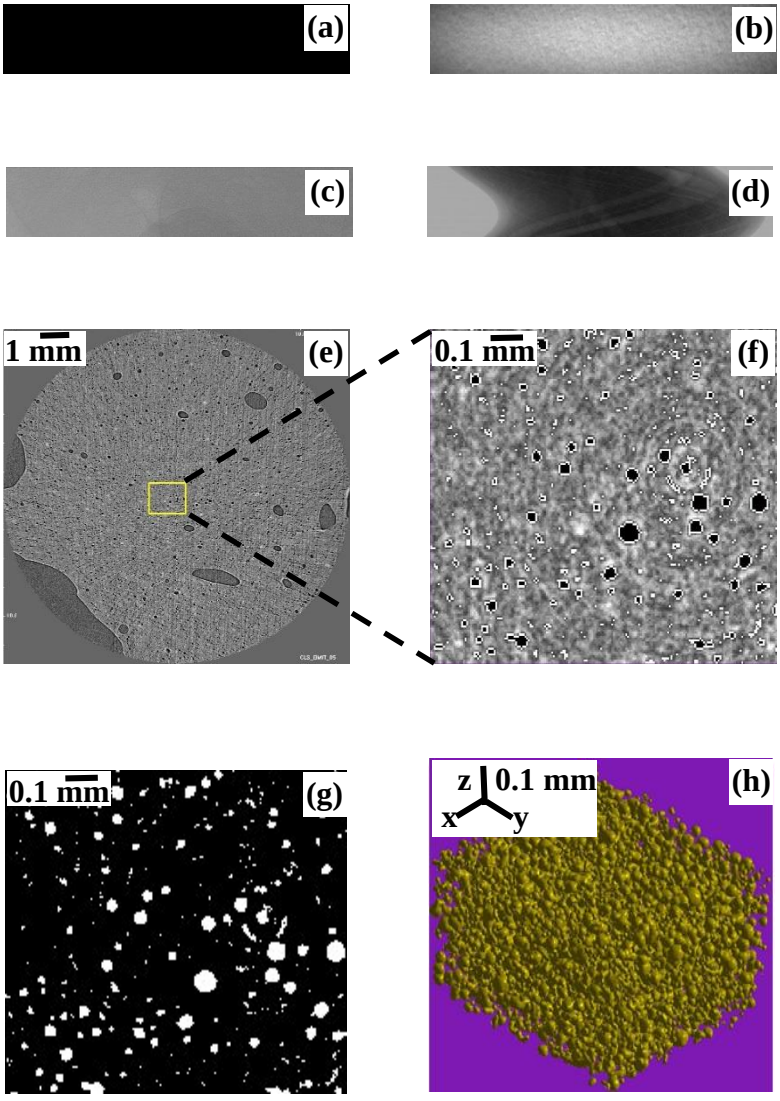

5.3.5. Radius Dependence of Bubble Volume Fraction [BVF(R)]

The radius dependence of bubble volume fraction [BVF(*R*)] is defined as the distribution of the contribution of gas bubbles at each size class (*i.e.*, 16 size classes, each 5 μm wide, from 0 to 80 μm) to the total gas volume fraction in the dough (Koksel, 2014). The BVF(*R*) in the dough is expressed in Eq. [2].

$$\mathrm{BVF}(R) = \int_0^\infty \frac{4}{3}\pi R^3 \mathrm{BSD}(R)\, \mathrm{d}R \qquad [2]$$

where *R* is the bubble radius (μm), and BSD(*R*) is the radius dependence of bubble size distribution on a number basis. For one bubble size class with the mean bubble radius of R_i, the BVF(R_i) in bread dough can be described as in Eq. [3].

$$\mathrm{BVF}(R_i) = \int_{R_i - \Delta R}^{R_i + \Delta R} \frac{4}{3}\pi {R_i}^3 \mathrm{BSD}(R_i)\mathrm{d}R_i \qquad [3]$$

where $R_i - \Delta R$ is the smallest bubble radius in this bubble size class, $R_i + \Delta R$ is the largest bubble radius in this bubble size class, and ΔR is half the width of this bubble size class. The frequency distributions of bubble sizes for BVF(*R*) were constructed by the procedure of 2D frequency counts (Origin graphing and analysis software, version 2016, Originlab Corporation, Northampton, MA, U.S.A.). Rather than using the BSD(*R*), the BVF(*R*) is used to minimize the effect of missing the consideration of smaller-sized bubbles that arise from limitations in image resolution, and also to emphasize the presence of the larger bubbles that have the largest contribution to changes in dough density (Campbell et al., 1991; Koksel, 2014).

At a fixed time after dough mixing, the BVF(*R*) was reported as the average of the 4 volumes of interest from three dough replicates for each dough formulation. The average BVF(*R*) was fitted by a lognormal distribution probability density function, shown in Eq. [4].

$$f(R) = \frac{1}{\sqrt{2\pi}\varepsilon R} \exp\left(\frac{-[\ln(R/R_0)]^2}{2\varepsilon^2}\right) \quad [4]$$

where R is the bubble radius (μm), R_0 is the median of the lognormal distribution, and ε is the width of the lognormal distribution (Bellido et al., 2006; Shimiya & Nakamura, 1997).

5.3.6. Statistical Analysis

Analysis of variance (ANOVA) using the Statistical Analysis Systems (SAS, version 9.4, Appendix 4c and 7) was conducted to evaluate the effects of wheat cultivar, the concentrations of water and salt, and mixing time on the gas volume fraction, median and width of the fitted lognormal BVF(R). For various wheat cultivars and salt contents, the difference in the slopes of linear fits of the median of fitted lognormal BVF(R) *vs.* time after mixing were analyzed by the F-test (linear fit comparison of parameters in Origin graphing and analysis software, version 2016, Originlab Corporation, Northampton, MA, U.S.A.).

5.4. Results and Discussion

5.4.1. The Gas Volume Fraction and BVF(R) in Doughs

At fixed FAB water and 2% salt, doughs made from the weaker wheat cultivar Harvest had a larger value of $\varphi_{X\text{-}ray}$ compared to those made from the stronger wheat cultivar Pembina (Table 5.1). When salt was reduced from 2% to 0, although statistically not significant, $\varphi_{X\text{-}ray}$ was again larger for Harvest when compared to Pembina, indicating that the weaker wheat cultivar entrained more gas at the end of mixing, in line with previous findings from dough density measurements (Campbell et al., 1993; Chin et al., 2005a).

Table 5.1: The gas volume fraction ($\varphi_{X\text{-}ray}$) in doughs

Dough formulation				[a] $\varphi_{X\text{-}ray}$ (%)
wheat cultivar	water content	salt content	mixing time	
Harvest	[b] FAB	0	3 min 44 s	7.04 ± 0.81[c]
Harvest	FAB	2%	5 min 14 s	10.18 ± 0.70[a]
Pembina	FAB-4	0	4 min 49 s	9.03 ± 0.54[b]
Pembina	FAB-4	2%	6 min 51 s	9.72 ± 0.25[a]
Pembina	FAB	0	4 min 49 s	6.88 ± 0.37[c]
Pembina	FAB	2%	6 min 51 s	7.42 ± 0.42[c]
Pembina	FAB+4	0	4 min 49 s	3.91 ± 0.07[d]
Pembina	FAB+4	2%	6 min 51 s	2.54 ± 0.38[e]

[a] $\varphi_{X\text{-}ray}$ is the gas volume fraction from X-ray microtomography analyses determined at the end of mixing, and values (mean ± SD, n = 12) labelled by the same letter are not significantly different ($P < 0.05$). [b] FAB is farinograph water absorption of wheat flour.

For Pembina doughs with a fixed salt content, the $\varphi_{X\text{-}ray}$ decreased with increasing water content (Table 5.1), indicating that higher water content doughs entrain a lower gas volume at the end of mixing, in agreement with the findings of Peighambardoust, Fallah, Hamer, & van der Goot (2010) determined by dough density measurements. In contrast, the gas volume entrained at the end of mixing increased with increasing water content in gluten-starch blended doughs (Koksel & Scanlon, 2012) and with other wheat flour doughs (Chin et al., 2005a). As water content is increased, the optimal development of dough is delayed (D'Appolonia & Gilles, 1971). Therefore, it takes a longer mixing time for higher water content doughs to reach their optimal development, contributing to a higher gas volume entrained (Chin et al., 2005a; Koksel & Scanlon, 2012). As

mixing time is fixed for doughs regardless of water content in our study, higher water content doughs appear to achieve a lower degree of development at the end of mixing and thus entrain a lower gas volume (D'Appolonia & Gilles, 1971; Peighambardoust et al., 2010).

At FAB water, the $\varphi_{X\text{-}ray}$ value of no-salt Harvest doughs was smaller compared to that of salted Harvest doughs (Table 5.1). Although statistically insignificant, a smaller value of $\varphi_{X\text{-}ray}$ was also seen for Pembina doughs with 0 salt and FAB water compared to that for Pembina doughs with 2% salt and FAB water. These results indicate a negative effect of salt reduction on dough's gas volume fraction at the end of mixing. From mixograph measurements, salt reduction has been observed to decrease the optimal mixing development time of dough (Danno & Hoseney, 1982a; Lang et al., 1992). In our study, no-salt doughs were mixed for a shorter time to reach their optimal development. The lower volume of gas bubbles entrained into no-salt doughs at the end of mixing can be attributed to the positive effect of mixing time on gas bubble entrainment (Kokawa et al., 2012; Koksel & Scanlon, 2012; Mehta et al., 2009; Trinh et al., 2013).

Figure 5.2: The radius dependence of bubble volume fraction (BVF(R)) tested (a) 0 min and (b) 45 min after optimal-mixing condition for Pembina dough with 0 salt and FAB water (replicate 1). Error bars show ± 1 SD, n = 4. Blue lines are the lognormal distribution function fitted to the BVF(R), (a) $r^2 = 0.985$ and (b) $r^2 = 0.784$.

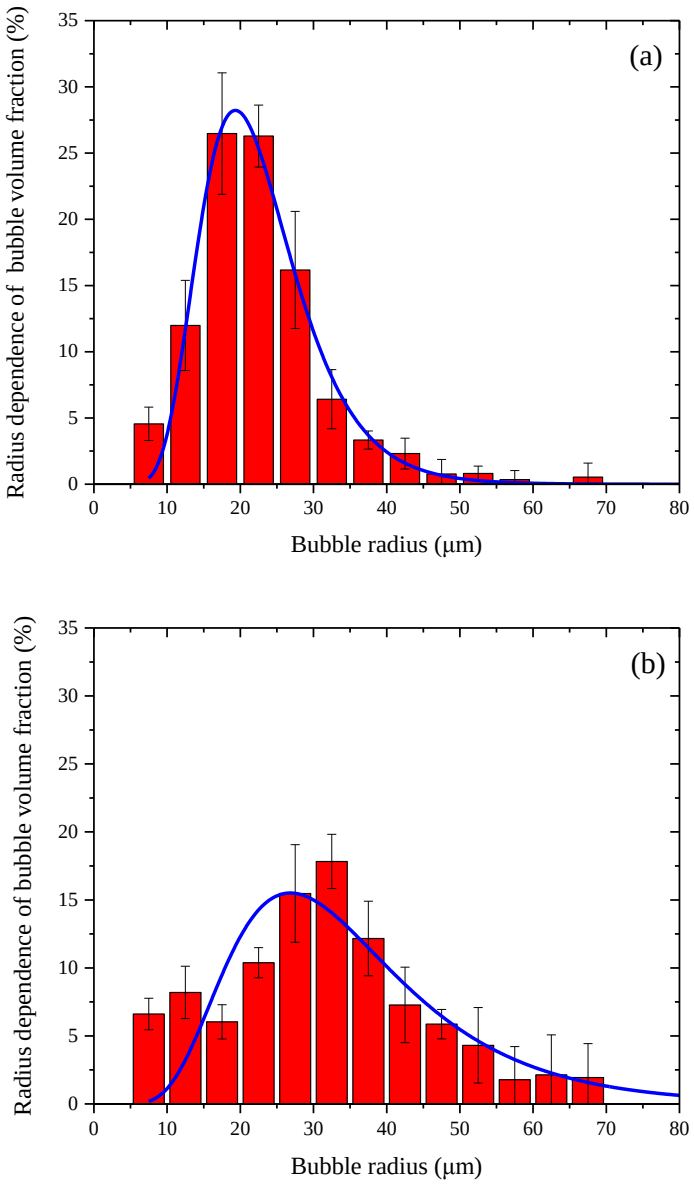

For optimally-mixed Pembina doughs with 0 salt and FAB water (replicate 1), the radius dependence of bubble volume fraction (BVF(R)) tested 0 min after mixing is presented in Figure 5.2a. The largest BVF(R) of the dough was seen for bubbles with radii from 15 to 25 μm. This

finding was confirmed for the rest of the dough replicates. For Pembina doughs varying in water and salt concentrations, the lognormal distribution probability density function (Eq. [4]) fitted well to the BVF(R) tested 0 min after mixing (over the bubble radius range from 5 to 80 μm), as shown as the blue line in Figure 5.2a (r^2 = 0.985). The median (R_0) and width (ε) obtained from the lognormal distribution is shown in Table 5.2 for Pembina doughs with various concentrations of water and salt. Regardless of water and salt concentrations, no significant change in the R_0 tested 0 min after mixing was observed. The width of the distribution (ε) of no-salt doughs was not statistically different across water contents, whereas ε of salted doughs was larger for FAB+4% doughs than at the water contents of FAB and FAB-4%.

5.4.2. The Time Evolution of Gas Bubbles in Optimally-Mixed Doughs

By comparing the BVF(R) tested 45min after mixing (Figure 5.2b) with that tested 0 min after mixing (Figure 5.2a) for the same replicate of Pembina dough with FAB water, the largest peak in dough's BVF(R) shifted to a larger bubble radius range (30 to 35 μm). Over the 45 min, the values of BVF(R) over the bubble radius range of 10 to 25 μm decreased, whereas these over the bubble radius range of 25 to 80 μm increased (Figure 5.2), as a result of shrinkage of smaller-sized bubbles and growth of larger-sized bubbles, due to disproportionation (Kokelaar et al., 1996; Leroy et al., 2008; Meinders & Van Vliet, 2004; Murray & Ettelaie, 2004; Shimiya & Yano, 1988; Turbin-Orger et al., 2015).

For Pembina doughs over a wide range of breadmaking strengths tested 45 min after mixing, the lognormal distribution function was still a reasonable fit for the BVF(R). For example, the lognormal distribution fitting curve for the BVF(R) of Pembina dough with FAB water (replicate 1) tested 45 min after mixing is shown as the blue line in Fig. 2b with a goodness of fit value of 0.784. However, at 0 min, the r^2 was higher (0.985), indicating that a better

characterization of lognormal BVF(R) in bread dough occurred at the shorter time. The contribution of the smallest bubble size class (*i.e.*, bubble radius of 5 to 10 μm) to total gas volume fraction of the dough increased over the 45 min following mixing (compare Figure 5.2b to Figure 5.2a), indicating a time-dependent increase in the total volume of the bubbles at this smallest size class. This finding can be explained as being due to the disproportionation-induced shrinkage of the bubbles at the size class next to the smallest size class. A decrease in those bubble sizes results in an increase in the number of smallest-sized bubbles, possibly increasing the total bubble volume corresponding to the smallest size class.

The parameters median (R_0) and width (ε) obtained from the lognormal distribution function fitted to the BVF(R)s tested 45 min after mixing are shown in Table 5.2. At a fixed salt content (*i.e.*, 0 or 2%), a larger value of R_0 was observed for FAB+4% doughs, indicating that higher water content promotes the growth of bubble sizes in the dough. The positive effect of higher water content on bubble growth has also been observed from 2D measurements of the bubble surface/volume ratio by X-ray microtomography (Mastromatteo et al., 2013) and the mean bubble diameter by confocal laser scanning microscopy (Upadhyay et al., 2012). As no effect of water on R_0 was observed at 0 min after mixing (Table 5.2), the water-induced increase in bubble sizes only becomes obvious after resting of the dough. Over 45 min, an increase in the R_0 (= 100% × (R_0 at 45 min – R_0 at 0 min) / R_0 at 0 min, Table 5.2) was 31% for the dough with no salt and FAB-4% water, 43% for the dough with no salt and FAB water, 85% for the dough with no salt and FAB+4% water, 31% for the dough with 2% salt and FAB-4% water, 43% for the dough with 2% salt and FAB water, and 88% for the dough with 2% salt and FAB+4% water. With increasing water, the proteins (a source of surfactants) in the dough liquid phase are diluted, resulting in

increased surface tension and decreased bubble stability in the dough (Salt et al., 2006). As such, increased water content promotes disproportionation in the dough.

Table 5.2: The median (R_0) and width (ε) of the fitted lognormal BVF(R) for Pembina doughs

Dough formulation		[a] R_0 (μm)		ε	
water content	salt content	0 min	45 min	0 min	45 min
FAB-4	0	22.8 ± 2.84[a]	30.6 ± 1.22[b]	0.35 ± 0.01[b]	0.47 ± 0.08[b]
FAB-4	2%	21.1 ± 1.52[a]	27.5 ± 1.35[b]	0.33 ± 0.02[b]	0.37 ± 0.04[b]
FAB	0	22.8 ± 2.90[a]	32.6 ± 0.44[b]	0.34 ± 0.02[b]	0.41 ± 0.03[b]
FAB	2%	20.7 ± 0.99[a]	29.6 ± 1.25[b]	0.34 ± 0.02[b]	0.46 ± 0.08[b]
FAB+4	0	21.0 ± 0.46[a]	38.8 ± 2.24[a]	0.37 ± 0.01[ab]	0.49 ± 0.16[ab]
FAB+4	2%	21.5 ± 0.92[a]	40.5 ± 2.98[a]	0.41 ± 0.03[a]	0.56 ± 0.05[a]

[a] R_0 or ε is tested at 0 and 45 min after the end of mixing, and values (mean ± SD, n = 12) labelled by the same letter are not significantly different ($P < 0.05$).

For doughs tested at 45 min after mixing, the higher water content condition (*i.e.*, FAB+4%) resulted in a larger value of ε for both no-salt and salted doughs (Table 5.2). But the effect of higher water content on ε was more significant for salted doughs, indicating that water-induced changes in the size distribution of bubbles become less observable as salt content in the dough is reduced. Like the value of R_0, ε tested at 45 min was larger than that tested 0 min after mixing for each dough formulation (Table 5.2), due to disproportionation (Guillermic et al., 2018; Koksel et al., 2016; Koksel, 2014). Over 45 min, an increase in ε (= 100% × (ε at 45 min – ε at 0 min) / ε at 0 min, Table 5.2) was 34% for the dough with no salt and FAB-4% water, 21% for the dough with no salt and FAB water, 33% for the dough with no salt and FAB+4% water, 12% for the dough with 2% salt and FAB-4% water, 35% for the dough with 2% salt and FAB water, and 37% for

the dough with 2% salt and FAB+4% water. As stronger doughs are formulated at higher salt content and/or lower water content, based on results from mixograph measurements (Baig & Hoseney, 1977; Danno & Hoseney, 1982a), the strongest dough system across 6 formulations (Table 5.2) is 2% salt and FAB-4% water, while the weakest one is no salt and FAB+4% water. The strongest dough system had the smallest increase in ε over time (*i.e.*, 12%), indicating that stronger doughs resist disproportionation (Sroan et al., 2009; van Vliet et al., 1992; van Vliet & Kokelaar, 1994; van Vliet, 1999). The largest increase in ε over time was seen not for the weakest dough system (no salt and FAB+4% water), but it (*i.e.*, 37%) was seen for the dough formulation of 2% salt and FAB+4% water. At FAB+4%, salted doughs were mixed for 6 min 51 s whereas no-salt doughs were mixed for 4 min 49 s (Table 5.1). A longer mixing time applied to salted doughs may enhance the depolymerization of gluten proteins in the dough, which in turn decreases the dough strength (Skerritt et al., 1999). As a result, disproportionation in salted and FAB+4% doughs was observed to a greater extent.

Over the time course of 40 min after mixing, the $\varphi_{X\text{-}ray}$ decreased with increasing time (Table 5.3). This time-dependent decrease in gas volume fraction is attributable to the diffusion of gas from the bubbles in the dough to the surrounding environment of the dough's sample container (Koksel et al., 2016).

Table 5.3: The gas volume fraction ($\varphi_{X\text{-}ray}$) of optimally-mixed doughs with FAB water as a function of time (min) after the end of mixing

Dough formulation		$\varphi_{X\text{-}ray}$ (%)				
wheat cultivar	salt content	0 min	10 min	20 min	30 min	40 min
Harvest	0	7.04 ± 0.81	6.73 ± 0.75	6.56 ± 0.68	6.11 ± 0.71	5.95 ± 0.64
Harvest	2%	10.18 ± 0.70	9.67 ± 0.77	9.68 ± 0.67	9.24 ± 0.65	8.86 ± 0.87
Pembina	0	6.88 ± 0.37	6.72 ± 0.46	6.40 ± 0.37	6.43 ± 0.57	6.03 ± 0.58
Pembina	2%	7.42 ± 0.42	7.24 ± 0.73	6.90 ± 0.49	6.83 ± 0.41	6.59 ± 0.50

The time-dependent change in the median (R_0) and width (ε) obtained from the lognormal distribution function fitted to the BVF(R)s are shown in Figure 5.3 and Figure 5.4, respectively, for optimally-mixed doughs with FAB water and 0 and 2 % salt contents. For all 4 dough formulations, R_0 had a positive linear relationship with time after mixing (Figure 5.3). The formulation of wheat flour doughs determined the slope of the line fitted to R_0 *vs.* time (Figure 5.3, dashed lines), and how good the linear relationship between the R_0 and time was (Figure 5.3, r^2 values). For the doughs made from the same wheat cultivar Harvest or Pembina, no-salt doughs showed larger slopes compared to the salted doughs (although statistically insignificant for Pembina doughs). This indicates that salt reduction may possibly cause a decrease in bubble stability and promote disproportionation. This effect is possibly due to a weakening of the gluten network and a decrease in strain hardening values of the doughs (Preston, 1989; van Vliet et al., 1992; van Vliet & Kokelaar, 1994; van Vliet, 1999) as well as due to a higher surface tension in the liquid phase of dough (Salt et al., 2006). The best linear fit of R_0 against time was seen for the strongest doughs made from the Pembina flour mixed with FAB water and 2% salt.

Figure 5.3: The median of the fitted lognormal BVF(R) of optimally-mixed doughs with FAB water as a function of time after the end of mixing. Dough formulations: Harvest flour and 0 salt (black squares), Harvest flour and 2% salt (red triangles), Pembina flour and 0 salt (blue circles), Pembina flour and 2% salt (green rhombuses). Error bars show ± 1 SD, n = 12. Linear fits (dashed lines): $y = 0.217^{a} x + 23.1$, $r^2 = 0.958$ (black), $y = 0.104^{b} x + 28.0$, $r^2 = 0.872$ (red), $y = 0.223^{a} x + 22.5$, $r^2 = 0.968$ (blue), $y = 0.197^{a} x + 20.4$, $r^2 = 0.989$ (green). For the slope of the linear fits, values labeled by the same letter are not significantly different ($P < 0.05$).

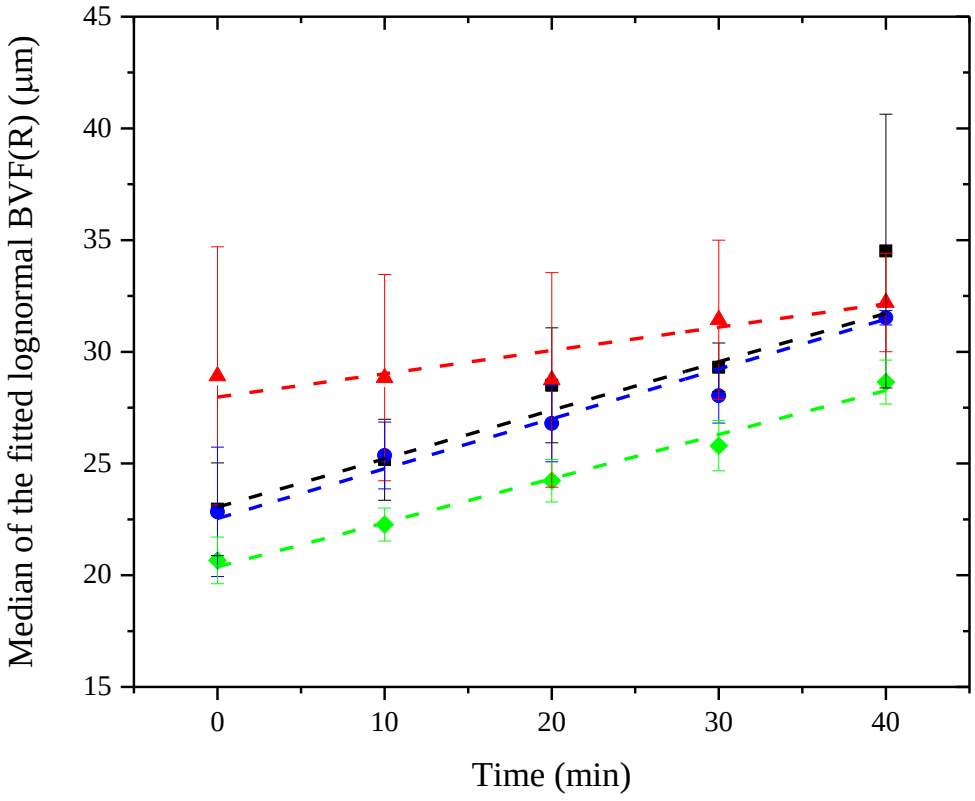

Figure 5.4: The width of the fitted lognormal BVF(R) of optimally-mixed doughs with FAB water as a function of time after the end of mixing. Dough formulations are the same as Figure 5.3. Error bars show ± 1 SD, n = 12.

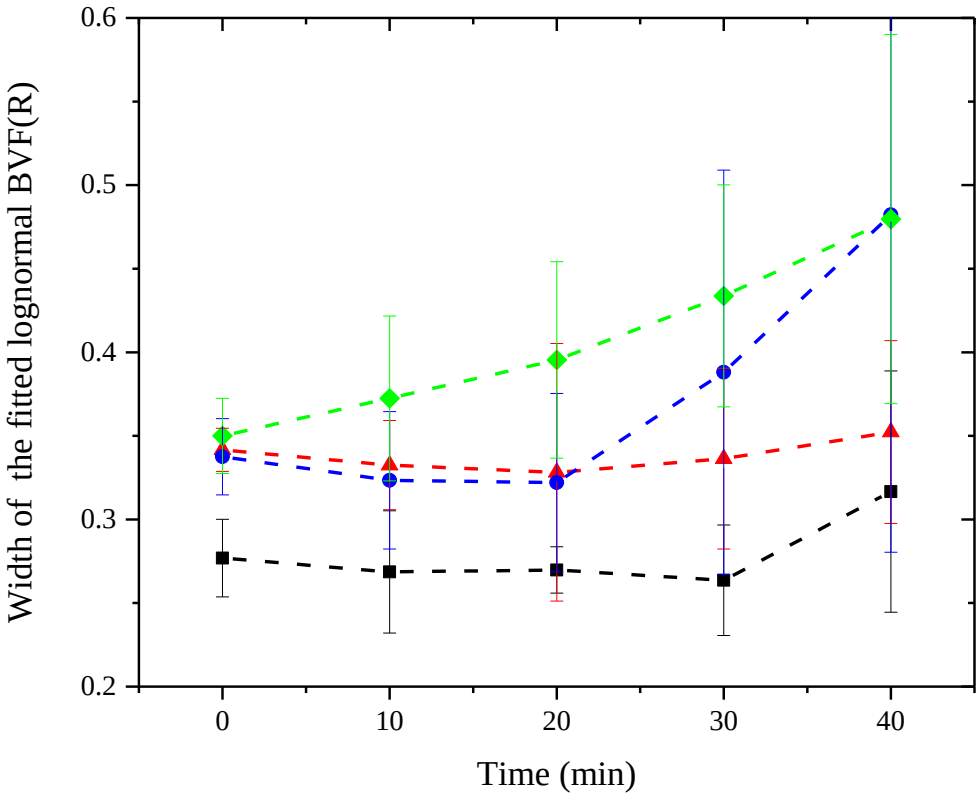

Unlike R_0, the response of ε for doughs studied did not show a clear relationship with time after mixing (Figure 5.4). The time dependence of ε was a function of the dough formulation (Figure 5.4). Compared to the salted doughs made from the same wheat cultivar, ε values for no-salt doughs were more responsive to time evolution (Figure 5.4, green *vs.* blue dashed lines for Pembina cultivar, red *vs.* black dashed lines for Harvest cultivar), indicating that salt reduction promoted disproportionation (Salt et al., 2006).

5.4.3. Effects of Mixing Time on Gas Volume Fraction and BVF(R) in Doughs

For doughs with the same salt content (0 or 2%), the $\varphi_{X\text{-}ray}$ increased with increasing mixing time for under-mixing, optimal-mixing and over-mixing conditions (Table 5.4). In agreement, Kokawa et al. (2012) reported that the total bubble number increased with increasing mixing time using fluorescence fingerprint image analyses. The positive effect of mixing time on the entrainment of gas bubbles in the dough has also been observed using an ultrasonic technique (Mehta et al., 2009) and benchtop X-ray tomography (Trinh et al., 2013). For overmixing, no-salt doughs had a larger value of $\varphi_{X\text{-}ray}$ compared to salted doughs (Table 5.4), indicating that the contribution of mixing time to increased gas entrainment is weakened with salt reduction.

Table 5.4: The median (R_0) and width (ε) of the fitted lognormal BVF(R) and gas volume fraction ($\varphi_{X\text{-}ray}$) for Pembina doughs with FAB water at various mixing conditions

Dough formulation		[a] $\varphi_{X\text{-}ray}$ (%)	R_0 (μm)	ε
salt content	mixing condition			
0	under-mixing	2.43 ± 0.70^{d}	21.3 ± 1.79^{b}	0.45 ± 0.09^{abc}
0	optimal-mixing	6.88 ± 0.37^{c}	22.8 ± 1.90^{ab}	0.34 ± 0.02^{c}
0	over-mixing	11.85 ± 1.73^{a}	31.8 ± 1.69^{a}	0.54 ± 0.08^{ab}
2%	under-mixing	2.67 ± 0.84^{d}	25.7 ± 1.16^{ab}	0.59 ± 0.08^{a}
2%	optimal-mixing	7.42 ± 0.42^{c}	20.7 ± 0.99^{b}	0.34 ± 0.02^{bc}
2%	over-mixing	10.20 ± 0.87^{b}	23.3 ± 0.22^{ab}	0.36 ± 0.02^{ab}

[a] $\varphi_{X\text{-}ray}$, R_0 or ε is tested at the end of mixing, and values (mean ± SD, n = 12) labelled by the same letter are not significantly different ($P < 0.05$).

At under- and over-mixing conditions, the radius dependence of bubble volume fraction [BVF(R)] tested at the end of mixing are illustrated in Figure 5.5 and Figure 5.6, respectively, for

the Pembina doughs with FAB water (replicate 1). At under-mixing conditions, the largest contribution to the total BVF(R) was provided by the bubbles with radii from 15 to 20 μm (Figure 5.5), which was evident for all 6 dough replicates. At over-mixing conditions, the bubbles over the radius range from 20 to 40 μm provided the largest contribution to the total BVF(R) (Figure 5.6), which was evident for all 6 dough replicates. This finding agrees with under-mixed doughs containing a higher volume of smaller-sized bubbles while over-mixed doughs contained a higher volume of larger-sized bubbles (Kokawa et al., 2012).

Figure 5.5: The radius dependence of bubble volume fraction (BVF(R)) tested at the end of under-mixing conditions (1 min) for Pembina dough with 0 salt and FAB water (replicate 1). Error bars show ± 1 SD, n = 4. Blue line is the lognormal distribution function fitted to the BVF(R), r^2 = 0.989.

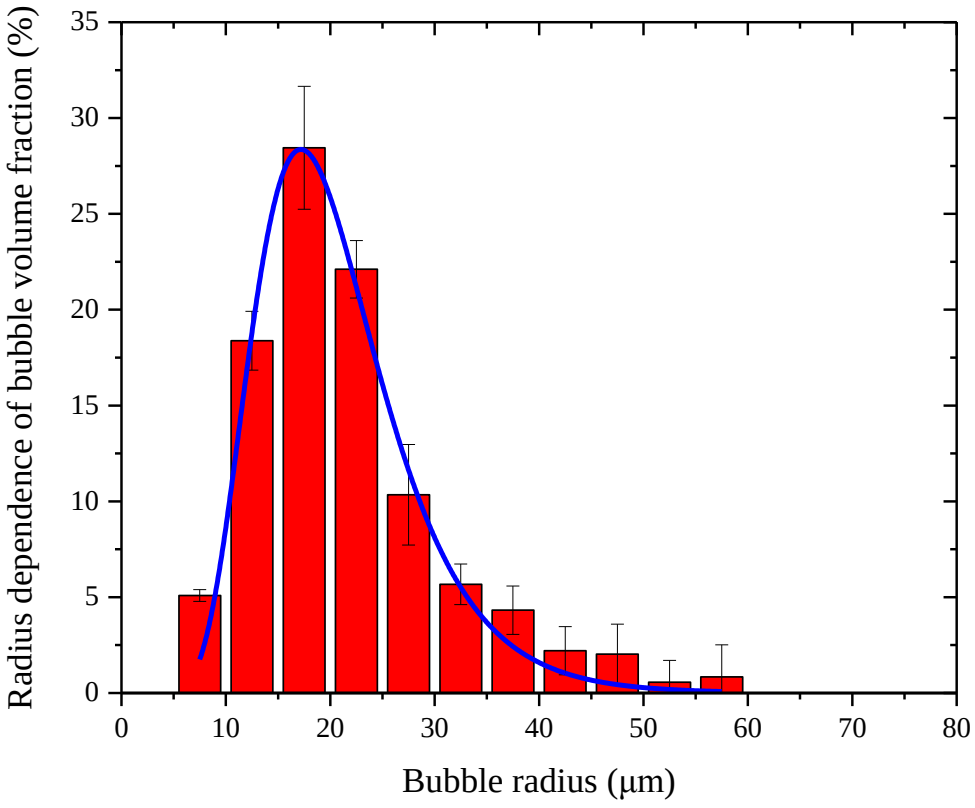

Figure 5.6: The radius dependence of bubble volume fraction (BVF(R)) tested at the end of over-mixing (10 min) conditions for Pembina dough with 0 salt and FAB water (replicate 1). Error bars show ± 1 SD, n = 4. Blue line is the lognormal distribution function fitted to the BVF(R), r^2 = 0.981.

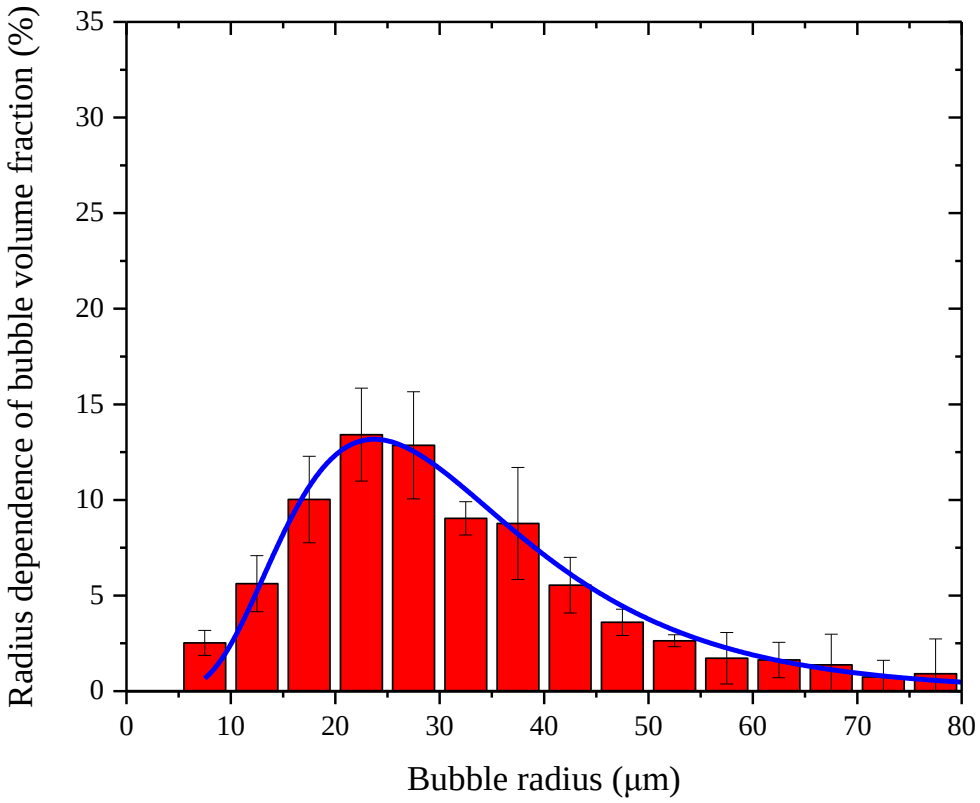

For both under- and over-mixed Pembina doughs with FAB water and no salt, the lognormal distribution function fitted well to the BVF(R) (Figure 5.5 and Figure 5.6). This finding was also observed for salted doughs (results not shown). The R_0 and ε obtained from the lognormal distribution fitted to BVF(R)s are shown in Table 5.4 for doughs with various salt and mixing conditions. Unlike the salted doughs for which no significant change was seen in R_0 across the three mixing conditions, no-salt doughs had a lower R_0 at the under-mixing conditions compared to that at the over-mixing conditions (Table 5.4). Since disproportionation is promoted by salt reduction (Salt et al., 2006), the median of the BVF(R) in no-salt doughs shifted towards larger

bubble sizes as mixing time increased. The ε of no-salt doughs increased from optimal- to over-mixing conditions, whereas the ε of salted doughs decreased from under- to over-mixing conditions (Table 5.4). Regardless of salt concentrations, changes in ε with mixing did not indicate how mixing time affected the rate of disproportionation.

5.5. Conclusions

The gas volume fraction of dough at the end of mixing is affected by dough formulation and mixing conditions. At a fixed mixing time, a higher gas volume was entrained when dough was made from a weaker wheat cultivar, lower water concentration, and/or higher salt concentration. At a fixed dough formulation, a higher gas volume was entrained as mixing time increased.

Synchrotron X-ray microtomography is an effective tool to investigate the size distribution of bubbles and its time evolution over a wide range of dough formulations (*i.e.*, wheat cultivar, concentration of water and salt) and mixing conditions (*i.e.*, under-, optimal- and over-mixing). Regardless of dough formulation and mixing condition, the lognormal distribution function fitted very well to the radius dependence of bubble volume fraction [BVF(R)] tested immediately after mixing. As disproportionation progressed over time following the end of mixing, the goodness of fit for a lognormal characterization of BVF(R) became less satisfactory. The parameters median (R_0) and width (ε) obtained from the lognormal fits to the BVF(R) were useful indicators of bubble dynamics arising from disproportionation.

The time evolution of gas bubbles in dough was demonstrated by a decrease in gas volume fraction and an increase in bubble sizes as a function of time after mixing. Higher water concentration promoted the time-dependent loss in the volume of gas from the dough to the

atmosphere. The time-dependent increase in bubble sizes due to disproportionation was enhanced as the water concentration increased, salt concentration decreased, and/or mixing time increased.

In dough systems, reduced salt content and/or increased water content exerted interactive effects on the bubble dynamics induced by disproportionation. The rate of disproportionation may be decreased by increasing salt concentration and/or decreasing water concentration. To produce low-sodium breads, lower water concentration can be considered to retard disproportionation that is promoted by salt reduction and in turn increase the bubble stability during breadmaking.

5.6. Acknowledgements

The authors acknowledge the financial support provided by Canada Bread Corp. (Toronto, Canada), the Saskatchewan Agricultural Development Fund, the Western Grains Research Foundation, and through a joint NSERC (Natural Sciences and Engineering Research Council of Canada)-CIHR (Canadian Institute of Health Research) Institute of Nutrition, Metabolism and Diabetes Funding Initiative for Sodium Reduction in the Canadian Food Supply, and CSC (China Scholarship Council). The authors would like to thank Andrea Stone, Nicole Avramenko, and Aleksandar Yovchev from the University of Saskatchewan for their technical support.

6. General Discussion and Conclusions

This thesis aimed to develop processing strategies for reduced- and low-sodium bread doughs with a better performance during breadmaking. By manipulating the wheat cultivar, water content and mixing time, the rheological properties and the gas phase of reduced salt content doughs were investigated. Dough rheological properties were examined using a combination of large- and small-strain rheological tests, *i.e.*, mixograph, dynamic oscillatory rheometry and creep-recovery tests. The mixograph has been used to evaluate how the strength of dough changes with salt reduction (Danno & Hoseney, 1982a; He et al., 1992). Dynamic oscillatory rheometry and creep-recovery tests have been conducted to study the effect of salt reduction on dough viscoelastic properties (Beck et al., 2012a; Jekle & Becker, 2012; Yovchev et al., 2017b). The gas phase in the dough, *i.e.*, the gas volume and bubble size distribution (BSD, the size distribution of bubbles on a number basis) as well as their time evolution, of dough have been investigated using synchrotron X-ray microtomography (Babin et al., 2006; Koksel et al., 2016). This powerful imaging technique has been conducted to acquire the BSD at the end of mixing and its evolution during resting time in non-yeasted doughs (Koksel et al., 2016) and study the growth of bubble sizes in yeasted doughs during proving (Babin et al., 2006).

The first study prepared doughs with a wide range of formulations, *i.e.*, four wheat cultivars, five water contents, eight salt contents, to examine how the response of dough mixograph parameters to salt reduction was manipulated by varying the wheat cultivar and water content (Chapter 3). Since mixograph parameters, *i.e.*, peak height (PKH) and energy to peak (ETP) are indicative of dough strength, their values increased when stronger wheat cultivars were used (Khatkar et al., 1996; Lukie, 2001), water content was lowered (Baig & Hoseney, 1977; Lang et al., 1992) and salt content was raised (Danno & Hoseney, 1982a; He et al., 1992). These previous findings are confirmed by outcomes from our mixograph measurements. By averaging for four

wheat cultivars, PKH and ETP measurements showed that the dough's response to salt reduction differed according to water content. Changes in dough's ETP with salt reduction indicated that an increase in the water content led to a better tolerance of dough to salt (NaCl) reduction. By averaging for five water contents, ETP values showed there was a cultivar-dependent tolerance of dough to salt reduction. According to the breadmaking strength and the salt reduction tolerance across four wheat cultivars, the weakest cultivar Harvest had the highest tolerance to salt reduction, and the strongest cultivar Roblin had the second highest tolerance to salt reduction. Due to their better tolerance to salt reduction, Harvest and Roblin were selected to prepare doughs for studying how dough viscoelastic properties responded to salt reduction (Chapter 4).

In Chapter 4, doughs were made from various formulations, *i.e.*, two wheat cultivars, five water contents, and three salt contents. How formulation affected dough's viscoelastic properties was examined using small-strain tests, *i.e.*, dynamic oscillatory rheometry with the parameters storage (elastic) modulus G' and loss (viscous) modulus G'', and creep-recovery tests with the parameter shear compliance J. Over a wide range of dough formulations, two constitutive models, *i.e.*, a power-law gel model and a Burgers model, were used to characterize the storage and loss modulus as a function of frequency, $G'(\omega)$ and $G''(\omega)$, as well as the shear compliance as a function of time $J(t)$. The power-law gel model fitted well to the data of $G'(\omega)$, $G''(\omega)$ and $J(t)$ in both linear and non-linear viscoelastic regions, whereas the Burgers model only fitted well to the $J(t)$ data in the non-linear viscoelastic region.

The parameter gel strength (S) from the power-law gel model interpreted changes in the strength and viscoelasticity with changes in dough formulation in the linear and non-linear viscoelastic tests well (Chapter 4). For example, higher S values were seen for doughs made from the stronger wheat cultivar, indicating that the strength and viscoelastic properties of doughs were

wheat cultivar dependent (Edwards et al., 2001; Miller & Hoseney, 1999; Yovchev et al., 2017c). A decrease in S values was seen with increasing water content, indicating a weakening effect of water on the dough (Meerts et al., 2017) due to the role of water as a mobility enhancer in dough systems (Masi et al., 1998). An increase in S was seen with reduced salt content, which has been interpreted as being due to the interactions between gluten proteins, water and salt in dough systems (Jekle & Becker, 2012). As water and salt compete to interact with gluten proteins, reduced salt content leads to more available sites on the surface of gluten proteins for water molecules to interact with (Jekle & Becker, 2012), resulting in an increase of immobile water molecules and a decrease of mobile water molecules, and these induce an increase in dough strength (Bushuk & Hlynka, 1964). In agreement with the results from Chapter 4, the $G'(\omega)$ and $G''(\omega)$ of dough also increased with reducing the salt content (Lynch et al., 2009; Wu et al., 2006). In contrast, the mixograph studies showed that dough strength (*i.e.*, PKH and ETP) decreased with salt reduction (Chapter 3). The contradictory results from mixograph (Chapter 3) and dynamic oscillatory rheometry (Chapter 4) may be due to different instrument limitation for detecting gluten's response to salt effect (Lynch et al., 2009). The dynamic oscillatory rheometry was able to differentiate the salt-induced responses of noodle doughs made from wheat cultivars varying in the content and quality of gluten (Wu et al., 2006). A reduction of salt content from 3% to 0% resulted in a decrease in the $G'(\omega)$ of doughs made from the wheat cultivar with lower content and quality of gluten (Wu et al., 2006). But this reduction level of salt resulted in an increase in the $G'(\omega)$ of doughs made from the wheat cultivar with higher content and quality of gluten (Wu et al., 2006).

Various gel strength parameters, *i.e.*, S', S" S^c and S^r, were derived by fitting the data of $G'(\omega)$, $G''(\omega)$, creep compliance $J_c(t)$ and recovery compliance $J_r(t)$, respectively, to the power-

law gel model. By averaging for two wheat cultivars, the slope value of a line for S' against NaCl reduction indicated that the response of dough's strength and viscoelasticity to salt (NaCl) reduction depended on water content (Figure 6.1). This finding is also evident for the other three S parameters from the linear (S'') and non-linear (S^c and S^r) viscoelastic tests (Chapter 4). The water-induced difference in dough's response to salt reduction is also confirmed by our PKH studies in Chapter 3. The absolute value of the slope of S^c against NaCl reduction for doughs varying in water content was determined as 148 for FAB-4%, 99 for FAB-2%, 91 for FAB, 25 for FAB+2% and 35 for FAB+4%. Therefore, it indicates that an increase in the dough's water content leads to a decrease in its sensitivity to salt reduction. This finding is consistent with our ETP results (Chapter 3). By averaging for five water contents and comparing the slope values of S' against NaCl reduction between wheat cultivars (Figure 6.2), a cultivar-dependent response of dough's strength and viscoelasticity to salt reduction was seen. This finding is in line with our studies of S'', S^c and S^r. The cultivar-dependent difference in the slopes of those S parameters against NaCl reduction also indicated that Harvest exhibited a better tolerance to salt reduction compared to Roblin. This finding agrees with outcomes from our ETP studies (Chapter 3).

Figure 6.1: Effects of salt reduction and changes in water content on dough gel strength (S') averaged for two wheat cultivars. S' was derived by fitting the G'(ω) data to the power-law gel model. Water contents are FAB-4% (black squares), FAB-2% (red triangles), FAB (blue circles), FAB+2% (green rhombuses), and FAB+4% (purple stars). Absolute values of slopes for linear fits (dashed lines): 73 (black), 167 (red), 327 (blue), 182 (green) and 117 (purple).

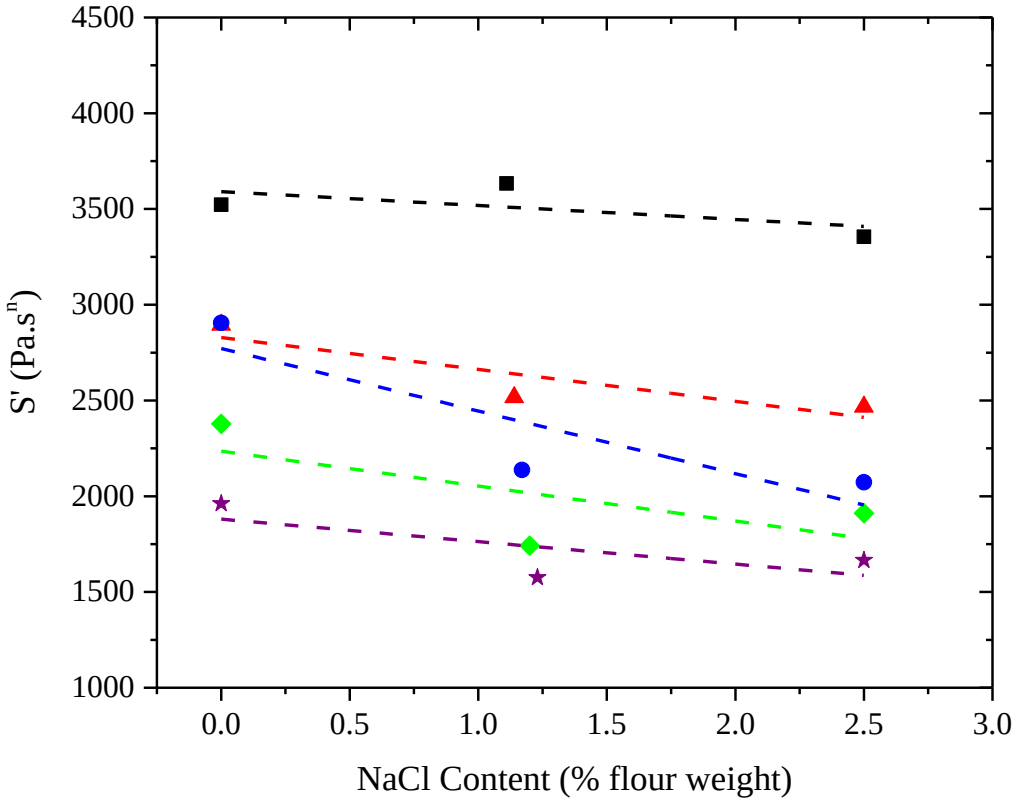

Figure 6.2: Effects of salt reduction and wheat cultivar on dough gel strength (S') averaged for five water contents. S' was derived by fitting the G'(ω) data to the power-law gel model. Wheat cultivars are Roblin (red triangles) and Harvest (green rhombuses). Absolute values of slopes for linear fits (dashed lines): 224 (red) and 121 (green).

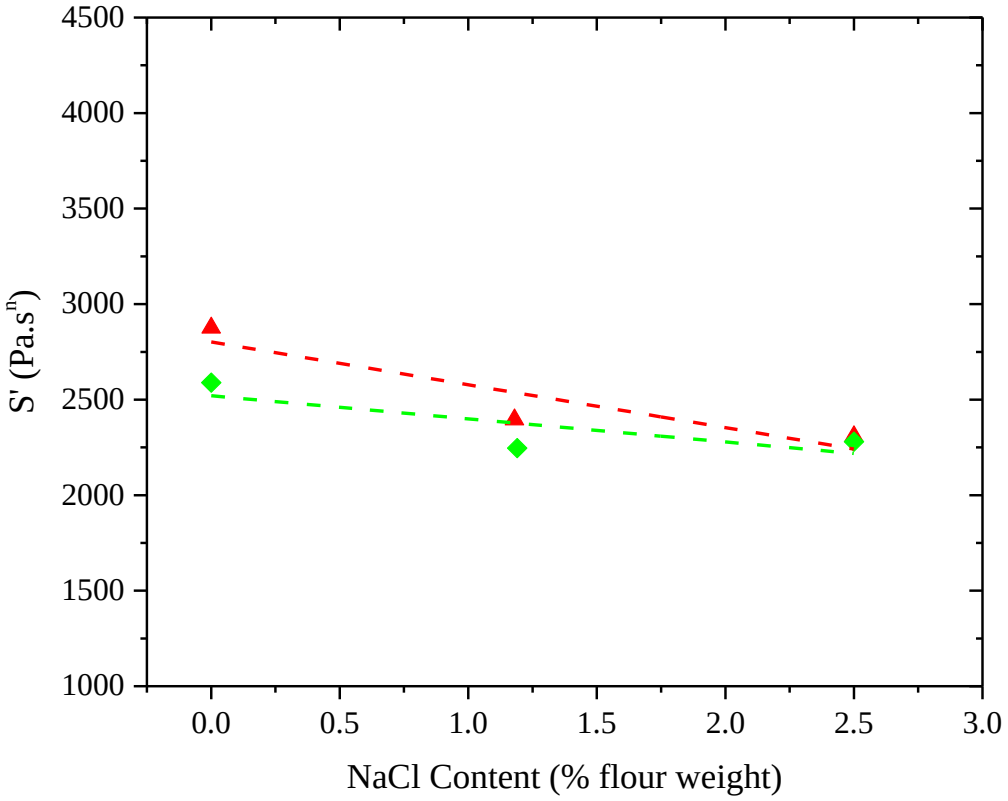

Mixing time and salt reduction are known to affect dough stickiness (Yovchev et al., 2017b). To examine the effects of mixing time and salt (NaCl) reduction on dough rheological properties, an analysis of *G'(ω)* was conducted for doughs varying in formulation (Appendix 3). The response of dough's S' to salt reduction is shown in Figure 6.3 by averaging for two wheat cultivars. With a reduction in the NaCl content, the S' of under-mixed doughs decreased, whereas that of optimally- and over-mixed doughs increased. This indicates that dough's response to salt reduction depends on the mixing condition. Compared to over-mixed doughs, optimally-mixed doughs had a lower absolute value of the slope of S' against NaCl reduction (Figure 6.3),

suggesting that using the optimal mixing time developed the dough so that it had a better tolerance to salt reduction. For each cultivar, the S' values of under-mixed doughs were lower than those of optimally- and over-mixed doughs (Figure 6.4), indicating that a sufficient mixing time is required for developing doughs. The response of dough's strength to mixing time depended on wheat cultivar.

Figure 6.3: Effects of salt reduction and mixing time on dough gel strength (S') averaged for two wheat cultivars held at a constant water content of FAB-4%. S' was derived by fitting the G'(ω) data to the power-law gel model. Mixing times are 1 min (black squares), optimal mixing time (red triangles) and 10 min (blue circles). Absolute values of slopes for linear fits (dashed lines): 347 (black), 73 (red) and 247 (blue).

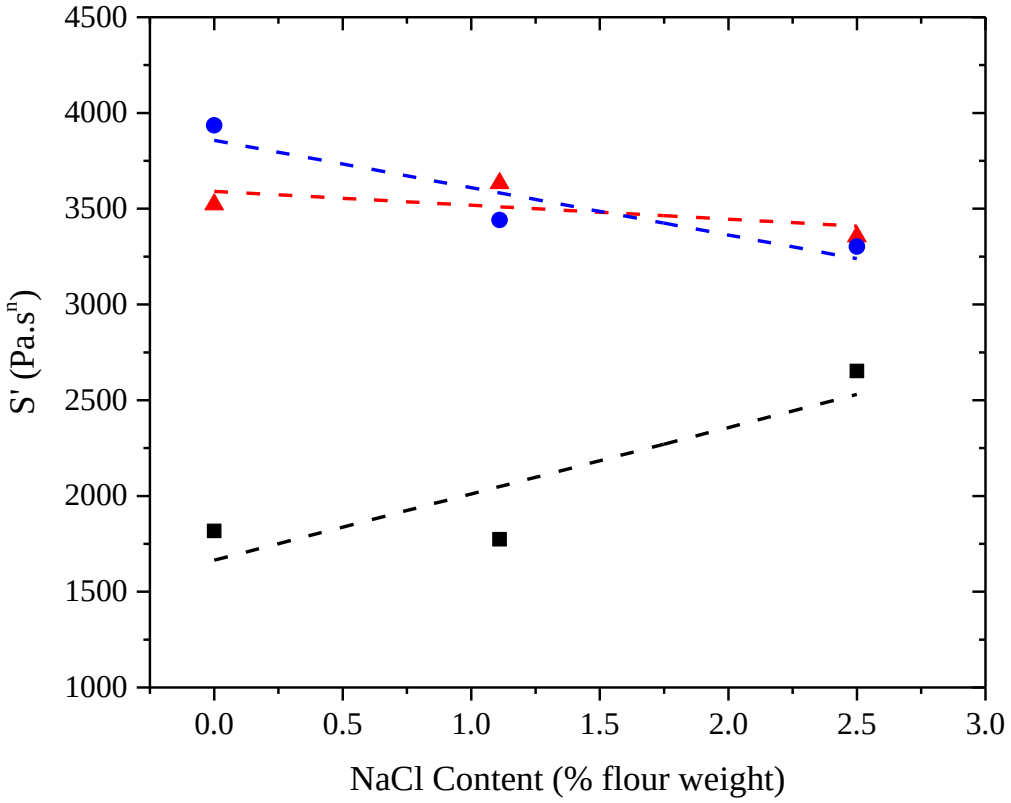

Figure 6.4: Effects of mixing time and wheat cultivar on dough gel strength (S') averaged for three salt contents held at a constant water content of FAB-4%. S' was derived by fitting the G'(ω) data to the power-law gel model. Mixing times are 1 min (under-mixing), optimal mixing time and 10 min (over-mixing). Wheat cultivars are Roblin (red triangles) and Harvest (green rhombuses).

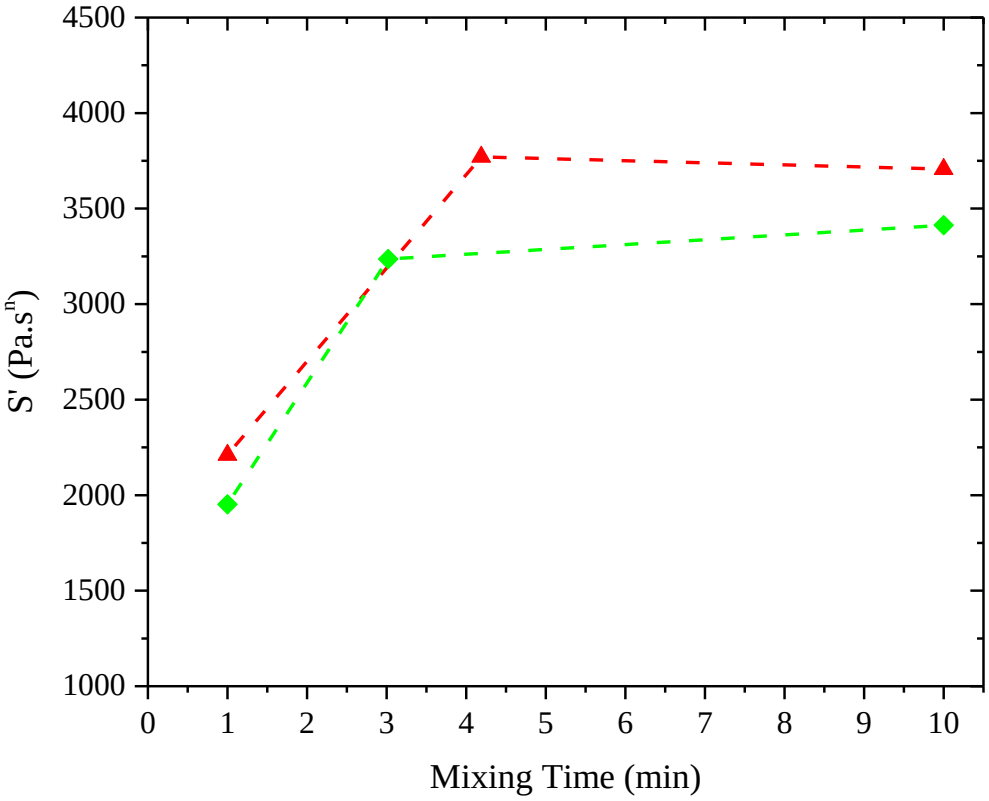

In Chapters 3 and 4, by using large- and small-strain tests, the rheological properties of doughs were measured to show that dough's response to salt (NaCl) reduction depended on wheat cultivar, water content and mixing time. While the response of dough strength parameters from large (*i.e.*, PKH and ETP) and small (*i.e.*, S', S'', S^c and S^r) strain rheological measurements had a similar response to changes in water content, their response to salt reduction did not follow the same trend. For the development of bread dough with a better tolerance to salt reduction, flour made from the wheat cultivar Harvest, increased water content, and optimal mixing time should be considered. To further investigate how the formulation and mixing conditions affect dough's

response to salt reduction on a microscopic level, the gas volume fraction ($\varphi_{X\text{-}ray}$) and radius dependence of bubble volume fraction [BVF(R)] at the end of mixing, as well as their changes with time after the completion of mixing, were examined using a high-resolution imaging technique — synchrotron X-ray microtomography (Chapter 5).

In Chapter 5, doughs were prepared from two wheat cultivars varying in breadmaking strength, three water contents, two salt contents and three mixing times. At the end of mixing, $\varphi_{X\text{-}ray}$ showed that a higher volume of gas was entrained into the dough made from a weaker cultivar, lower water content, higher salt content, and/or longer mixing time. Our findings are in line with previous studies of dough density (Campbell et al., 1993; Chin et al., 2005a; Kokawa et al., 2012; Koksel & Scanlon, 2012; Mehta et al., 2009; Peighambardoust et al., 2010; Trinh et al., 2013). The size distribution of bubbles in doughs varying in formulation and mixing conditions were investigated using a lognormal distribution function fitted to the BVF(R) with resultant parameters median (R_0) and width (ε). For 45 min following the end of mixing, the evolution of R_0 and ε of a lognormal-fitted BVF(R) distribution indicated a time-dependent shrinkage of smaller-sized bubbles and growth of larger-sized bubbles due to disproportionation (Kokelaar et al., 1996; Leroy et al., 2008; Meinders & Van Vliet, 2004; Murray & Ettelaie, 2004; Shimiya & Yano, 1988; Turbin-Orger et al., 2015). This disproportionation-induced change in the size distribution of bubbles became more observable when increasing water content, reducing salt content, and/or increasing mixing time. As such, salt (NaCl) reduction may possibly promote disproportionation in the dough during breadmaking, resulting in a poor crumb cell structure (Elmehdi et al., 2003; Hayman et al., 1998; Scanlon & Zghal, 2001). Therefore, it further emphasizes the importance of manipulating wheat cultivar, water content and mixing time to retard disproportionation induced by salt reduction.

Immediately after the end of mixing, the effects of wheat cultivar and salt (NaCl)reduction on $\varphi_{X\text{-}ray}$, R_0 and ε were investigated for doughs with the water content of FAB (Table 6.1). When reducing the salt content by 2%, the relative changes in $\varphi_{X\text{-}ray}$, R_0 and ε for Harvest doughs were greater than those of Pembina doughs, indicating that the stronger cultivar Pembina was more tolerant to salt reduction in terms of changes in the gas volume and size distribution of bubbles. This finding contradicts our mixograph studies which showed a better tolerance of the weaker cultivar Harvest to salt reduction. The cultivar-dependent tolerance of dough to salt reduction indicated by dough rheological parameters (Figures 3.3 and 6.2) differed from that indicated by dough's gas phase parameters (Table 6.1). The salt-induced response of dough rheological properties is primarily affected by the gluten-salt interaction (Preston, 1989), whereas the salt-induced response of dough's gas phase is affected by the gluten-salt and lipid-salt interactions (Salt et al., 2006). In terms of dough rheological studies, the cultivar-dependent content and composition of gluten affects dough's tolerance to salt reduction (Butow et al., 2002; Isaak et al., 2019). In terms of dough's gas phase, the cultivar-dependent content and composition of gluten and lipids both affect dough's tolerance to salt reduction (Salt et al., 2006). Therefore, the cultivar dependence of dough's tolerance to salt reduction demonstrated by dough rheological studies (Chapters 3 and 4) differed from that demonstrated by dough's gas phase studies (Chapter 5).

Table 6.1: Effects of salt reduction and wheat cultivar on the gas phase of doughs prepared with FAB water

Wheat cultivar	[a] Parameter's relative change (%) due to 2% salt reduction		
	$\varphi_{X\text{-}ray}$	R_0	ε
Harvest	-30.8	-20.6	-17.7
Pembina	-7.3	10.2	0

[a] FAB is farinograph water absorption of wheat flour. Parameters are the gas volume fraction ($\varphi_{X\text{-}ray}$) from X-ray microtomography analyses, the median (R_0) and width (ε) of the fitted lognormal radius dependence of bubble volume fraction [BVF(R)]. $\varphi_{X\text{-}ray}$, R_0 or ε (mean ± SD, n = 12) is tested at 0 min after the end of mixing. Relative change (%) = 100 % × (parameter at no salt condition - parameter at 2% salt condition) / parameter at 2% salt condition.

Due to a better tolerance to salt reduction, wheat flour from Pembina was selected to make the doughs to investigate the effects of water content and mixing time on the response of dough's gas phase to salt reduction. Although relative changes in $\varphi_{X\text{-}ray}$, R_0 and ε with salt reduction were seen to depend on water content, how increased water content affected the tolerance of dough's gas phase to salt reduction was not clearly revealed (Table 6.2). For Pembina doughs with the water content of FAB, relative changes in $\varphi_{X\text{-}ray}$, R_0 and ε with salt reduction differed according to the mixing time of the dough (Table 6.3). Rather than using mixing times like 1 min (under-mixing) and 10 min (over-mixing), using optimal mixing time contributed to develop the dough with a better tolerance to salt reduction in terms of parameters indicative of dough's gas phase (Table 6.3).

Table 6.2: Effects of salt reduction and water content on the gas phase of Pembina doughs

Water content (%)	Parameter's relative change (%) due to 2% salt reduction		
	$\varphi_{X\text{-}ray}$	R_0	ε
FAB-4	-7.1	8.4	6.1
FAB	-7.3	10.2	0
FAB+4	53.9	-2.4	-10.8

Table 6.3: Effects of salt reduction and mixing time on the gas phase of Pembina doughs prepared with FAB water

Mixing time (min)	Parameter's relative change (%) due to 2% salt reduction		
	$\varphi_{X\text{-}ray}$	R_0	ε
1	-9.9	-17.2	-23.7
[a] optimal mixing time	-7.3	10.2	0
10	16.2	36.0	50.0

[a] optimal mixing time: 4 min 49 s for no salt doughs and 6 min 51 s for 2% salt doughs.

Due to different results from the studies of dough's mixograph characteristics (Chapter 3) and gas phase parameters (Chapter 5) in an interpretation of the cultivar-dependent sensitivity of dough to salt (NaCl) reduction, baking tests on reduced salt doughs should be conduced in the future to ascertain the relationship between breadmaking performance and the sodium reduction tolerance of a given wheat cultivar, and in turn suitable wheat cultivars can be selected for reduced-sodium breadmaking. Secondly, the effect of increased water content on the gas phase of reduced-salt doughs was not clearly revealed (Chapter 5). To ensure that outcomes from fundamental studies of dough properties benefit industrial reduced-sodium breadmaking practice, a potential

future work is a study of the effects of wheat cultivar and water content on the quality of breads (*i.e.*, loaf volume and crumb cell structure) baked from reduced-salt doughs, and in turn screen wheat cultivars to determine the optimal water contents that will produce reduced-sodium breads with higher loaf volume and better crumb cell structure.

In conclusion, the breadmaking performance of reduced-salt (NaCl) doughs, *i.e.*, changes in the rheological properties, gas volume fraction and bubble size distribution of dough with salt reduction, can be improved if flour from a wheat cultivar with a better tolerance to salt reduction is used. In terms of dough rheological parameters, higher water contents may increase dough's tolerance to salt reduction. However, the relationship between water content and dough's tolerance to salt reduction was not clearly revealed in terms of dough's gas phase parameters. Outcomes from the studies on the rheological properties and the gas phase of dough suggest that using the optimal mixing time allows the dough to be developed so that it is more tolerant to salt reduction.

In terms of practical implications, the bakers and wheat breeders will benefit from outcomes from this thesis. For example, if bakers use the optimal mixing condition and wheat flours more tolerant to salt reduction during breadmaking, they will develop reduced sodium content dough with better handling properties, and in turn achieve a desirable product quality of bread baked from it. If wheat breeders have access to the mixograph results on the cultivar dependence of dough's tolerance to salt reduction, they will receive guidance for future wheat breeding programs due to a cultivar's suitability for reduced sodium breadmaking.

7. Bibliography

AACC International. (1999a). Approved methods of analysis, 11th Ed. Method 10-10.03. Optimized straight-dough bread-making method. *AACC International*, 1–8.

AACC International. (1999b). Approved methods of physical dough tests. Method No.54-40.02. Mixograph method. *AACC International*, 2–7.

AACC International. (2011). Approved methods of physical dough tests. Method No.54-21.02. Rheological behavior of flour by farinograph: Constant flour weight procedure. *AACC International*, 1–8. https://doi.org/10.1094/AACCIntMethod-54-21.02

Amemiya, J. I., & Menjivar, J. A. (1992). Comparison of small and large deformation measurements to characterize the rheology of wheat flour doughs. *Journal of Food Engineering*, *16*, 91–108. https://doi.org/10.1016/0260-8774(92)90022-X

Amon, M., & Denson, C. D. (1984). A study of the dynamics of foam growth: Analysis of the growth of closely spaced spherical bubbles. *Polymer Engineering and Science*, *24*, 1026–1034.

Arakawa, T., & Yonezawa, D. (1975). Compositional difference of wheat flour glutens in relation to their aggregation behaviors. *Agricultural and Biological Chemistry*, *39*(11), 2123–2128.

Arcand, J., Au, J. T. C., Schermel, A., & L'Abbe, M. R. (2014). A comprehensive analysis of sodium levels in the canadian packaged food supply. *American Journal of Preventive Medicine*, *46*(6), 633–642. https://doi.org/10.1016/j.amepre.2014.01.012

Autio, K., Flander, L., Kinnunen, A., & Heinonen, R. (2001). Bread quality relationship with rheological measurements of wheat flour dough. *Cereal Chemistry*, *78*(6), 654–657. https://doi.org/10.1094/CCHEM.2001.78.6.654

Babin, P., Della Valle, G., Chiron, H., Cloetens, P., Hoszowska, J., Pernot, P., … Dendievel, R. (2006). Fast X-ray tomography analysis of bubble growth and foam setting during

breadmaking. *Journal of Cereal Science*, *43*(3), 393–397. https://doi.org/10.1016/j.jcs.2005.12.002

Babin, P., Della Valle, G., Chiron, H., Cloetens, P., Hoszowska, J., Pernot, P., … Dendievel, R. (2008). In situ fast X-ray microtomography study of the evolution of cellular structure in bread dough during proving and baking. In G. M. Campbell, M. G. Scanlon, & L. D. Pyle (Eds.), *Bubbles in Food 2: Novelty, Health and Luxury* (pp. 265–272). St. Paul, MN, USA: Eagan Press.

Babin, P., Della Valle, G., Dendievel, R., Lassoued, N., & Salvo, L. (2005). Mechanical properties of bread crumbs from tomography based finite element simulations. *Journal of Materials Science*, *40*(22), 5867–5873. https://doi.org/10.1007/s10853-005-5021-x

Babin, P., Della Valle, G., Dendievel, R., Lourdin, D., & Salvo, L. (2007). X-ray tomography study of the cellular structure of extruded starches and its relations with expansion phenomenon and foam mechanical properties. *Carbohydrate Polymers*, *68*(2), 329–340. https://doi.org/10.1016/j.carbpol.2006.12.005

Baig, M. M., & Hoseney, R. C. (1977). Effects of mixer speed, dough temperature, and water absorption on flour-water mixograms. *Cereal Chemistry*, *54*(3), 605–615.

Bajd, F., & Serša, I. (2011). Continuous monitoring of dough fermentation and bread baking by magnetic resonance microscopy. *Magnetic Resonance Imaging*, *29*(3), 434–442. https://doi.org/10.1016/j.mri.2010.10.010

Baker, J. C., & Mize, M. D. (1941). The origin of the gas cell in bread dough. *Cereal Chemistry*, *18*, 19–34.

Baker, J. C., & Mize, M. D. (1946). Gas occlusion during dough mixing. *Cereal Chemistry*, *23*, 39–51.

Barigou, M., & Douaire, M. (2013). X-ray micro-computed tomography for resolving food microstructures. In K. Morris, V. J., Groves (Ed.), *Food Microstructures: Microscopy, Measurement and Modelling* (pp. 246–272). Cambridge, UK: Woodhead Publishing Limited. https://doi.org/10.1533/9780857098894.1.246

Barnes, H. A. (2000). *A Handbook of Elementary Rheology*. Aberystwyth, Wales: Institute of Non-Newtonian Fluid Mechanics, University of Wales.

Beck, M., Jekle, M., & Becker, T. (2012a). Impact of sodium chloride on wheat flour dough for yeast-leavened products. I. Rheological attributes. *Journal of the Science of Food and Agriculture*, *92*(3), 585–592. https://doi.org/10.1002/jsfa.4612

Beck, M., Jekle, M., & Becker, T. (2012b). Sodium chloride - sensory, preserving and technological impact on yeast-leavened products. *International Journal of Food Science and Technology*, *47*(9), 1798–1807. https://doi.org/10.1111/j.1365-2621.2012.03048.x

Bellido, G. G., Scanlon, M. G., & Page, J. H. (2009). Measurement of dough specific volume in chemically leavened dough systems. *Journal of Cereal Science*, *49*(2), 212–218. https://doi.org/10.1016/j.jcs.2008.10.002

Bellido, G. G., Scanlon, M. G., Page, J. H., & Hallgrimsson, B. (2006). The bubble size distribution in wheat flour dough. *Food Research International*, *39*(10), 1058–1066. https://doi.org/10.1016/j.foodres.2006.07.020

Bellido, G. G., Scanlon, M. G., Sapirstein, H. D., & Page, J. H. (2008). Use of a pressuremeter to measure the kinetics of carbon dioxide evolution in chemically leavened wheat flour dough. *Journal of Agricultural and Food Chemistry*, *56*(21), 9855–9861. https://doi.org/10.1021/jf801125f

Belton, P. S. (1999). Mini review: On the elasticity of wheat gluten. *Journal of Cereal Science*,

29(2), 103–107. https://doi.org/10.1006/jcrs.1998.0227

Belton, P. S. (2012). The molecular basis of dough rheology. In S. P. Cauvain (Ed.), *Breadmaking: Improving Quality* (second, pp. 337–351). Cambridge, UK: Woodhead Publishing Limited.

Belz, M. C. E., Ryan, L. A. M., & Arendt, E. K. (2012). The impact of salt reduction in bread: A review. *Critical Reviews in Food Science and Nutrition*, *52*(6), 514–524. https://doi.org/10.1080/10408398.2010.502265

Berland, S., & Launay, B. (1995a). Rheological properties of wheat flour doughs in steady and dynamic shear: Effect of water content and some additives. *Cereal Chemistry*, *72*(1), 48–52.

Berland, S., & Launay, B. (1995b). Shear softening and thixotropic properties of wheat flour doughs in dynamic testing at high shear strain. *Rheologica Acta*, *34*(6), 622–625. https://doi.org/10.1007/BF00712321

Bloksma, A. H. (1990a). Dough structure, dough rheology, and baking quality. *Cereal Foods World*, *35*, 237–244.

Bloksma, A. H. (1990b). Rheology of the breadmaking process. *Cereal Foods World*, *35*, 228–236.

Bloksma, A. H., & Bushuk, W. (1988). Rheology and chemistry of dough. In Y. Pomeranz (Ed.), *Wheat Chemistry and Technology* (pp. 131–219). St. Paul, MN, USA: AACC International Inc.

Bohlin, L., & Carlson, T. L.-G. (1980). Dynamic viscoelastic properties of wheat flour dough: Dependence on mixing time. *Cereal Chemistry*, *57*(3), 174–177.

Bonny, J. M., Rouille, J., Della Valle, G., Devaux, M. F., Douliez, J. P., & Renou, J. P. (2004). Dynamic magnetic resonance microscopy of flour dough fermentation. *Magnetic Resonance Imaging*, *22*(3), 395–401. https://doi.org/10.1016/j.mri.2004.01.020

Bushuk, W. (1987). Rheology: Theory and application to wheat flour doughs. In *Rheology of Wheat Products* (pp. 1–26). St. Paul, MN, USA: AACC International Inc.

Bushuk, W., & Hlynka, L. (1964). Water as a constituent of flour, dough, and bread. *Bakers Digest*, *38*(6), 43–46.

Butow, B. J., Gras, P. W., Haraszi, R., & Bekes, F. (2002). Effects of different salts on mixing and extension parameters on a diverse group of wheat cultivars using 2-g mixograph and extensigraph methods. *Cereal Chemistry*, *79*(6), 826–833. https://doi.org/10.1094/CCHEM.2002.79.6.826

Calderón-Domínguez, G., Farrera-Rebollo, R., Arana-Errasquín, R., & Mora-Escobedo, R. (2005). The effect of varying the mixing formula on the quality of a yeast sweet bread and also on the process conditions, as studied by surface response methodology. *International Journal of Food Science and Technology*, *40*(2), 157–164. https://doi.org/10.1111/j.1365-2621.2004.00926.x

Campbell, G. M., Herrero-Sanchez, R., Payo-Rodriguez, R., & Merchan, M. L. (2001). Measurement of dynamic dough density and effect of surfactants and flour type on aeration during mixing and gas retention during proofing. *Cereal Chemistry*, *78*(3), 272–277. https://doi.org/10.1094/CCHEM.2001.78.3.272

Campbell, G. M., & Mougeot, E. (1999). Creation and characterisation of aerated food products. *Trends in Food Science and Technology*, *10*(9), 283–296. https://doi.org/10.1016/S0924-2244(00)00008-X

Campbell, G. M., Rielly, C. D., Fryer, P. J., & Sadd, P. A. (1991). The measurement of bubble size distributions in an opaque food fluid. *Trans IChemE*, *69*, 67–76.

Campbell, G. M., Rielly, C. D., Fryer, P. J., & Sadd, P. A. (1993). Measurement and interpretation

of dough densities. *Cereal Chemistry*, *70*(5), 517–521.

Campbell, G. M., & Shah, P. (1999). Entrainment and disentrainment of air during bread dough mixing, and their effect on scale-up of dough mixers. In G. M. Campbell, C. Webb, S. S. Pandiella, & K. Niranjan (Eds.), *Bubbles in Food* (pp. 11–20). St. Paul, MN, USA: Eagan Press.

Campos, D. T., Steffe, J. F., & Ng, P. K. W. (1997). Rheological behavior of undeveloped and developed wheat dough. *Cereal Chemistry*, *74*(4), 489–494. https://doi.org/10.1094/CCHEM.1997.74.4.489

Carlson, T., & Bohlin, L. (1978). Free surface energy in the elasticity of wheat flour dough. *Cereal Chemistry*, *55*(4), 539–544.

Casutt, V., Preston, K. R., & Kilborn, R. H. (1984). Effects of fermentation time, inherent flour strength, and salt level on extensigraph properties of full-formula remix-to-peak processed doughs. *Cereal Chemistry*, *61*(5), 454–459.

Cauvain, S. P. (1998). Bread–the product. In S. P. Cauvain & L. S. Young (Eds.), *Technology of Breadmaking* (pp. 1–17). London, UK: Blackie Academic and Professional.

Cauvain, S. P., Whitworth, M. B., & Alava, J. M. (1999). The evolution of bubble structure in bread doughs and its effect on bread structure. In G. M. Campbell, C. Webb, S. S. Pandiella, & K. Niranjan (Eds.), *Bubbles in Food* (pp. 85–93). St. Paul, MN, USA: Eagan Press.

Centers for Disease Control and Prevention. (2012). Vital signs: Food categories contributing the most to sodium consumption - United States, 2007-2008. *Morbidity and Mortality Weekly Report*, *61*(5), 92–98.

Chamberlain, N., Collins, T., & Redman, B. I. (1970). *The Chorleywood bread process: Effect of reduced pressure during mixing. FMBRA Report No.40*. Chorleywood, Herts, UK: Flour

Millers and Bakers Research Association.

Chevallier, S., Zúñiga, R., & Le-Bail, A. (2012). Assessment of bread dough expansion during fermentation. *Food and Bioprocess Technology*, *5*(2), 609–617. https://doi.org/10.1007/s11947-009-0319-3

Chin, N. L., & Campbell, G. M. (2005a). Dough aeration and rheology: Part 1. Effects of mixing speed and headspace pressure on mechanical development of bread dough. *Journal of the Science of Food and Agriculture*, *85*(13), 2184–2193. https://doi.org/10.1002/jsfa.2236

Chin, N. L., & Campbell, G. M. (2005b). Dough aeration and rheology: Part 2. Effects of flour type, mixing speed and total work input on aeration and rheology of bread dough. *Journal of the Science of Food and Agriculture*, *85*(13), 2194–2202. https://doi.org/10.1002/jsfa.2237

Chin, N. L., Campbell, G. M., & Thompson, F. (2005a). Characterisation of bread doughs with different densities, salt contents and water levels using microwave power transmission measurements. *Journal of Food Engineering*, *70*(2), 211–217. https://doi.org/10.1016/j.jfoodeng.2004.09.024

Chin, N. L., Martin, P. J., & Campbell, G. M. (2005b). Dough aeration and rheology: Part 3. Effect of the presence of gas bubbles in bread dough on measured bulk rheology and work input rate. *Journal of the Science of Food and Agriculture*, *85*(13), 2203–2212. https://doi.org/10.1002/jsfa.2238

Chin, N. L., Martin, P. J., & Campbell, G. M. (2004). Aeration during bread dough mixing: I. Effect of direction and size of a pressure step-change during mixing on the turnover of gas. *Food and Bioproducts Processing*, *82*(4C), 261–267. https://doi.org/10.1205/fbio.82.4.261.56404

Chiotellis, E., & Campbell, G. M. (2003a). Proving of bread dough I Modelling the evolution of

the bubble size distribution. *Trans IChemE*, *81*(C), 194–206. https://doi.org/Doi 10.1205/096030803322437965

Chiotellis, E., & Campbell, G. M. (2003b). Proving of bread dough II Measurement of gas production and retention. *Trans IChemE*, *81*(C), 207–216. https://doi.org/10.1205/096030803322437974

Crowley, P., Grau, H., & Arendt, E. K. (2000). Influence of additives and mixing time on crumb grain characteristics of wheat bread. *Cereal Chemistry*, *77*(3), 370–375. https://doi.org/10.1094/CCHEM.2000.77.3.370

Czuchajowska, Z., Pomeranz, Y., & Jeffers, H. C. (1989). Water activity and moisture content of dough and bread. *Cereal Chemistry*, *66*(2), 128–132.

D'Appolonia, B. L., & Gilles, K. A. (1971). Effect of various starches in baking. *Cereal Chemistry*, *48*, 625–636.

Danno, G., & Hoseney, R. C. (1982a). Effect of sodium chloride and sodium dodecyl sulfate on mixograph properties. *Cereal Chemistry*, *59*(3), 202–204.

Danno, G., & Hoseney, R. C. (1982b). Effects of dough mixing and rheologically active compounds on relative viscosity of wheat proteins. *Cereal Chemistry*, *59*(3), 196–198.

De Guio, F., Musse, M., Benoit-Cattin, H., Lucas, T., & Davenel, A. (2009). Magnetic resonance imaging method based on magnetic susceptibility effects to estimate bubble size in alveolar products: application to bread dough during proving. *Magnetic Resonance Imaging*, *27*(4), 577–585. https://doi.org/10.1016/j.mri.2008.08.009

Demirkesen, I., Kelkar, S., Campanella, O. H., & Sumnu, G. (2014). Characterization of structure of gluten-free breads by using X-ray microtomography. *Food Hydrocolloids*, *36*, 37–44. https://doi.org/10.1016/j.foodhyd.2013.09.002

Dobraszczyk, B. J., & Morgenstern, M. P. (2003). Rheology and the breadmaking process. *Journal of Cereal Science*, *38*(3), 229–245. https://doi.org/10.1016/S0733-5210(03)00059-6

Dobraszczyk, B. J., & Roberts, C. A. (1994). Strain hardening and dough gas cell-wall failure in biaxial extension. *Journal of Cereal Science*, *20*, 265–274.

Dreese, P. . C., Faubion, J. M., & Hoseney, R. C. (1988). Dynamic rheological properties of flour, gluten, and gluten-starch doughs. II. Effect of various processing and ingredient changes. *Cereal Chemistry*, *65*(4), 354–359.

Du Cailar, G., Ribstein, J., & Mimran, A. (2002). Dietary salt and target organ damage in essential hypertension. *American Journal of Hypertension*, *15*(3), 222–229. https://doi.org/10.1016/S0895-7061(01)02287-7

Edwards, N. M., Dexter, J. E., Scanlon, M. G., & Cenkowski, S. (1999). Relationship of creep-recovery and dynamic oscillatory measurements to durum wheat physical dough properties. *Cereal Chemistry*, *76*(5), 638–645. https://doi.org/10.1094/CCHEM.1999.76.5.638

Edwards, N. M., Peressini, D., Dexter, J. E., & Mulvaney, S. J. (2001). Viscoelastic properties of durum wheat and common wheat dough of different strengths. *Rheologica Acta*, *40*(2), 142–153. https://doi.org/10.1007/s003970000147

Eliasson, A.-C., & Larsson, K. (1993). *Cereals in Breadmaking*. New York, USA: Marcel Dekker.

Elliott, P., Stamler, J., Nichols, R., Dayer, A. R., Stamler, R., Kesteloot, H., & Marmot, M. (1996). Intersalt revisited: Further analyses of 24 hour sodium excretion and blood pressure within and across populations. *British Medical Jounral*, *312*(7041), 1249–1253.

Elmehdi, H. M., Page, J. H., & Scanlon, M. G. (2003). Using ultrasound to investigate the cellular structure of bread crumb. *Journal of Cereal Science*, *38*(1), 33–42. https://doi.org/10.1016/S0733-5210(03)00002-X

Elmehdi, H. M., Page, J. H., & Scanlon, M. G. (2004). Ultrasonic investigation of the effect of mixing under reduced pressure on the mechanical properties of bread dough. *Cereal Chemistry*, *81*(4), 504–510. https://doi.org/10.1094/CCHEM.2004.81.4.504

Falcone, P. M., Baiano, A., Conte, A., Mancini, L., Tromba, G., Zanini, F., & Del Nobile, M. A. (2006). Imaging techniques for the study of food microstructure: A review. *Advances in Food and Nutrition Research*, *51*, 205–263. https://doi.org/10.1016/S1043-4526(06)51004-6

Falcone, P. M., Baiano, A., Zanini, F., Mancini, L., Tromba, G., Dreossi, D., … Del Nobile, M. A. (2005). Three-dimensional quantitative analysis of bread crumb by X-ray microtomography. *Journal of Food Science*, *70*(3), E265–E272.

Falcone, P. M., Baiano, A., Zanini, F., Mancini, L., Tromba, G., Montanari, F., & Del Nobile, M. A. (2004). A novel approach to the study of bread porous structure: Phase-contrast X-ray microtomography. *Food Engineering and Physical Properties*, *69*(1), 38–43. https://doi.org/10.1111/j.1365-2621.2004.tb17865.x

Farahnaky, A., & Hill, S. E. (2007). The effect of salt , water and temperature on wheat dough rheology. *Journal of Texture Studies*, *38*, 499–510. https://doi.org/10.1111/j.1745-4603.2007.00107.x

Faubion, J. M. (1987). Introduction. In H. Faridi & J. M. Faubion (Eds.), *Fundamentals of Dough Rheology* (pp. 1–8). St. Paul, MN, USA: AACC International Inc.

Faubion, J. M., & Hoseney, C. R. (1990). The viscoelastic properties of wheat flour doughs. In H. Faridi & J. M. Faubion (Eds.), *Dough Rheology and Baked Product Texture* (pp. 29–66). New York, USA: Van Nostrand Reinhold.

Ferry, J. D. (1961). Illustrations of viscoelastic behavior of polymeric systems. In *Viscoelastic Properties of Polymers* (pp. 20–60). New York, USA: John Wiley & Sons, Inc.

Fischer, P. W. F., Vigneault, M., Huang, R., Arvaniti, K., & Roach, P. (2009). Sodium food sources in the Canadian diet. *Applied Physiology, Nutrition, and Metabolism*, *34*(5), 884–892. https://doi.org/10.1139/h09-077

Fitzgerald, R. (2000). Phase-sensitive X-ray imaging. *Physics Today*, *53*(7), 23–26. https://doi.org/10.1063/1.1292471

Forbes, C., Evans, M., Hastings, N., & Peacock, B. (2017). *Statistical Distributions*. Hoboken, NJ, USA: John Wiley & Sons, Inc. https://doi.org/10.1007/978-3-319-65112-5

Gabriele, D., De Cindio, B., & D'Antona, P. (2001). A weak gel model for foods. *Rheologica Acta*, *40*(2), 120–127. https://doi.org/10.1007/s003970000139

Galal, A. M., Varriano-Marston, E., & Johnson, J. A. (1978). Rheological dough properties as affected by organic acids and salt. *Cereal Chemistry*, *55*(5), 683–691.

Gan, Z., Angold, R. E., Williams, M. R., Ellis, P. R., Vaughan, J. G., & Galliard, T. (1990). The microstructure and gas retention of bread dough. *Journal of Cereal Science*, *12*(1), 15–24. https://doi.org/10.1016/S0733-5210(09)80153-7

Gan, Z., Ellis, P. R., & Schofield, J. D. (1995). Gas cell stabilisation and gas retention in wheat bread dough. *Journal of Cereal Science*, *21*(3), 215–230. https://doi.org/10.1006/jcrs.1995.0025

Garrett, P. R. (1993). Recent developments in the understanding of foam generation and stability. *Chemical Engineering Science*, *48*(2), 367–392.

Gélinas, P., & Mckinnon, C. (2013). Experiments on dough rheology to improve screening of bread wheat cultivars. *International Journal of Food Science and Technology*, *48*(9), 1956–1961. https://doi.org/10.1111/ijfs.12176

Georgopoulos, T., Larsson, H., & Eliasson, A. C. (2004). A comparison of the rheological

properties of wheat flour dough and its gluten prepared by ultracentrifugation. *Food Hydrocolloids*, *18*(1), 143–151. https://doi.org/10.1016/S0268-005X(03)00059-6

Gómez, A., Ferrero, C., Calvelo, A., Añón, M. C., & Puppo, M. C. (2011). Effect of mixing time on structural and rheological properties of wheat flour dough for breadmaking. *International Journal of Food Properties*, *14*(3), 583–598. https://doi.org/10.1080/10942910903295939

Gras, P. W., Carpenter, H. C., & Anderssen, R. S. (2000). Modelling the developmental rheology of wheat-flour dough using extension tests. *Journal of Cereal Science*, *31*(1), 1–13. https://doi.org/10.1006/jcrs.1999.0293

Gras, P. W., & O'Brien, L. (1992). Application of a 2-gram mixograph to early generation selection for dough strength. *Cereal Chemistry*, *69*(3), 254–257.

Grenier, A., Lucas, T., Collewet, G., & Le Bail, A. (2003). Assessment by MRI of local porosity in dough during proving. Theoretical considerations and experimental validation using a spin-echo sequence. *Magnetic Resonance Imaging*, *21*(9), 1071–1086. https://doi.org/10.1016/S0730-725X(03)00194-2

Guillermic, R. M., Koksel, F., Sun, X., Hatcher, D. W., Nickerson, M. T., Belev, G. S., … Scanlon, M. G. (2018). Bubbles in noodle dough: Characterization by X-ray microtomography. *Food Research International*, *105*, 548–555. https://doi.org/10.1016/j.foodres.2017.11.050

Gundogdu, O., Nirgianaki, E., Che Ismail, E., Jenneson, P. M., & Bradley, D. A. (2007). Benchtop phase-contrast X-ray imaging. *Applied Radiation and Isotopes*, *65*(12), 1337–1344. https://doi.org/10.1016/j.apradiso.2007.07.009

Gupta, R. B., Khan, K., & Macritchie, F. (1993). Biochemical basis of flour properties in bread wheats. I. Effects of variation.pdf. *Journal of Cereal Science*, *18*, 23–41.

Halim, H. K., & Shoemaker, C. F. (1990). Effect of addition of α-, β -, and κ-casein, and Na-

caseinate on viscoelastic properties of skim milk curd. *Journal of Texture Studies*, *21*(3), 323–337.

Haraszi, R., Larroque, O. R., Butow, B. J., Gale, K. R., & Bekes, F. (2008). Differential mixing action effects on functional properties and polymeric protein size distribution of wheat dough. *Journal of Cereal Science*, *47*(1), 41–51. https://doi.org/10.1016/j.jcs.2007.01.007

Hardt, N. A., Boom, R. M., & van der Goot, A. J. (2014). Wheat dough rheology at low water contents and the influence of xylanases. *Food Research International*, *66*, 478–484. https://doi.org/10.1016/j.foodres.2014.10.011

Hayman, D., Hoseney, R. C., & Faubion, J. M. (1998). Bread crumb grain development during baking. *Cereal Chemistry*, *75*(5), 577–580. https://doi.org/10.1094/CCHEM.1998.75.5.577

He, H., & Hoseney, R. C. (1991). Differences in gas retention, protein solubility, and rheological properties between flours of different baking quality. *Cereal Chemistry*, *68*(5), 526–530.

He, H., & Hoseney, R. C. (1992). Factors controlling gas retention in nonheated doughs. *Cereal Chemistry*, *69*(1), 1–6.

He, H., Roach, R., & Hoseney, R. C. (1992). Effect of nonchaotropic salts on flour bread-making properties. *Cereal Chemistry*, *69*(4), 366–371.

Heertje, I., Vlist, P., Blonk, J. C. G., Hendrickx, H., & Brakenhoff, G. J. (1987). Confocal scanning laser microscopy in food research: Some observations. *Food Microstructure*, *6*, 115–120. https://doi.org/10.1086/302850

Hibberd, G. E. (1970). Dynamic viscoelastic behaviour of wheat flour doughs Part III: The influence of the starch granules. *Rheologica Acta*, *9*(4), 501–505. https://doi.org/10.1007/BF01985459

Hlynka, I. (1962). Influence of temperature, speed of mixing and salt on some rheological

properties of dough in the farinograph. *Cereal Chemistry*, *39*(14), 286–303.

Horst, R. H., & Winter, H. H. (2000). Stable critical gels of a copolymer of ethene and 1-butene achieved by partial melting and recrystallization. *Macromolecules*, *33*(20), 7538–7543. https://doi.org/10.1021/ma000361z

Horvat, D., Magdić, D., Simić, G., Dvojković, K., & Drezner, G. (2008). The relation between dough rheology and bread crumb properties in winter wheat. *Agriculturae Conspectus Scientificus*, *73*(1), 9–12.

Hoseney, R. C. (1986). Yeast-leavened products. In *Principles of Cereal Science and Technology* (pp. 1–203). St. Paul, MN, USA: AACC International Inc.

Hoseney, R. C. (1994). *Cereal Science and Technology*. (R. C. Hoseney, Ed.). St. Paul, MN, USA: AACC International Inc.

Hu, B., Nienow, A. W., & Pacek, A. W. (2003). The effect of sodium caseinate concentration and processing conditions on bubble sizes and their break-up and coalescence in turbulent, batch air/aqueous dispersions at atmospheric and elevated pressures. *Colloids and Surfaces B: Biointerfaces*, *31*, 3–11. https://doi.org/10.1016/S0927-7765(03)00038-9

Huang, H., & Kokini, J. L. (1999). Prediction of dough volume development which considers the biaxial extensional growth of cells. In G. M. Campbell, C. Webb, S. S. Pandiella, & K. Niranjan (Eds.), *Bubbles in Food* (pp. 113–120). St. Paul, MN, USA: Eagan Press.

Huang, S., Yun, S.-H., Quail, K., & Moss, R. (1996). Establishment of flour quality guidelines for northern style Chinese steamed bread. *Journal of Cereal Science*, *24*(2), 179–185. https://doi.org/10.1006/jcrs.1996.0051

Huebner, F. R. (1970). Comparative studies on glutenins from different classes of wheat. *Journal of Agricultural and Food Chemistry*, *18*(2), 256–259. https://doi.org/10.1021/jf60168a006

Huebner, F. R., & Wall, J. S. (1980). Wheat glutenin: Effect of dissociating agents on molecular weight and composition as determined by gel filtration chromatography. *Journal of Agricultural and Food Chemistry*, *28*(2), 433–438. https://doi.org/10.1021/jf60228a054

Hutton, T. (2002). Sodium technological functions of salt in the manufacturing of food and drink products. *British Food Journal*, *104*(2), 126–152. https://doi.org/10.1108/00070700210423635

Isaak, C., Sapirstein, H., Wu, Y., & Graf, R. (2019). Effects of water absorption and salt on discrimination of wheat gluten strength assessed by dough mixing and protein composition. *Journal of Cereal Science*.

Isaak, C. A. (2019). *Comparison of Physical and Biochemical Methods to Evaluate the Gluten Strength of Canadian Hard Red Winter Wheats*. University of Manitoba (MSc Thesis).

Ishida, N., Takano, H., Naito, S., Isobe, S., Uemura, K., Haishi, T., … Kano, H. (2001). Architecture of baked breads depicted by a magnetic resonance imaging. *Magnetic Resonance Imaging*, *19*(6), 867–874. https://doi.org/10.1016/S0730-725X(01)00410-6

Izuka, A., Winter, H. H., & Hashimoto, T. (1994). Temperature Dependence of Viscoelasticity of Polycaprolactone Critical Gels. *Macromolecules*, *27*(23), 6883–6888. https://doi.org/10.1021/ma00101a028

Jaishankar, A., & McKinley, G. H. (2014). A fractional K-BKZ constitutive formulation for describing the nonlinear rheology of multiscale complex fluids. *Journal of Rheology*, *58*(6), 1751–1788. https://doi.org/10.1122/1.4892114

Janssen, A. M., Vliet, T. V., & Vereijken, J. M. (1996). Fundamental and empirical rheological behaviour of wheat flour doughs and comparison with bread making performance. *Journal of Cereal Science*, *23*(1), 19–31. https://doi.org/10.1006/jcrs.1996.0002

Jekle, M., & Becker, T. (2011). Dough microstructure: Novel analysis by quantification using confocal laser scanning microscopy. *Food Research International*, *44*(4), 984–991. https://doi.org/10.1016/j.foodres.2011.02.036

Jekle, M., & Becker, T. (2012). Effects of acidification, sodium chloride, and moisture levels on wheat dough: I. Modeling of rheological and microstructural properties. *Food Biophysics*, *7*(3), 190–199. https://doi.org/10.1007/s11483-012-9257-0

Junge, R. C., Hoseney, R. C., & Varriano-Marston, E. (1981). Effect of surfactants on air incorporation in dough and the crumb grain of bread. *Cereal Chemistry*, *58*(4), 338–342.

Kaláb, M., Allan-Wojtas, P., & Miller, S. S. (1995). Microscopy and other imaging techniques in food structure analysis. *Trends in Food Science & Technology*, *6*, 177–186. https://doi.org/10.1016/S0924-2244(00)89052-4

Kamman, P. W. (1970). Factors affecting the grain and texture of white bread. *Bakers Digest*, *44*(2), 34–38.

Kansou, K., Chiron, H., Valle, G. D., Ndiaye, A., Roussel, P., & Shehzad, A. (2013). Modelling wheat flour dough proofing behaviour: Effects of mixing conditions on porosity and stability. *Food and Bioprocess Technology*, *6*(8), 2150–2164. https://doi.org/10.1007/s11947-012-0854-1

Karunakaran, C., Lahlali, R., Zhu, N., Webb, A. M., Schmidt, M., Fransishyn, K., … Hallin, E. (2015). Factors influencing real time internal structural visualization and dynamic process monitoring in plants using synchrotron-based phase contrast X-ray imaging. *Scientific Reports*, *5*, 1–13. https://doi.org/10.1038/srep12119

Kashyap, Y. S., Yadav, P. S., Roy, T., Sarkar, P. S., Shukla, M., & Sinha, A. (2008). Laboratory-based X-ray phase-contrast imaging technique for material and medical science applications.

Applied Radiation and Isotopes, *66*(8), 1083–1090. https://doi.org/10.1016/j.apradiso.2007.12.008

Kaufman, A., Cohen, D., & Yagel, R. (1993). Volume Graphics. *Computer*, *26*(7), 51–64. https://doi.org/10.1109/MC.1993.274942

Khatkar, B. S., Bell, A. E., & Schofield, J. D. (1995). The dynamic rheological properties of glutens and gluten sub-fractions from wheats of good and poor bread making quality. *Journal of Cereal Science*, *22*(1), 29–44. https://doi.org/10.1016/S0733-5210(05)80005-0

Khatkar, B. S., Bell, A. E., & Schofield, J. D. (1996). A comparative study of the inter-relationships between mixograph parameters and bread-making qualities of wheat flours and glutens. *Journal of the Science of Food and Agriculture*, *72*(1), 71–85. https://doi.org/10.1002/(SICI)1097-0010(199609)72:1<71::AID-JSFA625>3.0.CO;2-4

Khatkar, B. S., & Schofield, J. D. (2002). Dynamic rheology of wheat flour dough. II. Assessment of dough strength and bread-making quality. *Journal of the Science of Food and Agriculture*, *82*(8), 823–826. https://doi.org/10.1002/jsfa.1111

Kilborn, R. H., & Tipples, K. H. (1972). Factors affecting mechanical dough development. I. Effect of mixing intensity and work input. *Cereal Chemistry*, *49*, 34–47.

Kilborn, R. H., & Tipples, K. H. (1981). Canadian test baking procedures. I. GRL remix method and variations. *Cereal Foods World*, *26*, 624–628.

Kim, H. R., & Bushuk, W. (1995). Salt sensitivity of acetic acid-extractable proteins of wheat flour. *Journal of Cereal Science*, *21*(3), 241–250. https://doi.org/10.1006/jcrs.1995.0027

Kindelspire, J. Y., Glover, K. D., Caffé-Treml, M., & Krishnan, P. G. (2015). Dough strain hardening properties as indicators of baking performance. *Cereal Chemistry*, *92*(3), 293–301. https://doi.org/10.1094/CCHEM-12-13-0249-R

Kokawa, M., Fujita, K., Sugiyama, J., Tsuta, M., Shibata, M., Araki, T., & Nabetani, H. (2012). Quantification of the distributions of gluten, starch and air bubbles in dough at different mixing stages by fluorescence fingerprint imaging. *Journal of Cereal Science*, *55*(1), 15–21. https://doi.org/10.1016/j.jcs.2011.09.002

Kokelaar, J. J., & Prins, A. (1995). Surface rheological properties of bread dough components in relation to gas bubble stability. *Journal of Cereal Science*, *22*(1), 53–61. https://doi.org/10.1016/S0733-5210(05)80007-4

Kokelaar, J. J., van Vliet, T., & Prins, A. (1996). Strain hardening properties and extensibility of flour and gluten doughs in relation to breadmaking performance. *Journal of Cereal Science*, *24*(3), 199–214. https://doi.org/http://dx.doi.org/10.1006/jcrs.1996.0053

Koksel, F. (2014). *Use of ultrasound and X-ray microtomography to determine bubble size distributions in non-yeasted wheat (Triticum aestivum L.) flour dough*. University of Manitoba (PhD Thesis).

Koksel, F., Aritan, S., Strybulevych, A., Page, J. H., & Scanlon, M. G. (2016). The bubble size distribution and its evolution in non-yeasted wheat flour doughs investigated by synchrotron X-ray microtomography. *Food Research International*, *80*, 12–18. https://doi.org/10.1016/j.foodres.2015.12.005

Koksel, F., & Scanlon, M. G. (2012). Effects of composition on dough development and air entrainment in doughs made from gluten-starch blends. *Journal of Cereal Science*, *56*(2), 445–450. https://doi.org/10.1016/j.jcs.2012.05.013

Koksel, F., Strybulevych, A., Page, J. H., & Scanlon, M. G. (2014). Ultrasonic characterization of unyeasted bread dough of different sodium chloride concentrations. *Cereal Chemistry*, *91*(4), 327–332. https://doi.org/10.1094/CCHEM-10-13-0206-CESI

Kontogiorgos, V. (2011). Microstructure of hydrated gluten network. *Food Research International*, *44*(9), 2582–2586. https://doi.org/10.1016/j.foodres.2011.06.021

Kontogiorgos, V. (2017). Linear viscoelasticity of gluten: Decoupling of relaxation mechanisms. *Journal of Cereal Science*, *75*, 286–295. https://doi.org/10.1016/j.jcs.2017.04.001

Kontogiorgos, V., Shah, P., & Bills, P. (2016). Influence of supramolecular forces on the linear viscoelasticity of gluten. *Rheologica Acta*, *55*(3), 187–195. https://doi.org/10.1007/s00397-015-0901-8

Lachaise, J., Sahnoun, S., Dicharry, C., Mendiboure, B., & Salager, J. L. (1991). Improved determination of the initial structure of liquid foams. *Progress in Colloid and Polymer Science*, *84*, 253–256. https://doi.org/10.1007/BFb0115976

Laguna, L., Hernández, M. J., Salvador, A., & Sanz, T. (2013). Study on resistant starch functionality in short dough biscuits by oscillatory and creep and recovery tests. *Food and Bioprocess Technology*, *6*, 1312–1320. https://doi.org/10.1007/s11947-012-0785-x

Lampignano, V., Laverse, J., Mastromatteo, M., & Del Nobile, M. A. (2013). Microstructure, textural and sensorial properties of durum wheat bread as affected by yeast content. *Food Research International*, *50*(1), 369–376. https://doi.org/10.1016/j.foodres.2012.10.030

Lang, C. E., Neises, E. K., & Walker, C. E. (1992). Effects of additives on flour-water dough mixograms. *Cereal Chemistry*, *69*(6), 587–591.

Larsen, R. A. (1964). Hydration as a factor in bread flour quality. *Cereal Chemistry*, *41*, 181–187.

Larsson, H. (2002). Effect of pH and sodium chloride on wheat flour dough properties: Ultracentrifugation and rheological measurements. *Cereal Chemistry*, *79*(4), 544–545. https://doi.org/10.1094/CCHEM.2002.79.4.544

Larsson, H., Eliasson, A. C., Johansson, E., & Svensson, G. (2000). Influence of added starch on

mixing of dough made with three wheat flours differing in high molecular weight subunit composition: Rheological behavior. *Cereal Chemistry*, *77*(5), 633–639. https://doi.org/10.1094/CCHEM.2000.77.5.633

Lassoued, N., Babin, P., Della Valle, G., Devaux, M. F., & Réguerre, A. L. (2007). Granulometry of bread crumb grain: Contributions of 2D and 3D image analysis at different scale. *Food Research International*, *40*(8), 1087–1097. https://doi.org/10.1016/j.foodres.2007.06.004

Lazaridou, A., Duta, D., Papageorgiou, M., Belc, N., & Biliaderis, C. G. (2007). Effects of hydrocolloids on dough rheology and bread quality parameters in gluten-free formulations. *Journal of Food Engineering*, *79*(3), 1033–1047. https://doi.org/10.1016/j.jfoodeng.2006.03.032

Lee, L., Ng, P. K. W., Whallon, J. H., & Steffe, J. F. (2001). Relationship between rheological properties and microstructural characteristics of nondeveloped, partially developed, and developed doughs. *Cereal Chemistry*, *78*(4), 447–452. https://doi.org/10.1094/CCHEM.2001.78.4.447

Lefebvre, J. (2006). An outline of the non-linear viscoelastic behaviour of wheat flour dough in shear. *Rheologica Acta*, *45*(4), 525–538. https://doi.org/10.1007/s00397-006-0093-3

Lefebvre, J. (2009). Nonlinear, time-dependent shear flow behaviour, and shear-induced effects in wheat flour dough rheology. *Journal of Cereal Science*, *49*(2), 262–271. https://doi.org/10.1016/j.jcs.2008.10.010

Lefebvre, J., & Mahmoudi, N. (2007). The pattern of the linear viscoelastic behaviour of wheat flour dough as delineated from the effects of water content and high molecular weight glutenin subunits composition. *Journal of Cereal Science*, *45*(1), 49–58. https://doi.org/10.1016/j.jcs.2006.06.005

Lemlich, R. (1978). Prediction of changes in bubble size distribution due to interbubble gas diffusion in foam. *Industrial and Engineering Chemistry Fundamentals*, *17*(2), 89–93. https://doi.org/10.1021/i160066a003

Leroy, V., Fan, Y., Strybulevych, A., Bellido, G. G., Page, J. H., & Scanlon, M. G. (2008). Investigating the bubble size distribution in dough using ultrasound. In G. M. Campbell, M. G. Scanlon, & D. L. Pyle (Eds.), *Bubbles in Food 2: Novelty, Health and Luxury* (pp. 51–60). St. Paul, MN, USA: Eagan Press.

Leroy, V., Pitura, K. M., Scanlon, M. G., & Page, J. H. (2010). The complex shear modulus of dough over a wide frequency range. *Journal of Non-Newtonian Fluid Mechanics*, *165*, 475–478. https://doi.org/10.1016/j.jnnfm.2010.02.001

Létang, C., Piau, M., & Verdier, C. (1999). Characterization of wheat flour – water doughs . Part I : Rheometry and microstructure. *Journal of Food Engineering*, *41*, 121–132. https://doi.org/10.1016/S0260-8774(99)00082-5

Levine, H., & Slade, L. (1990). Influences of the glassy and rubbery states on the thermal, mechanical, and structural properties of doughs and baked products. In H. Faridi & J. M. Faubion (Eds.), *Dough Rheology and Baked Product Texture* (p. 157). New York, USA: Van Nostrand Reinhold.

Lim, K. S., & Barigou, M. (2004). X-ray micro-computed tomography of cellular food products. *Food Research International*, *37*(10), 1001–1012. https://doi.org/10.1016/j.foodres.2004.06.010

Limpert, E., Stahel, W. A., & Abbt, M. (2001). Log-normal distributions across the sciences: Keys and clues. *BioScience*, *51*(5), 341. https://doi.org/10.1641/0006-3568(2001)051[0341:LNDATS]2.0.CO;2

Linko, P., Härkönen, H., & Linko, Y. Y. (1984). Effects of sodium chloride in the processing of bread baked from wheat, rye and barley flours. *Journal of Cereal Science*, *2*(1), 53–62. https://doi.org/10.1016/S0733-5210(84)80008-9

Lucassen, J. (1981). Dynamic properties of free liquid films and foams. In E. H. Lucassen-Reynders (Ed.), *Anionic Surfactants* (pp. 217–265). New York, USA: Marcel Dekker, Inc.

Lukie, C. A. (2001). *Effects of genotype and environment on the breadmaking quality of Canada western extra strong red spring wheat cultivars*. University of Manitoba (MSc Thesis).

Lynch, E. J., Dal Bello, F., Sheehan, E. M., Cashman, K. D., & Arendt, E. K. (2009). Fundamental studies on the reduction of salt on dough and bread characteristics. *Food Research International*, *42*(7), 885–891. https://doi.org/10.1016/j.foodres.2009.03.014

MacRitchie, F. (1976). The liquid phase of dough and its role in baking. *Cereal Chemistry*, *53*(3), 318–326.

Magrabi, S. A., Dlugogorski, B. Z., & Jameson, G. J. (1999). Bubble size distribution and coarsening of aqueous foams. *Chemical Engineering Science*, *54*(18), 4007–4022. https://doi.org/10.1016/S0009-2509(99)00098-6

Maire, E., Fazekas, A., Salvo, L., Dendievel, R., Youssef, S., Cloetens, P., & Letang, J. M. (2003). X-ray tomography applied to the characterization of cellular materials. Related finite element modeling problems. *Composites Science and Technology*, *63*(16), 2431–2443. https://doi.org/10.1016/S0266-3538(03)00276-8

Mani, K., Eliasson, A.-C., Lindahl, L., & Tragardh, C. (1992). Rheological properties and breadmaking quality of wheat flour doughs made with different dough mixers. *Cereal Chemistry*, *69*(2), 222–225.

Mani, K., & Trligardh, C. (1992). Water content, water soluble fraction, and mixing affect

fundamental rheological properties of wheat flour doughs. *Journal of Food Science*, *57*(5), 1198–1201.

Manohar, R. S., & Rao, P. H. (1999). Effect of sugars on the rheological characteristics of biscuit dough and quality of biscuits. *European Food Research and Technology*, *209*, 281–285.

Marsh, D. (1998). Mixing and dough processing. In S. P. Cauvain & L. S. Young (Eds.), *Technology of Breadmaking* (pp. 81–119). London, UK: Blackie Academic and Professional.

Martin, A. H., Grolle, K., Bos, M. A., Cohen Stuart, M. A., & Van Vliet, T. (2002). Network forming properties of various proteins adsorbed at the air/water interface in relation to foam stability. *Journal of Colloid and Interface Science*, *254*(1), 175–183. https://doi.org/10.1006/jcis.2002.8592

Martin, P. J., Chin, N. L., Campbell, G. M., & Morrant, C. J. (2004). Aeration during bread dough mixing II. A population balance model of Aeration. *Food and Bioproducts Processing*, *82*(C4), 268–281. https://doi.org/10.1205/fbio.82.4.282.56408

Martinant, J. P., Nicolas, Y., Bouguennec, A., Popineau, Y., Soulnier, L., & Branlard, G. (1998). Relationships between mixograph parameters and indices of wheat grain quality. *Journal of Cereal Science*, *27*(2), 179–189. https://doi.org/10.1006/jcrs.1997.0156

Martz, H. E., Logan, C. M., Schneberk, D. J., & Shull, P. J. (2017). *X-Ray Imaging Fundamentals, Industrial Techniques and Applications*. Boca Raton, FL, USA: CRC Press.

Masi, P., Cavella, S., & Sepe, M. (1998). Characterization of dynamic viscoelastic behavior of wheat flour doughs at different moisture contents. *Cereal Chemistry*, *75*(4), 428–432. https://doi.org/10.1094/CCHEM.1998.75.4.428

Mastromatteo, M., Guida, M., Danza, A., Laverse, J., Frisullo, P., Lampignano, V., … Nobile, D. (2013). Rheological , microstructural and sensorial properties of durum wheat bread as

affected by dough water content. *Food Research International*, *51*(2), 458–466. https://doi.org/10.1016/j.foodres.2013.01.004

Mathai, A. M., & Pederzoli, G. (1977). *Characterizations of the Normal Probability Law*. New York, USA: John Wiley & Sons, Inc.

McCann, T. H., & Day, L. (2013). Effect of sodium chloride on gluten network formation, dough microstructure and rheology in relation to breadmaking. *Journal of Cereal Science*, *57*(3), 444–452. https://doi.org/10.1016/j.jcs.2013.01.011

Meerts, M., Cardinaels, R., Oosterlinck, F., Courtin, C. M., & Moldenaers, P. (2017). The impact of water content and mixing time on the linear and non-linear rheology of wheat flour dough. *Food Biophysics*, *12*(2), 151–163. https://doi.org/10.1007/s11483-017-9472-9

Mehta, K. L., Scanlon, M. G., Sapirstein, H. D., & Page, J. H. (2009). Ultrasonic investigation of the effect of effect of vegetable shortening and mixing time on the mechanical properties of bread dough. *Journal of Food Science*, *74*(9), 455–461. https://doi.org/10.1111/j.1750-3841.2009.01346.x

Meinders, M. B. J., & Van Vliet, T. (2004). The role of interfacial rheological properties on Ostwald ripening in emulsions. *Advances in Colloid and Interface Science*, *108-109*, 119–126. https://doi.org/10.1016/j.cis.2003.10.005

Melander, W., & Horváth, C. (1977). Salt effects on hydrophobic interactions in precipitation and chromatography of proteins: An interpretation of the lyotropic series. *Archives of Biochemistry and Biophysics*, *183*(1), 200–215. https://doi.org/10.1016/0003-9861(77)90434-9

MenJivar, J. A. (1990). Fundamental aspects of dough rheology. In H. Faridi & J. M. Faubion (Eds.), *Dough Rheology and Baked Product Texture* (pp. 1–28). New York, USA: Van

Nostrand Reinhold.

Miller, K. A., & Hoseney, R. C. (1999). Dynamic rheological properties of wheat starch-gluten doughs. *Cereal Chemistry*, *76*(1), 105–109. https://doi.org/doi:10.1094/CCHEM.1999.76.1.105

Miller, R. A., & Hoseney, R. C. (2008). Role of salt in baking. *Cereal Foods World*, *53*(1), 4–6. https://doi.org/10.1094/CFW-53-1-0004

Mills, E. N. C., Wilde, P. J., Salt, L. J., & Skeggs, P. (2003). Bubble formation and stabilization in bread dough. *Food and Bioproducts Processing*, *81*(3), 189–193. https://doi.org/http://dx.doi.org/10.1205/096030803322437956

Monsalve, A., & Schechter, R. S. (1984). The stability of foams: Dependence of observation on the bubble size distribution. *Journal of Colloid and Interface Science*, *97*(2), 327–335. https://doi.org/10.1016/0021-9797(84)90303-5

Mours, M., & Winter, H. H. (1996). Relaxation patterns of nearly critical gels. *Macromolecules*, *29*(22), 7221–7229. https://doi.org/10.1021/ma9517097

Muller, H. G. (1973). *An Introduction to Food Rheology*. London, UK: William Heinemann Ltd.

Murray, B. S., & Ettelaie, R. (2004). Foam stability: Proteins and nanoparticles. *Current Opinion in Colloid and Interface Science*, *9*, 314–320. https://doi.org/10.1016/j.cocis.2004.09.004

Navickis, L. L., Anderson, R. A., Bagley, E. B., & Jasberg, B. K. (1982). Viscoelastic properties of wheat flour doughs: Variation of dynamic moduli with water and protein content. *Journal of Texture Studies*, *13*, 249–264. https://doi.org/10.1111/j.1745-4603.1982.tb01399.x

Ng, T. (2008). *Linear to nonlinear rheology of bread dough and its constituents*. Massachusetts Institute of Technology (PhD Thesis).

Ng, T., McKinley, G. H., & Ewoldt, R. H. (2011). Large amplitude oscillatory shear flow of gluten

dough: A model power-law gel. *Journal of Rheology*, *55*(3), 627. https://doi.org/10.1122/1.3570340

Ng, T., McKinley, G. H., & Padmanabhan, M. (2006). Linear to non-linear rheology of wheat flour. *International Symposium on Food Rheology and Structure*, *16*, 265–274.

Noort, M. W. J., Bult, J. H. F., Stieger, M., & Hamer, R. J. (2010). Saltiness enhancement in bread by inhomogeneous spatial distribution of sodium chloride. *Journal of Cereal Science*, *52*(3), 378–386. https://doi.org/10.1016/j.jcs.2010.06.018

Oliver, J. R., & Allen, H. M. (1992). The prediction of bread baking performance using the farinograph and extensograph. *Journal of Cereal Science*, *15*(1), 79–89. https://doi.org/10.1016/S0733-5210(09)80058-1

Örnebro, J., Nylander, T., & Eliasson, A. C. (2000). Interfacial behaviour of wheat proteins. *Journal of Cereal Science*, *31*(2), 195–221. https://doi.org/10.1006/jcrs.1999.0297

Papoulia, K. D., Panoskaltsis, V. P., Kurup, N. V., & Korovajchuk, I. (2010). Rheological representation of fractional order viscoelastic material models. *Rheologica Acta*, *49*(4), 381–400. https://doi.org/10.1007/s00397-010-0436-y

Paredes, M. D. C., Rao, M. A., & Bourne, M. C. (1989). Rheological characteristics of salad dressings II: Effect of storage. *Journal of Texture Studies*, *20*, 235–250.

Paredes-Lopez, O., & Bushuk, W. (1982). Development and "undevelopment"of wheat dough by mixing: Physicochemical studies. *Cereal Chemistry*, *60*(1), 19–23.

Payne, P. I., & Corfield, K. G. (1979). Subunit composition of wheat glutenin proteins isolated by gel filtration in a dissociating medium. *Plant Breeding*, *88*, 83–88.

Pedersen, L., Kaack, K., Bergsøe, M. N., & Adler-Nissen, J. (2004). Rheological properties of biscuit dough from different cultivars, and relationship to baking characteristics. *Journal of*

Cereal Science, *39*(1), 37–46. https://doi.org/10.1016/S0733-5210(03)00064-X

Peighambardoust, S. H., Fallah, E., Hamer, R. J., & van der Goot, A. J. (2010). Aeration of bread dough influenced by different way of processing. *Journal of Cereal Science*, *51*(1), 89–95. https://doi.org/10.1016/j.jcs.2009.10.002

Peighambardoust, S. H., van der Goot, A. J., Boom, R. M., & Hamer, R. J. (2006). Mixing behaviour of a zero-developed dough compared to a flour-water mixture. *Journal of Cereal Science*, *44*(1), 12–20. https://doi.org/10.1016/j.jcs.2005.12.011

Peressini, D., Sensidoni, A., Pollini, C. M., & Cindio, B. (2000). Rheology of wheat doughs for fresh pasta production: influence of semolina-flour blends and salt content. *Journal of Texture Studies*, *31*(2), 163–182. https://doi.org/10.1111/j.1745-4603.2000.tb01415.x

Pinzer, B. R., Medebach, A., Limbach, H. J., Dubois, C., Stampanoni, M., & Schneebeli, M. (2012). 3D-characterization of three-phase systems using X-ray tomography: Tracking the microstructural evolution in ice cream. *Soft Matter*, *8*(17), 4584. https://doi.org/10.1039/c2sm00034b

Pon, C. R., Lukow, O. M., & Buckley, D. J. (1988). A multichannel, computer-based system for analyzing dough rheology. *Journal of Texture Studies*, *19*(4), 343–360. https://doi.org/10.1111/j.1745-4603.1988.tb00406.x

Preston, K. R. (1981). Effects of neutral salts upon wheat gluten protein properties. I. Relationship between the hydrophobic properties of gluten proteins and their extractability and turbidity in neutral salts. *Cereal Chemistry*, *58*(4), 317–324.

Preston, K. R. (1984). Gel filtration of neutral salt extracted gluten proteins varying in hydrophobic properties. *Cereal Chemistry*, *61*(1), 76–83.

Preston, K. R. (1985). Use of lyotropic salts to study the hydrophobic properties of wheat gluten

proteins. In *Gluten Proteins. Proceedings of the 2nd International Workshop on Gluten Proteins.* (pp. 207–217). TNO, Netherlands.

Preston, K. R. (1989). Effects of neutral salts of the lyotropic series on the physical dough properties of a Canadian red spring wheat flour. *Cereal Chemistry*, *66*(3), 144–148.

Proussevitch, A. A., Sahagian, D. L., & Carlson, W. D. (2007a). Statistical analysis of bubble and crystal size distributions: Application to Colorado Plateau basalts. *Journal of Volcanology and Geothermal Research*, *164*(3), 112–126. https://doi.org/10.1016/j.jvolgeores.2007.04.006

Proussevitch, A. A., Sahagian, D. L., & Carlson, W. D. (2007b). Statistical analysis of bubble and crystal size distributions: Formulations and procedures. *Journal of Volcanology and Geothermal Research*, *164*(3), 95–111. https://doi.org/10.1016/j.jvolgeores.2007.04.006

Puppo, M. C., Calvelo, A., & Añón, M. C. (2005). Physicochemical and rheological characterization of wheat flour dough. *Cereal Chemistry*, *82*(2), 173–181. https://doi.org/10.1094/CC-82-0173

Quoc, P. N., Zitha, P. L. J., & Currie, P. K. (2002). Effect of foam films on gas diffusion. *Journal of Colloid and Interface Science*, *248*(2), 467–476. https://doi.org/10.1006/jcis.2001.8155

Rao, M. A. (2007). *Rheology of Fluid and Semisolid Foods: Principles and Applications* (second). New York, USA: Springer.

Romano, A., Cavella, S., Toraldo, G., & Masi, P. (2013). 2D structural imaging study of bubble evolution during leavening. *Food Research International*, *50*(1), 324–329. https://doi.org/10.1016/j.foodres.2012.10.040

Romano, A., Toraldo, G., Cavella, S., & Masi, P. (2007). Description of leavening of bread dough with mathematical modelling. *Journal of Food Engineering*, *83*(2), 142–148.

https://doi.org/10.1016/j.jfoodeng.2007.02.014

Rouillé, J., Bonny, J. M., Della Valle, G., Devaux, M. F., & Renou, J. P. (2005). Effect of flour minor components on bubble growth in bread dough during proofing assessed by magnetic resonance imaging. *Journal of Agricultural and Food Chemistry*, *53*(10), 3986–3994. https://doi.org/10.1021/jf047953r

Sahi, S. S. (1994). Interfacial properties of the aqueous phases of wheat flour doughs. *Journal of Food Science*, *20*, 119–127.

Salovaara, H. (1982). Effect of partial sodium chloride replacement by other salts on wheat dough rheology and breadmaking. *Cereal Chemistry*.

Salt, L. J., Wilde, P. J., Georget, D., Wellner, N., Skeggs, P. K., & Mills, E. N. C. (2006). Composition and surface properties of dough liquor. *Journal of Cereal Science*, *43*(3), 284–292. https://doi.org/10.1016/j.jcs.2005.12.013

Salvador, A., Sanz, T., & Fiszman, S. M. (2006). Dynamic rheological characteristics of wheat flour-water doughs. Effect of adding NaCl, sucrose and yeast. *Food Hydrocolloids*, *20*, 780–786. https://doi.org/10.1016/j.foodhyd.2005.07.009

Sapirstein, H. D., Roller, R., & Bushuk, W. (1994). Instrumental measurement of bread crumb grain by digital image analysis. *Cereal Chemistry*, *71*(4), 383–391.

Scanlon, M. G., & Zghal, M. C. (2001). Bread properties and crumb structure. *Food Research International*, *34*(10), 841–864. https://doi.org/10.1016/S0963-9969(01)00109-0

Scourboutakos, M. J., & L'Abbé, M. R. (2013). Sodium levels in Canadian fast-food and sit-down restaurants. *Canadian Journal of Public Health*, *104*(1).

Seabourn, B. W., Xie, F., & Chung, O. K. (2008). Rapid determination of dough optimum mixing time for early generation wheat breeding lines using FT-HATR infrared spectroscopy. *Crop*

Science, *48*(4), 1575–1578. https://doi.org/10.2135/cropsci2007.12.0669

Shah, P., Campbell, G. M., McKee, S. L., & Rielly, C. D. (1998). Proving of bread dough: Modelling the growth of individual bubbles. *Food and Bioproducts Processing*, *76*, 73–79. https://doi.org/Doi 10.1205/096030898531828

Shehzad, A., Chiron, H., Della Valle, G., Kansou, K., Ndiaye, A., & Réguerre, A. L. (2010). Porosity and stability of bread dough during proofing determined by video image analysis for different compositions and mixing conditions. *Food Research International*, *43*(8), 1999–2005. https://doi.org/10.1016/j.foodres.2010.05.019

Shewry, P. R., & Jones, H. D. (2012). Improving wheat protein quality for breadmaking: the role of biotechnology. In S. P. Cauvain (Ed.), *Breadmaking: Improving Quality* (second, pp. 237–258). Cambridge, UK: Woodhead Publishing Ltd.

Shimiya, Y., & Nakamura, K. (1997). Changes in size of gas cells in dough and bread during breadmaking and calculation of critical size of gas cells that expand. *Journal of Texture Studies*, *28*(3), 273–288. https://doi.org/10.1111/j.1745-4603.1997.tb00117.x

Shimiya, Y., & Yano, T. (1987). Diffusion-controlled shrinkage and growth of an air bubble entrained in water and in wheat flour particles. *Agricultural and Biological Chemistry*, *51*(7), 1935–1940. https://doi.org/10.1271/bbb1961.51.1935

Shimiya, Y., & Yano, T. (1988). Rates of shrinkage and growth of air bubbles entrained in wheat flour dough. *Agricultural and Biological Chemistry*, *52*, 2879–2883.

Shimuzu, K., & Crow, E. L. (1988). History, genesis, and properties. In E. L. Crow & K. Shimuzu (Eds.), *Lognormal Distributions: Theory and Applications* (pp. 1–22). New York, USA: Marcel Dekker, Inc.

Shuey, W. C. (1972). *The Farinograph Handbook*. St. Paul, MN, USA: AACC International Inc.

Singh, N., Inderpreet, K. B., Singh, R. P., & Hardeep, S. G. (2003). Effect of different additives on mixograph and bread making properties of Indian wheat flour. *Journal of Food Engineering*, *56*(1), 89–95. https://doi.org/10.1016/S0260-8774(02)00151-6

Skeggs, P. K., & Kingswood, K. (1981). Mechanical dough development-polit scale studies. *Cereal Chemistry*, *58*(4), 256–260.

Skendi, A., Papageorgiou, M., & Biliaderis, C. G. (2010). Influence of water and barley β-glucan addition on wheat dough viscoelasticity. *Food Research International*, *43*(1), 57–65. https://doi.org/10.1016/j.foodres.2009.08.012

Skerritt, J. H., Luch, H., & Bekes, F. (1999). Depolymerization of the glutenin macropolymer during dough mixing: I. Changes in levels, molecular weight distribution, and overall composition. *Cereal Chemistry*, *76*(3), 395–401. https://doi.org/10.1094/CCHEM.1999.76.3.395

Sliwinski, E. L., Kolster, P., & van Vliet, T. (2004). Large-deformation properties of wheat dough in uni- and biaxial extension. Part I. Flour dough. *Rheologica Acta*, *43*(4), 306–320. https://doi.org/10.1007/s00397-003-0345-4

Smith, J. R., Smith, T. L., & Tschoegl, N. W. (1970). Rheological properties of wheat doughs III. Dynamic shear modulus and its dependence on amplitude, frequency and dough composition. *Rheologica Acta*, *9*, 239–252. https://doi.org/10.1360/zd-2013-43-6-1064

Sofou, S., Muliawan, E. B., Hatzikiriakos, S. G., & Mitsoulis, E. (2008). Rheological characterization and constitutive modeling of bread dough. *Rheologica Acta*, *47*(4), 369–381. https://doi.org/10.1007/s00397-007-0248-x

Song, Y., & Zheng, Q. (2007). Dynamic rheological properties of wheat flour dough and proteins. *Trends in Food Science and Technology*, *18*(3), 132–138.

https://doi.org/10.1016/j.tifs.2006.11.003

Spies, R. (1990). Application of rheology in the bread industry. In H. Faridi & J. M. Faubion (Eds.), *Dough Rheology and Baked Product Texture* (pp. 343–361). New York, USA: Van Nostrand Reinhold.

Sroan, B. S., Bean, S. R., & MacRitchie, F. (2009). Mechanism of gas cell stabilization in bread making. I. The primary gluten-starch matrix. *Journal of Cereal Science*, *49*(1), 32–40. https://doi.org/10.1016/j.jcs.2008.07.003

Steffe, J. F. (1996). *Rheological Methods in Agricultural Engineering*. East Lansing, USA: Freeman Press. https://doi.org/10.1016/0260-8774(94)90090-6

Stevenson, P. (2010). Inter-bubble gas diffusion in liquid foam. *Current Opinion in Colloid and Interface Science*, *15*(5), 374–381. https://doi.org/10.1016/j.cocis.2010.05.010

Stojceska, V., Butler, F., Gallagher, E., & Keehan, D. (2007). A comparison of the ability of several small and large deformation rheological measurements of wheat dough to predict baking behaviour. *Journal of Food Engineering*, *83*(4), 475–482. https://doi.org/10.1016/j.jfoodeng.2007.02.043

Suchy, J., Lukow, O. M., & Ingelin, M. E. (2000). Dough microextensibility method using a 2-g mixograph and a texture analyzer. *Cereal Chemistry*, *77*(1), 39–43. https://doi.org/10.1094/CCHEM.2000.77.1.39

Takano, H., Ishida, N., Koizumi, M., & Kano, H. (2002). Imaging of the fermentation process of bread dough and the grain structure of baked breads. *Journal of Food Science*, *67*(1), 244–250.

Tanaka, K., Furukawa, K., & Matsumoto, H. (1967). The effect of acid and salt on the farinogram and extensigram of dough. *Cereal Chemistry*, *44*(6), 675–680.

Tanner, R. I., Qi, F., & Dai, S.-C. (2008). Bread dough rheology and recoil. I. rheology. *Journal of Non-Newtonian Fluid Mechanics*, *148*(1-3), 33–40. https://doi.org/10.1016/j.jnnfm.2007.04.006

Thorvaldsson, K., Stading, M., Nilsson, K., Kidman, S., & Langton, M. (1999). Rheology and structure of heat-treated pasta dough: Influence of water content and heating rate. *LWT - Food Science and Technology*, *32*, 154–161.

Tietze, S., Jekle, M., & Becker, T. (2016). Possibilities to derive empirical dough characteristics from fundamental rheology. *Trends in Food Science and Technology*, *57*, 1–10. https://doi.org/10.1016/j.tifs.2016.08.016

Tipples, K. H., Preston, K. R., & Kilborn, R. H. (1982). Implications of the term "strength" as related to wheat and flour quality. *Bakers Digest*, *56*(6), 16–20.

Tkachuk, R., & Hlynka, I. (1968). Some properties of dough and gluten in D2O. *Cereal Chemistry*, *45*(1), 80–87.

Trater, A. M., Alavi, S., & Rizvi, S. S. H. (2005). Use of non-invasive X-ray microtomography for characterizing microstructure of extruded biopolymer foams. *Food Research International*, *38*(6), 709–719. https://doi.org/10.1016/j.foodres.2005.01.006

Trinh, L., Lowe, T., Campbell, G. M., Withers, P. J., & Martin, P. J. (2013). Bread dough aeration dynamics during pressure step-change mixing: Studies by X-ray tomography, dough density and population balance modelling. *Chemical Engineering Science*, *101*, 470–477. https://doi.org/10.1016/j.ces.2013.06.053

Tronsmo, K. M., Magnus, E. M., Baardseth, P., Schofield, J. D., Aamodt, A., & Faergestad, E. M. (2003). Comparison of small and large deformation rheological properties of wheat dough and gluten. *Cereal Chemistry*, *80*(5), 1–4. https://doi.org/10.1094/CCHEM.2003.80.5.587

Tronsmo, K. M., Magnus, E. M., Færgestad, E. M., & Schofield, J. D. (2003). Relationships between gluten rheological properties and hearth loaf characteristics. *Cereal Chemistry*, *80*(5), 575–586. https://doi.org/10.1094/CCHEM.2003.80.5.575

Turbin-Orger, A., Babin, P., Boller, E., Chaunier, L., Chiron, H., Della Valle, G., … Salvo, L. (2015). Growth and setting of gas bubbles in a viscoelastic matrix imaged by X-ray microtomography: the evolution of cellular structures in fermenting wheat flour dough. *Soft Matter*, *11*(17), 3373–3384. https://doi.org/10.1039/C5SM00100E

Turbin-Orger, A., Boller, E., Chaunier, L., Chiron, H., Della Valle, G., & Réguerre, A. L. (2012). Kinetics of bubble growth in wheat flour dough during proofing studied by computed X-ray micro-tomography. *Journal of Cereal Science*, *56*(3), 676–683. https://doi.org/10.1016/j.jcs.2012.08.008

Unbehend, L., Lindhauer, M. G., & Meuser, F. (2004). Physical and microscopic studies of flour-water systems. *European Food Research and Technology*, *219*(5), 514–521. https://doi.org/10.1007/s00217-004-0975-5

Upadhyay, R., Ghosal, D., & Mehra, A. (2012). Characterization of bread dough: Rheological properties and microstructure. *Journal of Food Engineering*, *109*(1), 104–113. https://doi.org/10.1016/j.jfoodeng.2011.09.028

Uthayakumaran, S., Gras, P. W., Stoddard, F. L., & Bekes, F. . (1999). Effect of varying protein content and glutenin-to-glutenin roatio on the funtional properties of wheat dough. *Cereal Chemistry*, *76*(3), 389–394. https://doi.org/10.1094/CCHEM.1999.76.3.389

Van Bockstaele, F., De Leyn, I., Eeckhout, M., & Dewettinck, K. (2008a). Rheological properties of wheat flour dough and their relationship with bread volume. I. Creep-Recovery measurements. *Cereal Chemistry*, *85*(6), 753–761. https://doi.org/10.1094/CCHEM-85-6-

0762

Van Bockstaele, F., De Leyn, I., Eeckhout, M., & Dewettinck, K. (2008b). Rheological properties of wheat flour dough and their relationship with bread volume. II. Dynamic oscillation measurements. *Cereal Chemistry*, *85*(6), 762–768. https://doi.org/10.1094/CCHEM-85-6-0762

Van Bockstaele, F., De Leyn, I., Eeckhout, M., & Dewettinck, K. (2011). Non-linear creep-recovery measurements as a tool for evaluating the viscoelastic properties of wheat flour dough. *Journal of Food Engineering*, *107*(1), 50–59. https://doi.org/10.1016/j.jfoodeng.2011.06.001

van Duynhoven, J. P. M., van Kempen, G. M. P., van Sluis, R., Rieger, B., Weegels, P., van Vliet, L. J., & Nicolay, K. (2003). Quantitative assessment of gas cell development during the proofing of dough by magnetic resonance imaging and image analysis. *Cereal Chemistry*, *80*(4), 390–395. https://doi.org/10.1094/CCHEM.2003.80.4.390

van Vliet, T. (1999). Physical factors determining gas cell stability in a dough during bread making. In G. M. Campbell, C. Webb, S. S. Pandiella, & K. Niranjan (Eds.), *Bubbles in Food* (pp. 121–127). St. Paul, MN, USA: Eagan Press.

van Vliet, T. (2008). Strain hardening as an indicator of bread-making performance: A review with discussion. *Journal of Cereal Science*, *48*(1), 1–9. https://doi.org/10.1016/j.jcs.2007.08.010

van Vliet, T., Janssen, A. M., Bloksma, A. H., & Walstra, P. (1992). Strain hardening of dough as a requirement for gas retention. *Journal of Texture Studies*, *23*, 439–460.

van Vliet, T., & Kokelaar, J. J. (1994). Biaxial strain hardening in relation to foam formation and stability towards disproportionation. In C. Gallegos, A. Guerrero, J. Munoz, & M. Berjano (Eds.), *Progress and Trends in Rheology IV, Proceedings of the 4th European Rheology*

Congress (pp. 201–203). Darmstadt, Germany: Steinkopff.

Venerus, D. C. (2001). Diffusion-induced bubble growth in viscous liquids of finite and infinite extent. *Polymer Engineering and Science*, *41*(8), 1390–1398.

Venerus, D. C. (2015). Diffusion-induced bubble growth and collapse in yield stress fluids. *Journal of Non-Newtonian Fluid Mechanics*, *215*, 53–59. https://doi.org/10.1016/j.jnnfm.2014.11.001

Venerus, D. C., & Yala, N. (1997). Transport analysis of diffusion-induced bubble growth and collapse in viscous liquids. *AIChE Journal*, *43*(11), 2948–2959. https://doi.org/10.1002/aic.690431108

Venerus, D. C., Yala, N., & Bernstein, B. (1998). Analysis of diffusion-induced bubble growth in viscoelastic liquids. *Journal of Non-Newtonian Fluid Mechanics*, *75*(1), 55–75. https://doi.org/10.1016/S0377-0257(97)00076-1

Vu, R. H., Rangayyan, R. M., Deglint, H. J., & Boag, G. S. (2007). Segmentation and analysis of neuroblastoma. *Journal of the Franklin Institute*, *344*, 257–284. https://doi.org/10.1016/j.jfranklin.2006.11.002

Walstra, P. (2003). *Physical Chemistry of Foods*. New York, USA: Marcel Dekker.

Wang, F. C., & Sun, X. S. (2002). Creep-recovery of wheat flour doughs and relationship to other physical dough tests and breadmaking performance. *Cereal Chemistry*, *79*(4), 567–571. https://doi.org/10.1094/CCHEM.2002.79.4.567

Wang, S., Austin, P., & Bell, S. (2011). It's a maze: the pore structure of bread crumbs. *Journal of Cereal Science*, *54*, 203–210. https://doi.org/10.1016/j.jcs.2011.05.004

Wehrle, K., Grau, H., & Arendt, E. K. (1997). Effects of lactic acid, acetic acid, and table salt on fundamental rheological properties of wheat dough. *Cereal Chemistry*, *74*(6), 739–744.

https://doi.org/10.1094/CCHEM.1997.74.6.739

Whitworth, M. B. (2008). X-ray microtomography of structure formation in bread and cakes during baking. In G. M. Campbell, M. G. Scanlon, & D. L. Pyle (Eds.), *Bubbles in Food 2: Novelty, Health and Luxury* (pp. 273–286). St. Paul, MN, USA: Eagan Press.

Whitworth, M. B., & Alava, J. M. (1999). Imaging and measurement of bubbles in bread doughs. In G. M. Campbell, C. Webb, S. S. Pandiella, & K. Niranjan (Eds.), *Bubbles in Food* (pp. 221–231). St. Paul, MN, USA: Eagan Press.

Williams, A. (1975). *Breadmaking: The Modern Revolution*. London, UK: Hutchinson Benham.

Wilson, A. J., Wooding, A. R., & Morgenstern, M. P. (1997). Comparison of work input requirement on laboratory-scale and industrial-scale mechanical dough development mixers. *Cereal Chemistry, 74*(6), 715–721. https://doi.org/10.1094/CCHEM.1997.74.6.715

World Health Organization. (2007). Cost-effectiveness of interventions to reduce dietary salt intake. In *Reducing Salt Intake in Populations: Report of a WHO Forum and Technical Meeting, 5-7 October 2006* (pp. 1–32). Paris, France: WHO Press.

Wu, J., Beta, T., & Corke, H. (2006). Effects of salt and alkaline reagents on dynamic rheological properties of raw oriental wheat noodles. *Cereal Chemistry*, *83*(2), 211–217. https://doi.org/10.1094/CC-83-0211

Yannas, I. (2004). Linear viscoelastic constitutive equations. In *Linear Viscoelastic Behavior* (pp. 73–99). New York, USA: Dover Publications.

Yovchev, A., Stone, A. K., Hucl, P. J., Scanlon, M. G., & Nickerson, M. T. (2017a). Effects of salt , polyethylene glycol , and water content on dough rheology for two red spring wheat varieties. *Cereal Chemistry, 94*(3), 513–518.

Yovchev, A., Briggs, C. E., Stone, A. K., Hucl, P. J., Nickerson, M. T., & Scanlon, M. G. (2017b).

Effect of salt reduction on dough handling and the breadmaking quality of Canadian western red spring wheat varieties. *Cereal Chemistry*, *94*(4), 752–759. https://doi.org/10.1094/CCHEM-02-17-0026-R

Yovchev, A., Briggs, C. E., Stone, A. K., Scanlon, M. G., Tyler, R. T., Hucl, P. J., & Nickerson, M. T. (2017c). Interrelationships of flour, dough, and bread properties under reduced salt level conditions. *Cereal Chemistry*, *94*(4), 760–769. https://doi.org/10.1094/CCHEM-12-16-0285-R

Yovchev, A., Scanlon, M. G., & Nickerson, M. T. (2015). The impact of salt reduction in baked goods. *Canadian Food Insights*, 31–33.

Zghal, M. C. (2001). *The relationship between bread physical texture and its structure determinced by digital image analysis*. University of Manitoba (MSc Thesis).

Zghal, M. C., Scanlon, M. G., & Sapirstein, H. D. (1999). Prediction of bread crumb density by digital image analysis. *Cereal Chemistry*, *76*(5), 734–742. https://doi.org/10.1094/CCHEM.1999.76.5.734

Zghal, M. C., Scanlon, M. G., & Sapirstein, H. D. (2001). Effects of flour strength, baking absorption, and processing conditions on the structure and mechanical properties of bread crumb. *Cereal Chemistry*, *78*(1), 1–7. https://doi.org/10.1094/CCHEM.2001.78.1.1

Zghal, M. C., Scanlon, M. G., & Sapirstein, H. D. (2002). Cellular structure of bread crumb and its influence on mechanical properties. *Journal of Cereal Science*, *36*(2), 167–176. https://doi.org/10.1006/jcrs.2001.0445

Zheng, H., Morgenstern, M. P., Campanella, O. H., & Larsen, N. G. (2000). Rheological properties of dough during mechanical dough development. *Journal of Cereal Science*, *32*(3), 293–306. https://doi.org/10.1006/jcrs.2000.0339

Zounis, S., & Quail, K. J. (1997). Predicting test bakery requirements from laboratory mixing tests. *Journal of Cereal Science, 25*(2), 185–196. https://doi.org/10.1006/jcrs.1996.0075

8. Appendices

Appendix 1: Calibration of NaCl Content in Bread Dough according to Health Canada's Target of 330 mg Sodium/100g Bread

(a) Conversion of 330 mg sodium/100 g bread into % NaCl on a basis of flour weight

Molecular weight of Na = 23 g mol^{-1}

Molecular weight of NaCl = 58.44 g mol^{-1}

As Health Canada's target = 330 mg sodium/100 g bread, then:

NaCl (g) in 100g bread = 58.44 g mol^{-1} × 0.33 g / 23 g mol^{-1} = 0.838 g

If bread moisture = 38%, then:

Moisture (g) in 100 g bread = 38 g

As weight of bread (g) = dry flour solids (g) + NaCl (g) + moisture (g), then:

100 g = dry flour solids (g) + 0.838 g + 38 g

dry flour solids (g) = 100 g – 0.838 g – 38 g = 61.16 g

If moisture content of flour = 14%, then:

Moisture (g) in 100 g flour = 14 g

dry flour solids (g) / weight of flour (g) = (100 g – 14 g) / 100 g

61.16 g / weight of flour (g) = 0.86

weight of flour (g) = 71.12 g

NaCl (% flour weight basis) = 0.838 g / 71.12 g × 100% = 1.18% (~1.2%)

(b) Conversion of 1.18% NaCl into molarity of NaCl in the dough made by a 10 g mixograph

As our doughs were prepared using a 10 g mixograph, the weight of flour, water and NaCl for dough preparations were calibrated on a basis of 10 g flour weight.

As the moisture content of *Pembina* flour was determined as 11.9%, and weight of *Pembina* flour used for dough preparation was calibrated on a basis of 14% moisture content of flour, then:

weight (g) of flour used = (100 – 14) / (100 – 11.9) × 10 g = 9.76 g

moisture (mL) in flour = 9.76 g × 11.9% / 1 g mL^{-1} = 1.16 mL

According to AACC method No. 54-21.01 on a basis of 10 g flour (14% moisture basis),

farinograph absorption (FAB)% = [flour used (g) + added water (mL) – 10] / 0.1

If FAB of *Pembina* flour is 61.6%, then:

61.6 = (9.76 + added water (mL) – 10) / 0.1

added water (mL) = 61.6 × 0.1 + 10 – 9.76 = 6.4 mL

Water (L) in dough = [moisture in flour (mL) + added water (mL)] / 1000 mL L^{-1}

= (1.16 mL + 6.4 mL) / 1000 mL L^{-1} = 7.56 × 10^{-3} L

According to Health Canada's target of 1.18% NaCl on a basis of flour weight, then:

moles of NaCl in dough = 9.76 g × 1.18% / 58.44 g mol^{-1} = 0.002 mol

Molarity of NaCl in dough = 0.002 mol / 7.56 × 10^{-3} L = 0.2607 mol L^{-1}

1.18% NaCl is calibrated into molarity of NaCl in the doughs, shown in Table 1.

Table 1 Molarity of NaCl in doughs made from various wheat cultivars

Wheat cultivar	Moisture (%) of flour	Weight (g) of flour used	FAB (%)	Water (L) in dough	NaCl (mol) in dough	NaCl (mol L^{-1}) in dough
Pembina	11.9	9.76	61.6	7.56 × 10^{-3}	0.002	0.2607
Roblin	12	9.77	65	7.9 × 10^{-3}	0.002	0.2532
McKenzie	11.9	9.76	64.1	7.81 × 10^{-3}	0.002	0.2523
Harvest	12.2	9.79	65.5	7.96 × 10^{-3}	0.002	0.2513

According to the value of NaCl (mol L^{-1}) in dough for each cultivar (Table 1), then:

NaCl (mol L^{-1}) in the water of doughs averaged for the four wheat cultivars = 0.2543 mol L^{-1} (~ 0.25 mol L^{-1})

(c) Conversion of 0.25 mol L^{-1} NaCl into % NaCl (flour weight basis) in the doughs

If water absorption of *Pembina* dough is held at FAB+2% (= 63.6%), then:

water (L) in dough = [1.16 mL + (63.6 × 0.1 + 10 – 9.76) mL] / 1000 mL L^{-1} = 7.76×10^{-3} L

If molarity of NaCl is held at 0.25 mol L^{-1}, then:

moles of NaCl in dough = 0.25 mol L^{-1} × 7.76×10^{-3} L = 1.94×10^{-3} mol

% NaCl on a basis of flour weight = 100% × (1.94×10^{-3} mol × 58.44 g mol^{-1}) / 9.76 g = 1.16%

As 0.25 mol L^{-1} NaCl is held constant for doughs made from various cultivars and water absorptions, % NaCl (flour weight basis) in doughs is shown in Table 2.

Table 2 Calibration of 0.25 mol L^{-1} NaCl into % NaCl (flour weight basis) in the doughs

Water absorption (%) of dough	% NaCl (flour weight basis)			
	Pembina	Roblin	McKenzie	Harvest
FAB-4%	1.07	1.12	1.11	1.13
FAB-2%	1.10	1.15	1.14	1.16
FAB	1.13	1.18	1.17	1.19
FAB+2%	1.16	1.21	1.20	1.22
FAB+4%	1.19	1.24	1.23	1.25

Appendix 2: Custom-Written MATLAB (Version 7.12.0.635) Code

```
function mriGUI_3a
ScreenSize = get(0,'ScreenSize');
set(gcf, 'doublebuffer', 'on', ...
        'clipping', 'off', ...
        'color', [0.5,0.1,0.7], ...
        'name', 'RKS Digitize', ...
        'menubar','none', ...
        'resize','on', ...
        'numbertitle','off', ...
        'Units','Pixels',...
        'Position' , ...
        [ScreenSize(1) ScreenSize(2) ScreenSize(3) ScreenSize(4)], ...
        'CloseRequestFcn', @mri_closereq);

   tif_files = dir('*.tif');
   numberOfTIFFs = length(tif_files);
   disp(['Number of Tiff Files : ' num2str(numberOfTIFFs)]);
   for k = 1 : length(tif_files)
      lb_string(k,:) = tif_files(k).name;
   end
  WIDTH = 220;
  % ListBox of files
  uicontrol('style','listbox', ...
     'fontw','bold', ...
     'Tag','liste', ...
     'ForegroundColor','Black', ...
     'Background','White', ...
     'Min', 1, ...
     'Max', numberOfTIFFs, ...
     'String',lb_string, ...
     'FontSize', 8, ...
     'value', 1, ...
     'Units','pixels', ...
     'Position', [25 760 WIDTH 270], ...
     'Callback', @process);

  % Set Position Button
  uicontrol('style','pushbutton',...
     'String', 'Set Position',...
     'Tag','setposition',...
     'fontw','bold', ...
     'ForegroundColor','Black', ...
     'Background',[0.9 0.9 0], ...
     'FontSize', 14, ...
```

```
        'Units','pixels', ...
        'Position', [25 700 WIDTH 40],...
        'Callback', @setPosition);

    % Slider Adjustment
    % Gamma Slider
    uicontrol('style','slider',...
        'Tag','hGamma',...
        'String', 'SetGamma', ...
        'Min',10, ...
        'Max',16, ...
        'SliderStep', [1/100 , 20/100 ], ...
        'Value',10,...
        'ForegroundColor','Black', ...
        'Background',[0.4,0.5,0.6], ...
        'Units','pixels', ...
        'Position', [25 645 WIDTH 20],...
        'Callback', @process);
    % Gamma text
    uicontrol('style','text',...
        'Tag','hGammaText',...
        'String', 'Gamma : 1', ...
        'FontSize',10, ...
        'FontWeight', 'Bold', ...
        'HorizontalAlignment','Left',...
        'ForegroundColor','Yellow', ...
        'Background',[0.5,0.1,0.7], ...
        'Units','pixels', ...
        'Position', [25 665 WIDTH 20]);
%
    % Contrast Slider
    uicontrol('style','slider',...
        'Tag','hAdjust',...
        'String', 'SetContrast', ...
        'Min',1, ...
        'Max',100, ...
        'SliderStep', [1/100 , 10/100 ], ...
        'Value',1,...
        'ForegroundColor','Black', ...
        'Background',[0.4,0.0,0.6], ...
        'Units','pixels', ...
        'Position', [25 600 WIDTH 20],...
        'Callback', @process);
    % Contrast text
    uicontrol('style','text',...
        'Tag','hContrastText',...
```

```
    'String', 'Contrast : 0.1000', ...
    'FontSize',10, ...
    'FontWeight', 'Bold', ...
    'HorizontalAlignment','Left',...
    'ForegroundColor','Yellow', ...
    'Background',[0.5,0.1,0.7], ...
    'Units','pixels', ...
    'Position', [25 620 WIDTH 20]);

% Slider Binarization
uicontrol('style','slider',...
    'Tag','hAdjustBinary',...
    'String', 'SetContrast', ...
    'Min',1, ...
    'Max',100, ...
    'Value',1,...
    'ForegroundColor','Black', ...
    'Background',[0.4,0.4,0.4], ...
    'Units','pixels', ...
    'Position', [25 555 WIDTH 20],...
    'Callback', @process);

% Binarization text
uicontrol('style','text',...
    'Tag','hBinaryText',...
    'String', 'Binarization : 0.0100', ...
    'FontSize',10, ...
    'FontWeight', 'Bold', ...
    'HorizontalAlignment','Left',...
    'ForegroundColor','Yellow', ...
    'Background',[0.5,0.1,0.7], ...
    'Units','pixels', ...
    'Position', [25 575 WIDTH 20]);

 % Zoom Image
uicontrol('style','checkbox', ...
    'Tag','hZoomCheck',...
    'String', 'Zoom Image', ...
    'Min',0, ...
    'Max',1, ...
    'Value',0,...
    'ForegroundColor','Black', ...
    'Background',[0.5,0.1,0.7], ...
    'FontSize', 12, ...
    'Units','pixels', ...
    'Position', [25 525 WIDTH 20],...
```

```
    'Callback', @process);

% Raw Image
uicontrol('style','checkbox', ...
    'Tag','hRawCheck',...
    'String', 'Raw Image', ...
    'Min',0, ...
    'Max',1, ...
    'Value',0,...
    'ForegroundColor','Black', ...
    'Background',[0.5,0.1,0.7], ...
    'FontSize', 12, ...
    'Units','pixels', ...
    'Position', [25 500 WIDTH 20],...
    'Callback', @process);

% Slider Filter
uicontrol('style','slider',...
    'Tag','hImageFilter',...
    'String', 'SetContrast', ...
    'Min',1, ...
    'Max',30, ...
    'Value',1,...
    'ForegroundColor','Black', ...
    'Background',[0.9,0.2,0.2], ...
    'Units','pixels', ...
    'Position', [25 475 WIDTH 20],...
    'Callback', @process);

% Filter Text
uicontrol('style','text',...
    'Tag','hFilterText',...
    'String', 'Filter Size : ', ...
    'FontSize',14, ...
    'FontWeight', 'Bold', ...
    'HorizontalAlignment','Left',...
    'ForegroundColor',[0.9,0.2,0.2], ...
    'Background',[0.5,0.1,0.7], ...
    'Units','pixels', ...
    'Position', [25 425 WIDTH 40]);

uicontrol('style','text',...
    'Tag','hImageText',...
    'String', 'Selected Image %', ...
    'FontSize',12, ...
    'FontWeight', 'Bold', ...
```

```
    'HorizontalAlignment','Left',...
    'ForegroundColor',[0.9,0.5,0.5], ...
    'Background',[0.5,0.1,0.7], ...
    'Units','pixels', ...
    'Position', [25 400 WIDTH 40]);

uicontrol('style','text',...
    'Tag','hImageSelection',...
    'String', '', ...
    'FontSize',12, ...
    'FontWeight', 'Bold', ...
    'HorizontalAlignment','Left',...
    'ForegroundColor','Yellow', ...
    'Background',[0.5,0.1,0.7], ...
    'Units','pixels', ...
    'Position', [840 35 360 40]);

% Create the button group.
hRadio = uibuttongroup('visible','on', ...
    'Title', ' 3D Connectivity ', ...
    'Tag','rbtnGroup', ...
    'FontSize',10, ...
    'FontWeight', 'Bold', ...
    'Background',[0.5,0.1,0.7], ...
    'Units', 'pixels', ...
    'Position',[25 300 WIDTH 90]);

uicontrol('Style', 'radiobutton', ...
    'parent', hRadio, ...
    'HandleVisibility','off', ...
    'Tag', '3d06', ...
    'FontSize',12, ...
    'FontWeight', 'Bold', ...
    'Units',    'pixels', ...
    'Background',[0.5,0.1,0.7], ...
    'Position', [10, 10, 80, 22], ...
    'String',   ' 6', ...
    'Value',    1);

uicontrol('Style', 'radiobutton', ...
    'parent', hRadio, ...
    'HandleVisibility','off', ...
    'Tag', '3d18', ...
    'FontSize',12, ...
    'FontWeight', 'Bold', ...
    'Units',    'pixels', ...
```

```
        'Background',[0.5,0.1,0.7], ...
        'Position', [10, 30, 100, 22], ...
        'String',   '18', ...
        'Value',    0);

    uicontrol('Style', 'radiobutton', ...
        'parent', hRadio, ...
        'HandleVisibility','off', ...
        'Tag', '3d26', ...
        'FontSize',12, ...
        'FontWeight', 'Bold', ...
        'Units',    'pixels', ...
        'Background',[0.5,0.1,0.7], ...
        'Position', [10, 50, 80, 22], ...
        'String',   '26', ...
        'Value',    0);

    % Buttons
    uicontrol('style','pushbutton',...
        'String', 'Process All',...
        'fontw','bold', ...
        'ForegroundColor','Black', ...
        'Background',[0.0 0.6 0.2], ...
        'FontSize', 14, ...
        'Units','pixels', ...
        'Position', [25 190 WIDTH 100],...
        'Callback', @processAll);

    uicontrol('style','pushbutton',...
        'String', 'Create 3D',...
        'Tag','birak',...
        'fontw','bold', ...
        'ForegroundColor','Black', ...
        'Background',[0.0 0.6 0.2], ...
        'FontSize', 14, ...
        'Units','pixels', ...
        'Position', [25 70 WIDTH 100],...
        'Callback', @create3D);
end
%%
function setPosition(hObj, event) %#ok<INUSD>
    valCheckBox = get(findobj('Tag','hZoomCheck'), 'Value');

    if ~valCheckBox
        set(findobj('tag','setposition'), 'Background',[0.0 0.8 0.1]);
        rect = guidata(findobj('tag','setposition'));
```

```
if isempty(rect)
   h = imrect(gca, [11 11 624 624]);
else
   h = imrect(gca, ceil(rect));
end
setColor(h,'g')

% Calculate the Percentage

lbVal = get(findobj('Tag','liste'),'Value');
lbString = get(findobj('Tag','liste'),'String');
I = imread(lbString(lbVal,:)); % get the image
[m, n, ~] = size(I);
imageSize = m * n;

addNewPositionCallback(h, @(p) title( ...
                              sprintf('%s%%', ...
                                    mat2str(fix(p), 4), ...
                                    num2str(p(3)*p(4) / imageSize, '%1.3f')), ...
                                    'Color', 'y', ...
                                    'FontSize', 14) ...
                             );
% rect control
fcn = makeConstrainToRectFcn('imrect', get(gca, 'XLim'), get(gca, 'YLim'));
setPositionConstraintFcn(h, fcn);
position = wait(h);
set(findobj('tag','setposition'), 'Background', [0.9 0.9 0.0]);
guidata(findobj('tag','setposition'), position);
rectangle('Position',[position(1) position(2) position(3) position(4)], ...
                'LineWidth',3, 'EdgeColor','y');

set(findobj('Tag','hImageText'),'String', ['Selected Image %', ...
   num2str((position(3)*position(4) / imageSize)*100, '%1.1f')]);
set(findobj('Tag','hImageSelection'),'String',  ...
   sprintf('Selected Area (x,y:%4.0f,%4.0f) w:%4.0f h:%4.0f',...
   [position(1) position(2) position(3) position(4)]))

process();

fileID = fopen([datestr(now,'report_ddmmyy') '.htm'],'w');
fprintf(fileID,'<!DOCTYPE html>\n<html>\n<body>\n<h1>---------- Bubble
Distribution ----------</h1>');
fprintf(fileID,['<h2>Selected Area x, y:', num2str(position(1),'%4.0f'), ', '
num2str(position(2),'%4.0f'), ' Width : ', num2str(position(3),'%4.0f'), ' px Height : ',
num2str(position(4),'%4.0f'), ' px']);
fclose(fileID);
```

```
    end
end
%%
function setPicture(hObj, event)  %#ok<INUSD>
    val = get(hObj, 'Value');
    lbstring = get(hObj, 'String');
    I = imread(lbstring(val,:));

    % disp(size(I))
    valSlide = get(findobj('Tag', 'hAdjust'), 'Value')/100;

    % Calculate the center of the image

    rect = guidata(findobj('tag','setposition'));
    rect= ceil(rect);
    if isempty(rect)
        rect = [11 11 624 624];
    end

    Is = I(rect(2):rect(2)+rect(4), rect(1):rect(1)+rect(3));
    K = imadjust(Is,[0.001 valSlide],[0 1]);
    %I(rect(2):rect(2)+rect(4), rect(1):rect(1)+rect(3)) = K;

    valCheckBox = get(findobj('Tag','hZoomCheck'), 'Value');

    if valCheckBox
        imshow(K);
        drawnow
    else
        imshow(I);
        rectangle('Position',[rect(1) rect(2) rect(3) rect(4)], ...
                          'LineWidth',3, 'EdgeColor','y');
        drawnow
    end
end
%%
function MBW = calculateBoundry(BW)

        iMBW = zeros(size(BW));
        valSlideFilter = fix(get(findobj('Tag','hImageFilter'), 'Value'));
        set(findobj('Tag','hFilterText'),'String', ...
                    ['Filter Size : ' num2str(valSlideFilter)]);

        BW = bwareaopen(BW, valSlideFilter);
        [B, ~] = bwboundaries(BW, 8,'noholes');
        for k = 1:length(B)
```

```
            boundary = B{k};
              for j = 1: length(boundary)
                 iMBW(boundary(j,1), boundary(j,2)) = 1;
              end
        end
        MBW = iMBW;
end
%%
function process(hObj, event) %#ok<INUSD>
    lbVal = get(findobj('Tag','liste'),'Value');
    lbString = get(findobj('Tag','liste'),'String');

    [~, name, ~] = fileparts(lbString(lbVal,:));

    I = imread(lbString(lbVal,:));
    disp([name ' is on view'])
    rect = guidata(findobj('tag','setposition'));
    rect= ceil(rect);
    if isempty(rect)
        rect = [11 11 624 624];
    end
    Is = I(rect(2):rect(2)+rect(4), rect(1):rect(1)+rect(3));

    valSlideGamma = get(findobj('Tag','hGamma'), 'Value')/10;
    valSlideAdjust = get(findobj('Tag','hAdjust'), 'Value')/100;
    valSlideBinary = get(findobj('Tag','hAdjustBinary'), 'Value')/100;

    set(findobj('Tag','hGammaText'),...
        'String', sprintf('Gamma : %1.2f',valSlideGamma));
    set(findobj('Tag','hContrastText'),...
        'String', sprintf('Contrast : %.4f',valSlideAdjust));
    set(findobj('Tag','hBinaryText'),...
        'String', sprintf('Binarization : %.4f',valSlideBinary));

    K = imadjust(Is, [0.0001 valSlideAdjust], [0 1], valSlideGamma);
    BW = im2bw(K, valSlideBinary);
    cBW = uint16(calculateBoundry(~BW))*65536;

    %I(rect(2):rect(2)+rect(4), rect(1):rect(1)+rect(3)) = cBW;

    valCheckBox = get(findobj('Tag','hZoomCheck'), 'Value');
    valRawImageBox = get(findobj('Tag','hRawCheck'), 'Value');

    if valCheckBox
        if ~valRawImageBox
            %imshow(K);
```

```
            imshow(cBW+K);
            drawnow
        else
            %imshow(Is);
            imshow(cBW+Is);
            drawnow
        end
    else
        imshow(I);
        rectangle('Position',[rect(1) rect(2) rect(3) rect(4)], ...
                          'LineWidth',3, 'EdgeColor','y');
        drawnow
    end
    imwrite(logical(cBW),[name '.bmp'],'bmp');
end
%%
function processAll(hObj, event) %#ok<INUSD>
% This function process all tiff image files listed in the listbox
% it uses the selected contrast, binarization and filtering values
% from the GUI
    delete('*.bmp')
    delete('*.txt')
    disp('---  Process All Selected --- ');

    for i = 1 : get(findobj('Tag', 'liste'), 'MAX')
%    set the first picture as a value
        set(findobj('Tag', 'liste'), 'Value', i)
        setPicture(findobj('Tag', 'liste'));

        process(); % process the file in the sequence

    end
    fillCirclesBMP(); % first fill circles and do calculation
    processTxt();

end
%%
function fillCirclesBMP()
% This function fill the cicrles and then calculates
% centroid of the circles, perimeter, area and diameter
% in order to write a TXT file

    bmp_files = dir('*.bmp'); % get the list of BMP files
    t = zeros(1, length(bmp_files));
    fig = false; % be carefull default is false
```

```
    for n = 1 : length(bmp_files)
        % tic;
        [~, name, ~] = fileparts(bmp_files(n).name);
        % disp(bmp_files(n).name);
        % read the image
        BWo = imread(bmp_files(n).name);
        BW = imfill(BWo,4,'holes');
        % Objects touching image borders removed but 3D is better
        % BW = imclearborder(BW, 8);
        %imwrite(BW, bmp_files(n).name, 'bmp');

        fid = fopen([name '.txt'],'w');
        if fig, figure(1), imshow(BW), hold on, end
        %[B, L, N, A] = bwboundaries(BWo);
        [B, L] = bwboundaries(BW,8,'noholes');
        stats = regionprops(L, 'Area', 'Perimeter','Centroid','EquivDiameter');
        for k = 1:length(B)

            boundary = B{k};
            centroid = stats(k).Centroid;
            perimeter= stats(k).Perimeter;
            area = stats(k).Area;
            dia = stats(k).EquivDiameter;
            if fig
               plot(boundary(:,2), ...
                  boundary(:,1),'r','LineWidth',2);
               plot(centroid(1), centroid(2),'b+','LineWidth',2);
            end
            fprintf(fid,'%d,%3.3f,%3.3f,%3.3f,%3.3f,%3.3f\n', k, centroid(1), centroid(2), ...
                    perimeter, area, dia);
        end
        fclose(fid);
    end
end
%%
function processTxt()

    txt_files = dir('*.txt');
    maxArea = zeros(1,length(txt_files));
    numberofBubbles = zeros(1,length(txt_files));
    totalArea = zeros(1,length(txt_files));
    % read the txt files
    for n = 1 : length(txt_files)
        % [~, name, ext] = fileparts(txt_files(n).name);

        D = load(txt_files(n).name);
```

```
    disp([txt_files(n).name ' is being processed.']);
    maxArea(n) = max(D(:,5));
    totalArea(n) = sum(D(:,5));
    numberofBubbles(n) = length(D);
end
% check image size consistency
bmp_files = dir('*.bmp');
for n = 1 : length(bmp_files)
    info = imfinfo(bmp_files(n).name);
    imageWidth(n) = info.Width;
    imageHeight(n) = info.Height;
end
if (length(unique(imageWidth)) > 1 ||  length(unique(imageHeight)) > 1)
    error('Image Sizes are not consistent. Calculation Stopped.')
else
    totalVolume = imageWidth(1)*imageHeight(1)*length(txt_files);
    totalBubbleVolume = sum(totalArea);
    bubblePercent = totalBubbleVolume/totalVolume;
    % do not forget the print bubblePercent
    % fprintf('\nBubble Percent %% %2.3f\n', bubblePercent*100)
end

for n = 1 : length(bmp_files)
    %[~, name, ext] = fileparts(bmp_files(n).name);
    % read the image
    BWo = imread(bmp_files(n).name);
    BW = imfill(BWo,4,'holes');
    data3D(:,:,n) = BW;%(128:256,128:256);
end
unitVolume = 1;

switch get(get(findobj('Tag','rbtnGroup'), 'SelectedObject'),'Tag')
        case '3d06',  res = 6;
        case '3d18',  res = 18;
        case '3d26',  res = 26;
end

% disp(['Before Cleaning : ', num2str(sum(data3D(:))/totalVolume*100)]);
% Save data3D connection options before cleaning
data3D6 = imclearborder(data3D, 6);
data3D18 = imclearborder(data3D, 18);
data3D26 = imclearborder(data3D, 26);

data3D = imclearborder(data3D, res); % Choose Connection
cleanBubblePercent = sum(data3D(:))/totalVolume;
```

```
    [L, NUM] = bwlabeln(data3D, res); % 6, 18, 26
    bin = histc(L(:),unique(1:NUM));
    volume = bin.*unitVolume;
    radius = (3*bin/(pi*4)).^(1/3);

    vDist = histc(volume,unique(volume));
    rDist = histc(radius,unique(radius));
    disp('----------------- Bubble Distribution ----------------')
    fprintf('\n   Total Bubble Percent of Selected Volume%% %2.3f\n\n', bubblePercent*100);
    fprintf('   Total Bubble Percent After Border Cleaning\n');
    fprintf('  6 Point Connectivity : %% %2.3f\n', sum(data3D6(:))/totalVolume*100);
    fprintf(' 18 Point Connectivity : %% %2.3f\n', sum(data3D18(:))/totalVolume*100);
    fprintf(' 26 Point Connectivity : %% %2.3f\n', sum(data3D26(:))/totalVolume*100);
    fprintf('\n  %d Point Connectivity is Selected by the User\n', res);

    fprintf('\n   Volume   Radius  Number\n');
    fprintf('----------------------------\n');
    fprintf('%8.3f-%8.3f-%5d  \n', [unique(volume)'; unique(radius)'; vDist']);
    % process result in HTML format
    % HTML output
    volume = unique(volume)';
    radius = unique(radius)';
    vDist = vDist';

    fileID = fopen([datestr(now,'report_ddmmyy') '.htm'],'a');
    %fprintf(fileID,'<!DOCTYPE        html>\n<html>\n<body>\n<h1>-----------------        Bubble
Distribution ----------------</h1>');
    fprintf(fileID,'<h3>\nTotal  Bubble  Percent  of  Selected  Volume  %%  %2.3f  \n\n</h3>',
bubblePercent*100);
    fprintf(fileID,'<h3>\nTotal  Bubble  Percent  of  Selected  Volume  %%  %2.3f  After  Border
Cleaning\n\n</h3>', cleanBubblePercent*100);
    fprintf(fileID,'<h3>\n  %d Point 3D Connectivity is Selected by the User\n</h3>', res);

    fprintf(fileID,'<table>');
    fprintf(fileID,'<tr>\n<th>Volume</th><th>Radius</th><th>Number</th></tr>');
    for i = 1: length(volume)
        fprintf(fileID,['<tr>\n<th>', num2str(volume(i)), '</th>\n<th>', ...
            num2str(radius(i)), '</th>\n<th>', num2str(vDist(i)), '</th>\n</tr>']);
    end
     fprintf(fileID,'</table>');
% <p>My first paragraph.</p>
    fprintf(fileID,'</body>\n</html>');
    fclose(fileID);
end
%%
function create3D(src,evnt) %#ok<INUSD>
```

```
    bmp_files = dir('*.bmp');

    for n = 1 : length(bmp_files)
        % [~, name, ext] = fileparts(bmp_files(n).name);
        % disp(bmp_files(n).name);
        % read the image
        BWo = imread(bmp_files(n).name);
        BW = imfill(BWo,4,'holes');
        data3D(:,:,n) = BW;%(128:256,128:256);
    end

    data3D = imclearborder(data3D, 26);
    D = squeeze(data3D*64);
    D = padarray(D,[3 3 3], 'both');
    % Create an isosurface
    Ds = smooth3(D);
    surface = isosurface(Ds,3);
    % Display the surface
      hiso = patch('Vertices',surface.vertices,...
                   'Faces',surface.faces,...
                   'FaceColor',[.85,.75,.05],...
                   'EdgeColor','none');
      view(45,30)
      axis tight
      daspect([1,1,1])
      lightangle(45,30);
      set(gcf,'Renderer','zbuffer');
      lighting phong
      isonormals(Ds, hiso)
      set(hiso,'SpecularColorReflectance',0,'SpecularExponent',50)
end
%%
function mri_closereq(src,evnt) %#ok<INUSD>
% User-defined close request function
% to display a question dialog box
   selection = questdlg('Close xRaY GUI?',...
      'Close Request Function',...
      'Yes','No','Yes');
   switch selection,
      case 'Yes',
         delete(gcf)
      case 'No'
      return
   end
end
```

Appendix 3: Dough Formulation for Studying the Effects of Mixing Time and Salt Reduction on Dough Rheological Properties

Wheat cultivar	[a] Water content	[b] Salt content	[c] Mixing time
Roblin	FAB-4%	0	1 min
Harvest		0.25 mol L^{-1}	Optimal mixing time
		2.5%	10 min

[a] To eliminate dough handling difficulties, *i.e.*, sticky dough, induced by higher water contents, doughs were prepared at a constant water content of FAB-4%.

[b] The salt (NaCl) content of 0.25 mol L^{-1} was determined due to Health Canada's sodium reduction target (Appendix 1).

[c] The mixing time of 1 and 10 min refers to the under- and over-mixing conditions.

Appendix 4: Statistical Application Systems (SAS) Code

(a) Three-way ANOVA

```
data parameter;
input parameter cultivar $ water $ salt $;
datalines;
proc glimmix data=parameter;
class cultivar water salt;
model parameter=cultivar|water|salt;
lsmeans cultivar/ adjust=tukey plot=mean(join) lines;
lsmeans water/ adjust=tukey plot=mean(join) lines;
lsmeans salt/ adjust=tukey plot=mean(join) lines;
lsmeans cultivar*water/adjust=tukey plot=mean(sliceby=water join) lines;
slice cultivar*water/sliceby=water diff adjust=tukey lines;
slice cultivar*water/sliceby=cultivar diff adjust=tukey lines;
lsmeans cultivar*salt/adjust=tukey plot=mean(sliceby=salt join) lines;
slice cultivar*salt/sliceby=salt diff adjust=tukey lines;
slice cultivar*salt/sliceby=cultivar diff adjust=tukey lines;
lsmeans water*salt/adjust=tukey plot=mean(sliceby=salt join) lines;
slice water*salt/sliceby=salt diff adjust=tukey lines;
slice water*salt/sliceby=water diff adjust=tukey lines;
lsmeans cultivar*water*salt/adjust=tukey plot=mean(sliceby=cultivar*water join) lines;
slice cultivar*water*salt/sliceby=water*salt diff adjust=tukey lines;
lsmeans cultivar*water*salt/adjust=tukey plot=mean(sliceby=cultivar*salt join) lines;
slice cultivar*water*salt/sliceby=cultivar*water diff adjust=tukey lines;
lsmeans cultivar*water*salt/adjust=tukey plot=mean(sliceby=water*salt join) lines;
slice cultivar*water*salt/sliceby=cultivar*salt diff adjust=tukey lines;
run;
quit;
```

(b) One-way ANOVA

```
data parameter;
input parameter cultivar $ water $ salt $;
datalines;
proc glimmix data=parameter;
class cultivar water salt;
model parameter=cultivar|water|salt;
lsmeans cultivar/ adjust=tukey plot=mean(join) lines;
lsmeans water/ adjust=tukey plot=mean(join) lines;
lsmeans salt/ adjust=tukey plot=mean(join) lines;
run;
```

(c) Comparison between means

```
data parameter;
input parameter sample $;
datalines;
proc glimmix data= parameter;
class sample;
model parameter=sample;
lsmeans sample/ adjust=tukey plot=mean(join) lines;
run;
proc means data=parameter;
class sample;
run;
```

(d) Pearson correlation coefficients

```
data correlation;
input cultivar$ salt$ water$ a b;
datalines;
proc print;
proc corr data= correlation;
run;
proc gplot data= correlation;
plot a*b;
run;
quit;
```

Appendix 5: Effects of Wheat Cultivar, Water and Salt on Dough Mixograph Parameters

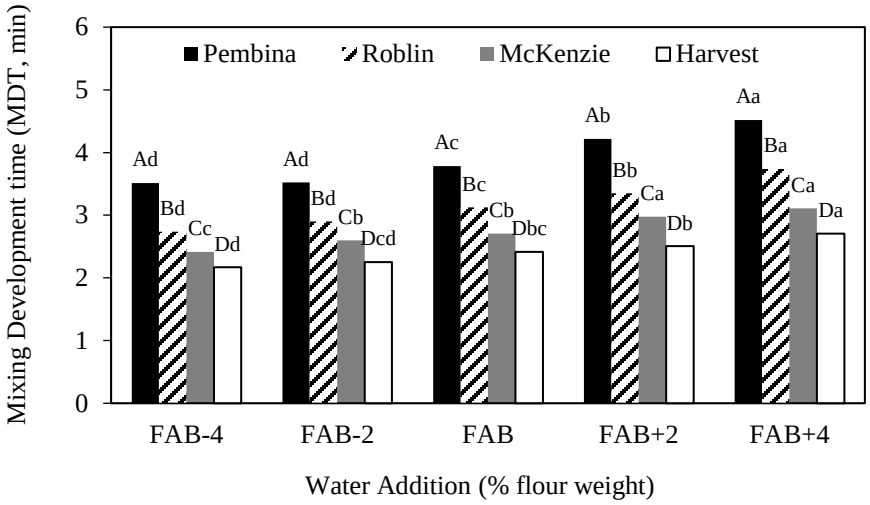

Fig. 1. Effects of wheat cultivar and water addition on mixing development time (MDT)

[a] For the same water addition, columns labeled by the same upper-case letters are not significantly different ($P<0.05$).

[b] For the same wheat cultivar, columns labeled by the same lower-case letters are not significantly different ($P<0.05$).

[c] FAB: farinograph water absorption.

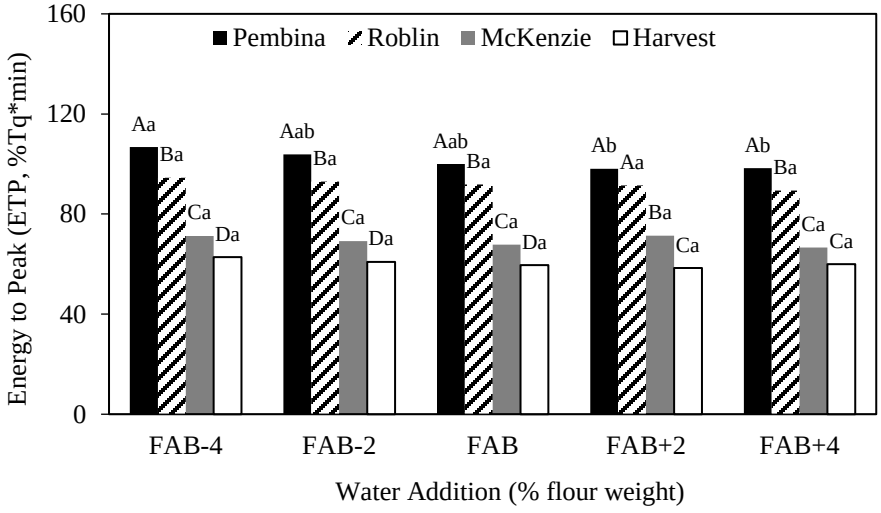

Fig. 2. Effects of wheat cultivar and water addition on energy to peak (ETP)

[a] For the same water addition, columns labeled by the same upper-case letters are not significantly different ($P<0.05$).

[b] For the same wheat cultivar, columns labeled by the same lower-case letters are not significantly different ($P<0.05$).

[c] FAB: farinograph water absorption.

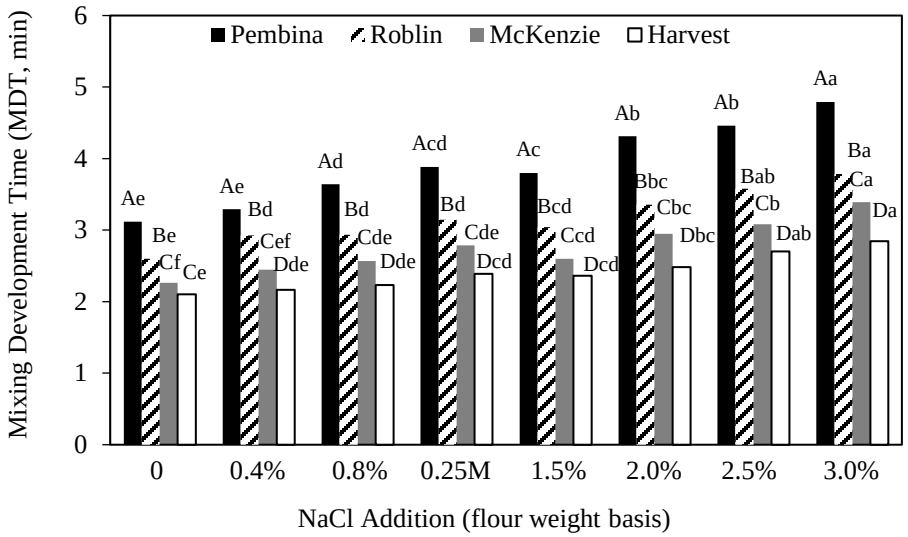

Fig. 3. Effects of wheat cultivar and NaCl addition on mixing development time (MDT)

[a] For the same NaCl addition, columns labeled by the same upper-case letters are not significantly different (P<0.05). [b] For the same wheat cultivar, columns labeled by the same lower-case letters are not significantly different (P<0.05). [c] 0.25M (mol/L), NaCl addition to bread dough recommended by Health Canada.

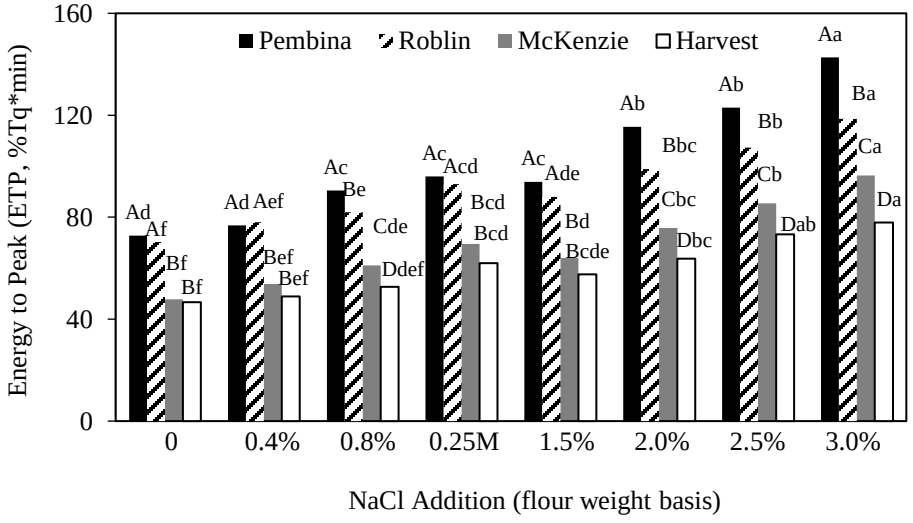

Fig. 4. Effects of wheat cultivar and NaCl addition on energy to peak (ETP)

[a] For the same NaCl addition, columns labeled by the same upper-case letters are not significantly different (P<0.05). [b] For the same wheat cultivar, columns labeled by the same lower-case letters are not significantly different (P<0.05). [c] 0.25M (mol/L), NaCl addition to bread dough recommended by Health Canada.

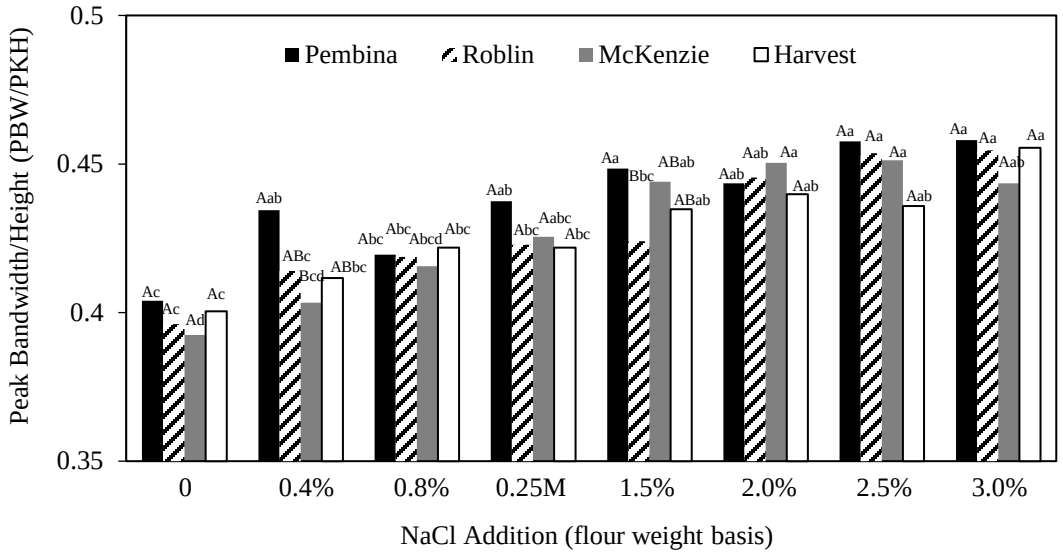

Fig. 5. Effects of wheat cultivar and NaCl addition on peak bandwidth/height (PBW/PKH)

[a] For the same NaCl addition, columns labeled by the same upper-case letters are not significantly different (P<0.05). [b] For the same wheat cultivar, columns labeled by the same lower-case letters are not significantly different (P<0.05). [c] 0.25M (mol/L), NaCl addition to bread dough recommended by Health Canada.

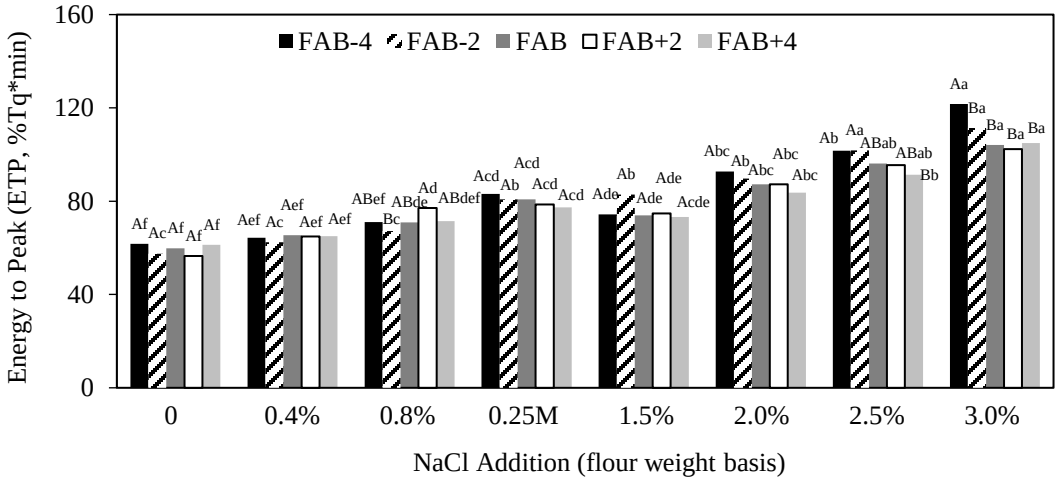

Fig. 6. Effects of water and NaCl addition on energy to peak (ETP)

[a] For the same NaCl addition, columns labeled by the same upper-case letters are not significantly different (P<0.05). [b] For the same water addition, columns labeled by the same lower-case letters are not significantly different (P<0.05). [c] 0.25M (mol/L), NaCl addition to bread dough recommended by Health Canada. [d] FAB: farinograph water absorption.

Appendix 6: Effects of Cultivar (C), Water (W) and Salt (S) on Rheological Model Parameters

Parameters	Cultivar	Water	Salt	C*W	C*S	W*S	C*W*S
S'	0.0673ns	<.0001*	<.0001*	0.0344*	0.4507ns	0.2556ns	0.428ns
S''	<.0001*	<.0001*	<.0001*	0.0222*	0.0737ns	0.1448ns	0.7155ns
S^c	<.0001*	<.0001*	<.0001*	0.0586ns	0.0194*	0.0022ns	0.1004ns
S^r	<.0001*	<.0001*	<.0001*	<.0001*	<.0001*	0.0013*	0.2598ns
n'	0.3076ns	0.1541ns	0.215ns	0.0865ns	0.5077ns	0.4355ns	0.8131ns
n''	0.0118*	0.0321*	0.0023*	0.4171ns	0.6388ns	0.5962ns	0.6291ns
n^c	<.0001*	<.0001*	0.7858ns	<.0001*	0.0033*	0.0041*	0.0196*
n^r	<.0001*	<.0001*	0.0395*	<.0001*	0.0071*	0.0084*	0.0414*
R_1^c	<.0001*	<.0001*	<.0001*	0.0613ns	0.2761ns	0.4697ns	0.7666ns
R_1^r	0.7018ns	<.0001*	0.02*	0.5532ns	0.0148*	0.2385ns	0.7357ns
R_2^c	<.0001*	<.0001*	0.0007*	<.0001*	0.6342ns	0.2383ns	0.1788ns
R_2^r	0.0969ns	<.0001*	0.0059*	0.185ns	0.0056*	0.1446ns	0.6001ns
λ^c	<.0001*	<.0001*	0.0008*	<.0001*	0.4305ns	0.0017*	0.0036*
λ^r	<.0001*	<.0001*	<.0001*	<.0001*	0.2754ns	0.0007*	0.0013*
η_0^c	<.0001*	<.0001*	0.0093*	<.0001*	0.0048*	0.0670ns	0.4169ns
η_0^r	0.0017*	<.0001*	0.3206ns	0.0022*	0.0232*	0.3843ns	0.1668ns

P values labeled by * = significant, 'ns'= not significant.

Appendix 7: Effects of Cultivar, Water, Salt and Mixing on Dough's Gas Phase Parameters

(a) Pembina and Harvest doughs with FAB water and 2 salt levels tested immediately after optimal mixing

Effect	df	R_0	ε
Salt	1	0.3671ns	0.0369*
Cultivar	1	0.0678ns	0.0237*
Salt*Cultivar	1	0.0742ns	0.0606ns

P values labeled by * = significant, 'ns'= not significant.

(b) Pembina doughs with 3 water levels and 2 salt levels tested immediately after optimal mixing

Effect	df	R_0	ε
Salt	1	0.2559ns	0.3090ns
Water	2	0.6074ns	0.0015*
Salt*Water	2	0.5689ns	0.0840ns

P values labeled by * = significant, 'ns'= not significant.

(c) Pembina doughs with FAB water and 2 salt levels tested immediately after three various mixing conditions

Effect	df	R_0	ε
Salt	1	0.2373ns	0.7192ns
Mixing	2	0.0326*	0.0073*
Salt*Mixing	2	0.0283*	0.0148*

P values labeled by * = significant, 'ns'= not significant.